A Thesis for the Degree of Ph.D. in Science

Chemistry and biology of pharmacological active compounds from natural products

June 2014

Graduate School of Science and Technology
Keio University

Takahiro Fujimaki

Contents

Chapter 1

Introduction

1-1. Natural products for drug discovery

Humans have long used natural products for medical purposes. In particular, plants have been classically used over the centuries. Since beginning of the 19th century when the development of the analytical chemistry, isolation and purification of the active components of medicinal plants and demonstration of their values for medicine were become popular. In 1815, F. W. Sertürner isolated morphine (Figure 1-1) from opium extracts and found that its ability for the analgesic [1]. This success brought the importance to seek "active principles" of medicinal plants, and discovery of bioactive natural products, such as quinine (Figure 1-1) and cocaine (Figure 1-1) [2].

The use of other natural resources for medicine, such as actinomycetes and fungi, began with the identification of penicillin's antibacterial activity by Fleming [3] and its isolation by Chain and Florey [4]. This discovery of the world's first antibiotic was a trigger that produced a large number of other antibiotic compounds, and many of them were commercialized and are still used in clinical care. Since about 1970s, pharmaceutical industry began using natural products for development of various diseases. For instance, Taxol (Figure 1-1) isolated from *Taxus brevifolia* [5] was used for anti-cancer drug and cyclosporine (Figure 1-1) isolated from *Trichoderma polysporum* [6,7] was used for immunosuppressant .

When the human genome project started in 1990, function analysis of the protein has become the main focus in the growing research fields of biology. The concept of drug discovery also shifted to understanding of disease mechanism at the molecular level and

to screening for medicines targeting optimal bio-molecules (proteins) in organism. From this kind of circumstance, since about 1990s, combinatorial chemistry got the attention as discovery tool of drugs, and many pharmaceutical companies have been using in favor of high-throughput screening (HTS) based on molecular targets requiring large libraries of synthesis compounds. In contrast, these companies have deemphasized natural products research for drug development because of incompatibility with HTS, difficult of synthesis and unstable supply. Sorafenib (Figure 1-2) is one of the combinatorial compounds that can be identified as an approved drug, but the expected surge in productivity of clinical drug using the screening combining HTS and combinatorial chemistry has not come true, and the number of New Chemical Entities (NCEs) is declining yearly.

Against this backdrop, many major pharmaceutical companies became interested in natural products as drug-seeds, because of high structural diversity and various unique biological activities of natural products. Recently, the use of natural products for drug discovery is not only directly adoption of compounds isolated from natural products but also diversity-oriented synthesis based on a hint from partial structure of nature. For instance, halichondrin B (Figure 1-2) isolated from the marine sponge *Halichondria okadai* [8,9] was total synthesized and its partial structure were approved as eribulin (Figure 1-2) [10] for treatment of cancer. Furthermore, recent reports showed that 34% of 1073 small molecule NCEs from 1981 to 2010 were classified as natural products or derivatives [11]. Moreover, 16% of these NECs were total synthesis, but the pharmacophore was from natural product [11]. These reports suggested that natural

products are expected to be the source of novel leads for drug development.

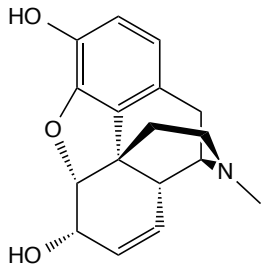

morphine

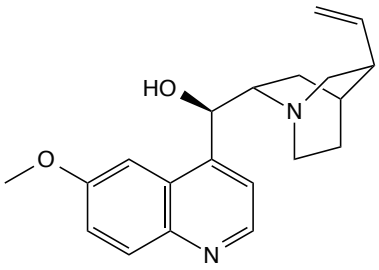

quinine

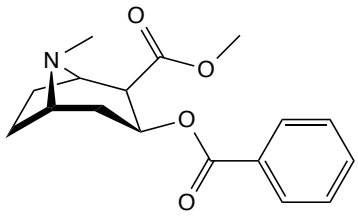

cocaine

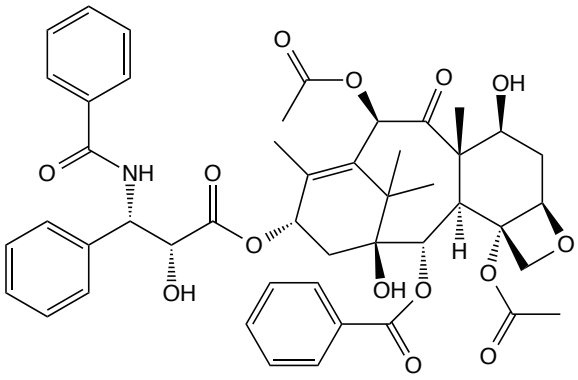

taxol

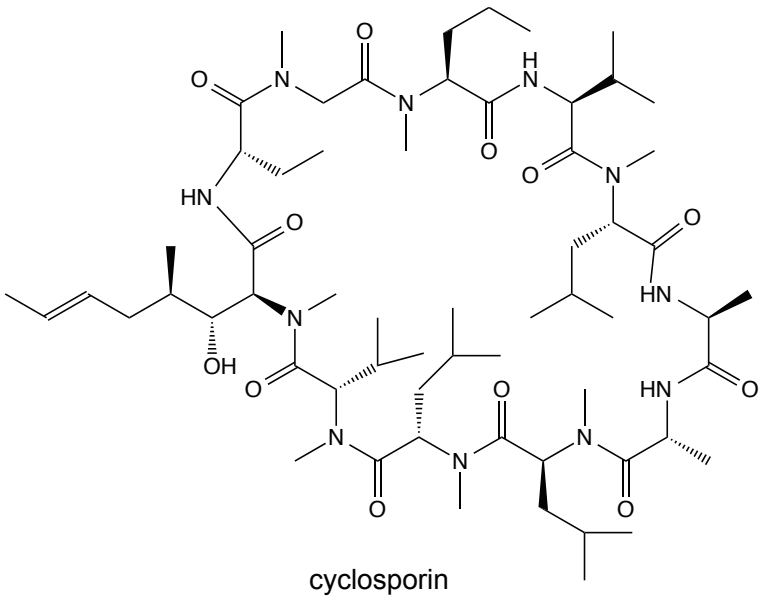

cyclosporin

Figure 1-1. Structures of physiological active compounds derived from natural products.

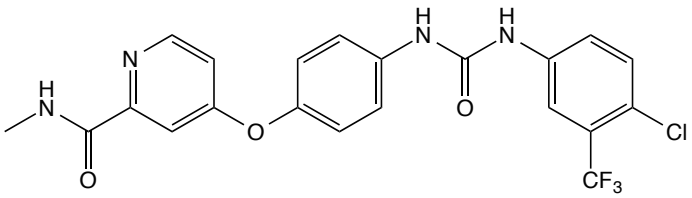

sorafenib

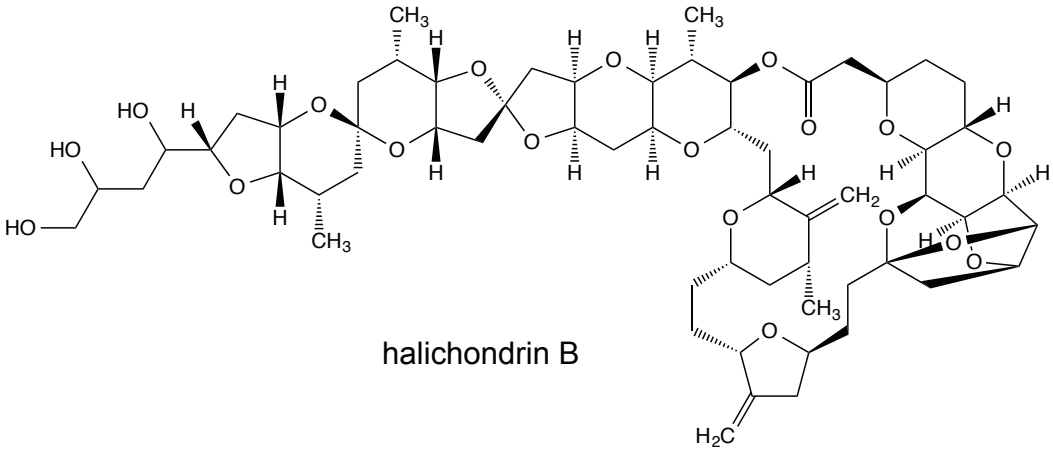

halichondrin B

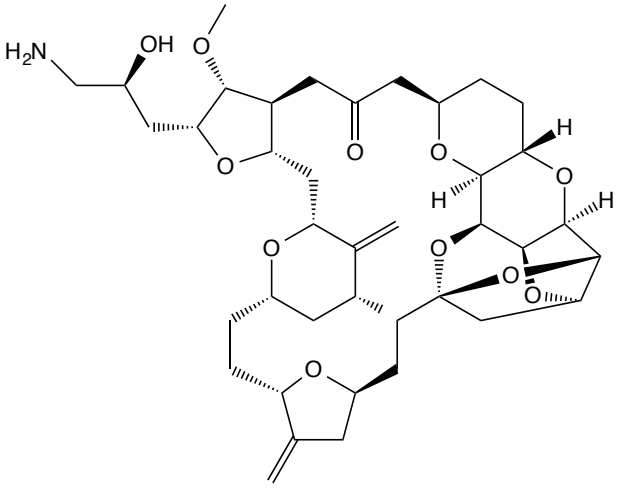

eribulin

Figure 1-2. Structures of sorafenib, halichondrin B and eribulin.

1-2. Prostate cancer

There are approximately 240,000 new diagnoses and 33,000 deaths resulting from prostate cancer each year in the USA [12]. In Japan, the number of deaths caused by prostate cancer is on an increasing trend rapidly, and is expected to reach second, only after lung cancer in 2020. Moreover, prostate cancer is one of the diseases common in the elderly, thus, there is an urgent need to treat prostate cancer as aging of the population continue in Japan.

The androgen receptor (AR), nuclear hormone receptor, plays an important role in the development and progression of prostatic diseases, and the AR can be activated by androgens, such as testosterone and dihydrotestosterone (DHT); therefore, the androgen deprivation therapy (ADT) is effective in decreasing prostate-specific antigen (PSA) levels and reducing the tumor size with early treatment [13,14]. ADT include multiple approaches, such as surgical castration by bilateral orchiectomy, administration of estrogens, luteinizing hormone-releasing hormone (LH-RH) agonists or antagonists therapy, treatment of 5α-reductase (an enzyme that convert testosterone to DHT) inhibition and anti-androgen therapy [13]. These therapies are generally used in combination with others to improve the effect of treatment. However, long-term ADT eventually cause cancer recurrence, specifically called castrate-resistant prostate cancer (CRPC) [12,15]. Although CRPC has been mis-comprehended as “androgen independent”, recent research revealed that CRPC is still driven by hormones [16]. Therefore, new AR antagonists and new agents targeting the metabolic pathways that

lead to the production of androgens have been developed for the treatment of CRPC [15,17].

Enzalutamide (Figure 1-3) is the second generation AR antagonist that has been approved for the treatment of CRPC [18,19]. The first generation AR antagonists, such as flutamide (Figure 1-3) and bicalutamide (Figure 1-3), induce AR mutations and exhibit partial agonist after the long-term therapy [20,21], however, enzalutamide shows antagonism to these AR mutations, in particular W741C, which resistant to bicalutamide [18]. Furthermore, besides the competing with androgens, enzalutamide exhibit unprecedented antagonism including inhibiting translocation of AR to the nucleus, impairing bond of AR to DNA and disturbing co-activator recruiting [18].

Recently, however, it has been shown that F876L mutant AR resistant to enzalutamide in the laboratory level [22]. This easy acquirement of tolerance may result from the structural similarities among existing AR antagonists. In fact, enzalutamide has common partial structure with both flutamide and bicalutamide including anilide and trifluoromethyl group. Other type of clinical AR antagonist is only steroid type (e.g., chlomadinone acetate (Figure 1-3)), therefore, development of an AR antagonist possessing novel structure is an attractive strategy to overcome prostate cancers that are resistant to the known AR antagonists.

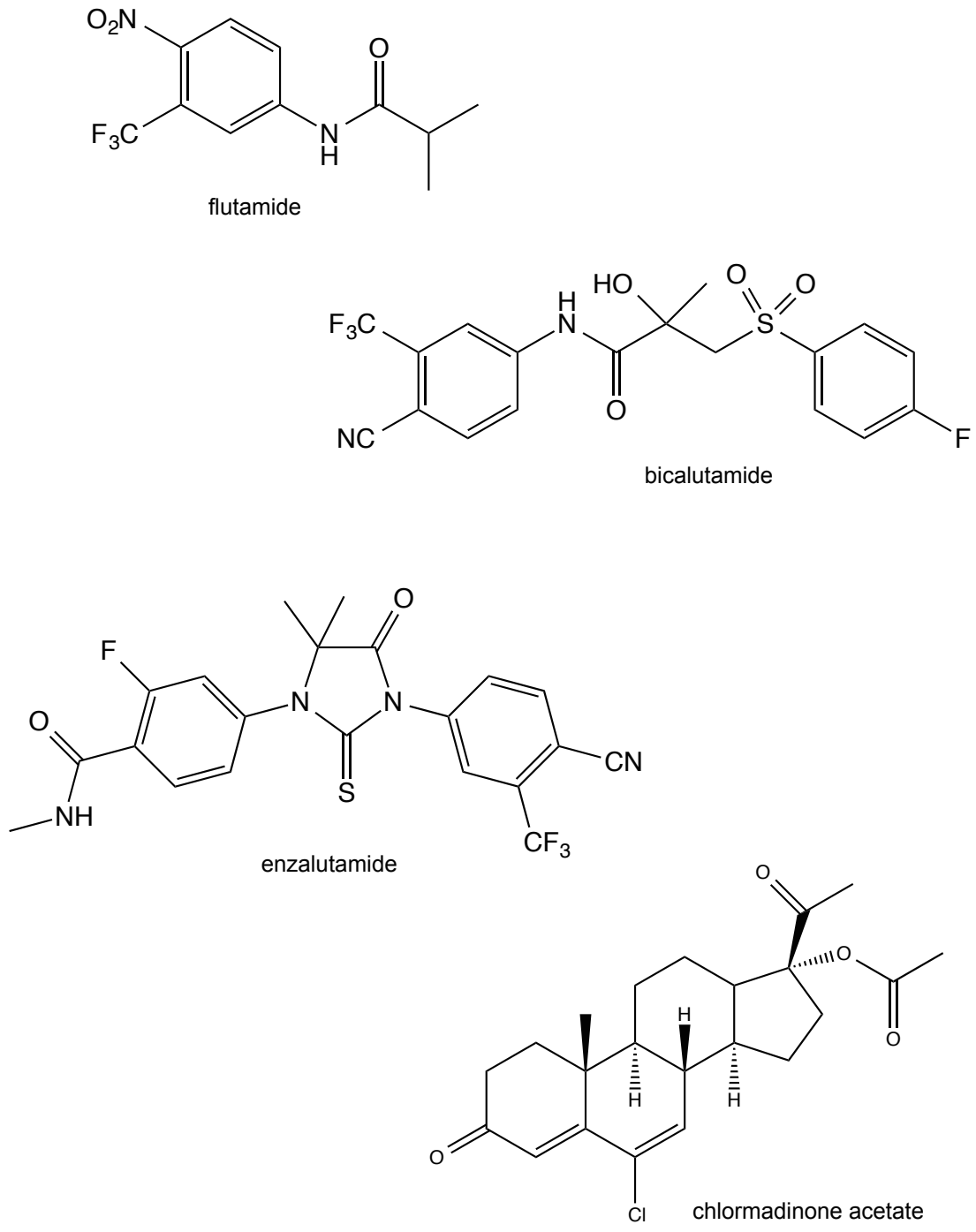

Figure 1-3. Structures of clinical AR antagonists for prostate cancer.

1-3. Parkinson's disease

Parkinson's disease (PD) is the second most common neurodegenerative disease, affecting 1% of the population over 55 years of age [23]. PD is characterized by progressive dopaminergic neuronal cell death in the substantia nigra par compacta of the midbrain. The main symptoms of PD are movement disorders such as rest tremors, bradykinesia/akinesia, muscular rigidity, postural instability, and gait abnormalities. The pathological characteristic of the brain with PD is Lewy bodies, witch are composed mainly of α-synuclein and ubiquitin. Oral administration of L-dopa (Figure 1-4), precursor to dopamine, is the most widely used and effective treatment for PD. However, L-dopa also leads to motor complication (e.g., dyskinesia, dystonia and end-of-dose akinesia) and its effective time of therapy wear off after 5-10 years of treatment [24]. Another class of antiparkinsonian drugs such as dopamine agonists (e.g., bromocriptine), anticholinergic agents (e.g., trihexyphenidyl), monoamine oxidase B (MAO-B) inhibitors (e.g., selegiline) and catechol-*O*-methyltransferase (COMT) inhibitors (e.g., entacapone), which only ameliorate the symptoms of PD, like L-dopa, and there are no therapies to completely cure patients with the disorder (Figure 1-4) [25].

The cause of PD remains unclear, but several pathogenic mechanisms have been suggested, including oxidative stress and mitochondria dysfunction. The oxidative stress accompanied by a disturbance of mitochondria function that has been in postmortem brain tissue from PD patients. Thus, several small antioxidant molecules

have been studied as treatment for PD [26,27,28], and some inhibitors of mitochondrial respiratory chain, such as rotenone, paraquat, 1-methyl-4-phenylpyridinium (MPP^+) and its precursor 1-methyl-4-phenyl-1,2,3,6-tetrahydropyridine (MPTP) have been used as mimicking agents for various PD models (Figure 1-5) [29,30]. The identification of PD-associated genetic mutations from familial forms of PD (PINK1, Dj-1, LRKK2, parkin and α-synuclein) is another approach for studies of PD, and has revealed that involvement of molecular chaperon and the ubiquitin-proteasome system in PD pathogenesis [31,32].

However, effective drugs or approach to therapies for PD have not been found by these researches so far. These failures may arise from a lack of understanding about the fundamental pathogenesis of PD upstream oxidative stress or mitochondria stress. Therefore, in order to develop innovative treatment for PD, it is necessary to investigate new target molecules and new molecular pathways of PD by using compounds which possess novel structure or ability.

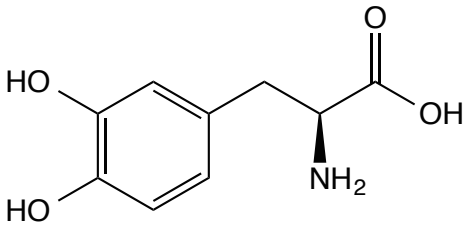

L-dopa

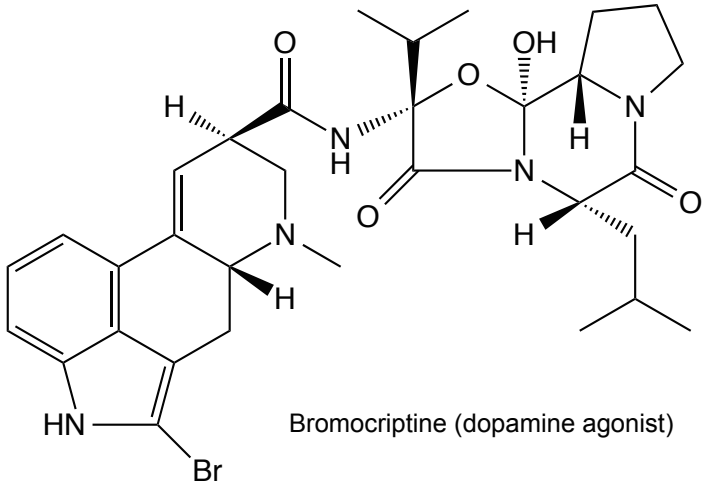

Bromocriptine (dopamine agonist)

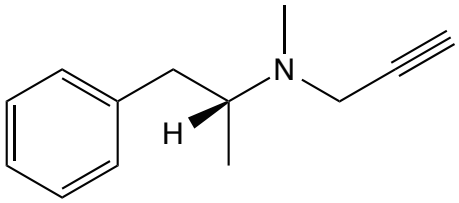

Selegiline (MAO-B inhibitor)

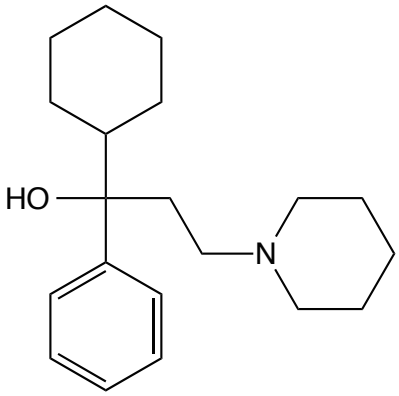

Trihexyphenidyl (anticholinergic agent)

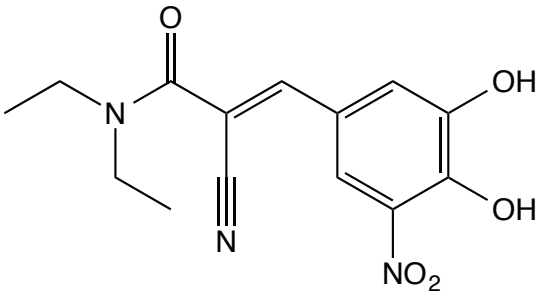

Entacapone (COMT inhibitor)

Figure 1-4. Structures of anti-PD drugs.

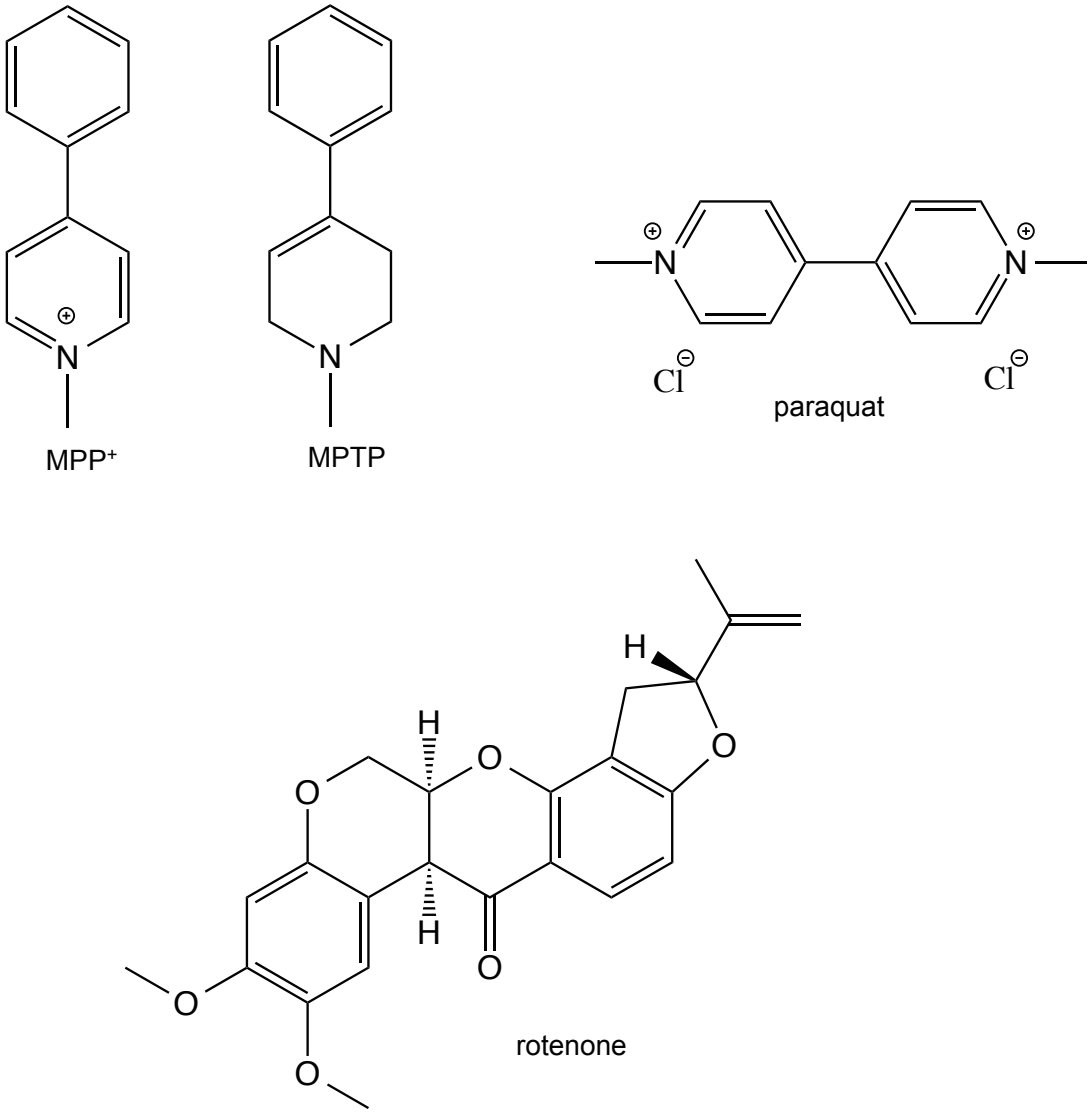

Figure 1-5. Structures of mimicking agents for PD.

Chapter 2

Isolation, structure elucidation and evaluation of pharmacological effect of a novel androgen antagonist, arabilin, produced by *Streptomyces* sp. MK756-CF1

2-1. Introduction

One of the effective prostate cancer treatments is treatment of AR antagonists. AR antagonists can be classified into two structural types, steroidal and nonsteroidal compounds [33,34]. Steroidal AR antagonists, such as chlomadinone acetate (Figure 1-3), often exhibit side effects because of cross-reactivity with other steroid hormone nuclear receptors, such as estrogen receptor and progesterone receptor. On the other hand, anilide-type compounds, such as flutamide (Figure 1-3) and bicalutamide (Figure 1-3), are representative of nonsteroidal AR antagonists. Although these anilide-type AR antagonists have been clinically used for prostate cancer therapy, prostate cancer almost always advances to a hormone-refractory state after long-term treatment with AR antagonists [35]. The mutation in AR is considered a possible reason for rendering prostate cancer cells hormone refractory [36]. The most commonly reported AR mutation are point mutation of ligand binding domain including T877A [37], W741C, W741L [38], H874Y [39,40]. Furthermore, anilide-type AR antagonists act as agonists toward hormone-refractory prostate cancer cells in some cases [38,41,42]. Thus, development of a new type of AR antagonist is an attractive strategy to overcome prostate cancers that are resistant to the known AR antagonists.

In the course of screening for a new type of AR antagonist, the author isolated a novel compound, arabilin, with two known structural isomers, spectinabilin and SNF4435C, from *Streptomyces* sp. MK756-CF1. In this chapter, the isolation, structure elucidation and biological activities of arabilin are reported.

2-2. Result and discussion

2-2-1. Screening for binding inhibitors of DHT and AR

To acquire a new type of AR antagonist with a nonsteroidal/nonanilidetype structure, the author first screened more than 2000 microbial extracts to find inhibitors, which could inhibit the binding of DHT to AR using a [^{3}H] DHT-AR *in vitro* binding assay. In the course of screening, the author found that the culture broth extract of strain MK756-CF1 inhibited the binding of DHT to AR.

2-2-2. Taxonomy of the producing strain

Strain MK756-CF1 produced spore chains on aerial mycelia, which developed from branched substrate mycelia. The partial gene sequence (1412 bp) coding 16S ribosomal RNA of MK756-CF1 showed high homology with those of members of the genus *Streptomyces*, such as *Streptomyces spectabilis* (National Institute of Technology and Evaluation Biological Research Center (NBRC) 13423^T 1408/1413 bp, 99%) and *Streptomyces flavofungini* (NBRC 13371^T 1391/1412 bp, 98%). These phenotypic and genotypic properties implied that strain MK756-CF1 belonged to the genus *Streptomyces*.

2-2-3. Isolation of arabilin, spectinabilin and SNF4435C

The cultivation of strain MK756-CF1 was carried out in sixty 500-mL Erlenmeyer flasks containing pressed wheat (2.4 kg) because this solid-state fermentation enabled the strain to produce abundant active components. After fermentation, the culture was extracted with ethanol (2 L), filtrated and concentrated *in vacuo*. This suspension was adjusted to pH 7.0, followed by extraction with ethyl acetate (3 L) twice, and the organic layer was concentrated to give a pink oily residue (2.2 g). Thus, the obtained crude active oil was subsequently subjected to silica gel column chromatography (Silica gel 60, 60–230 μm; Merck, Darmstadt, Germany) using an n-hexane-ethyl acetate stepwise system. One active fraction (n-hexane-ethyl acetate, 2:1) was further purified by preparative octadecyl silyl (ODS) HPLC (Sun Fire, 10 μm, 19 x 250 mm; Waters, Milford, MA, USA) with 80% aqueous methanol to give a pure novel compound, arabilin (3.3 mg) (Figure 2-1). Another active fraction obtained by silica gel column chromatography (n-hexane-ethyl acetate, 1:1) was also further purified by preparative ODS HPLC to give spectinabilin (3.0 mg) [43] and SNF4435C (6.0 mg) [44] (Figure 2-1). Spectinabilin and SNF4435C were reported as a weak inhibitor of Rauscher leukemia virus reverse transcriptase [43] and a potent immunosuppressant [44], respectively. The isolation procedure of these compounds was shown in Figure 2-2.

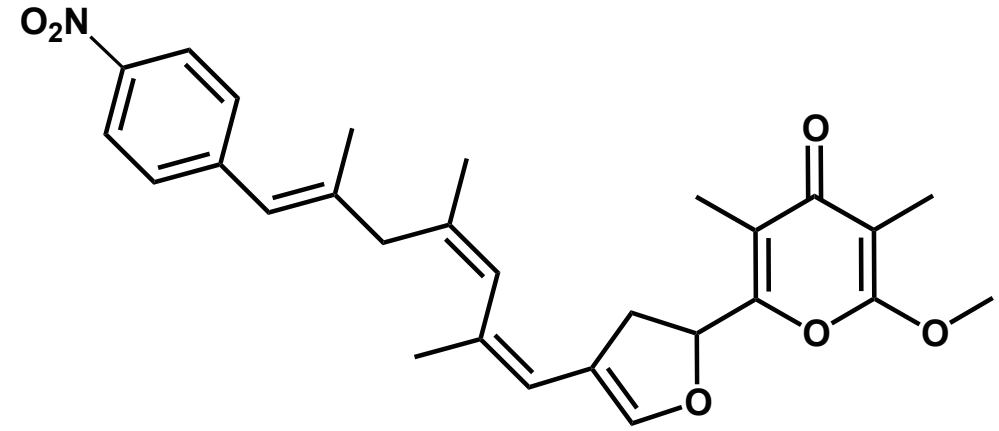

arabilin

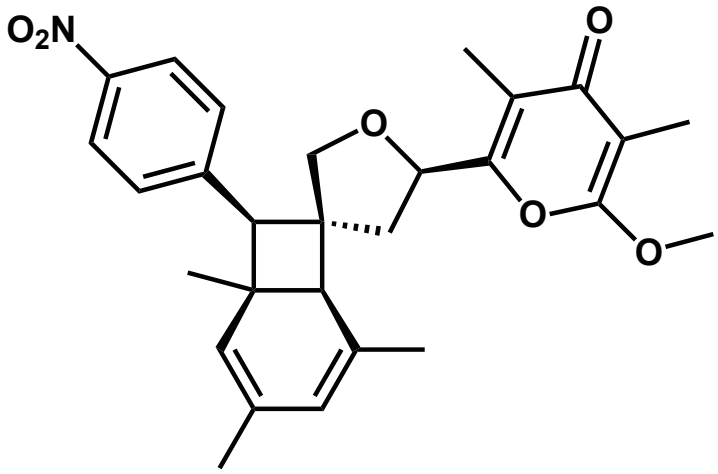

SNF4435C

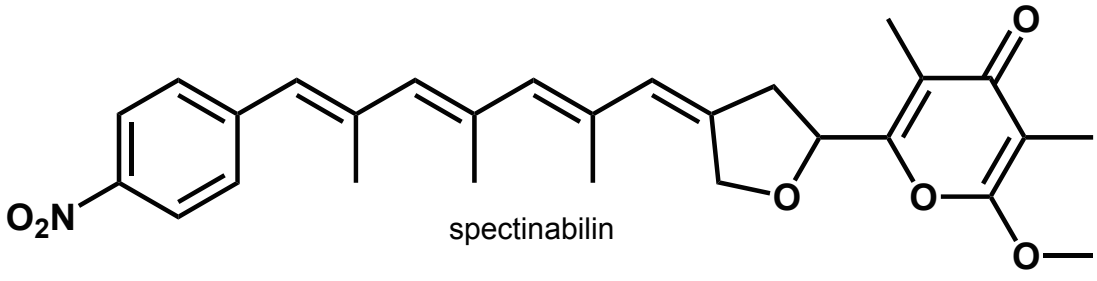

spectinabilin

Figure 2-1. Structures of arabilin, SNF4435C and spectinabilin.

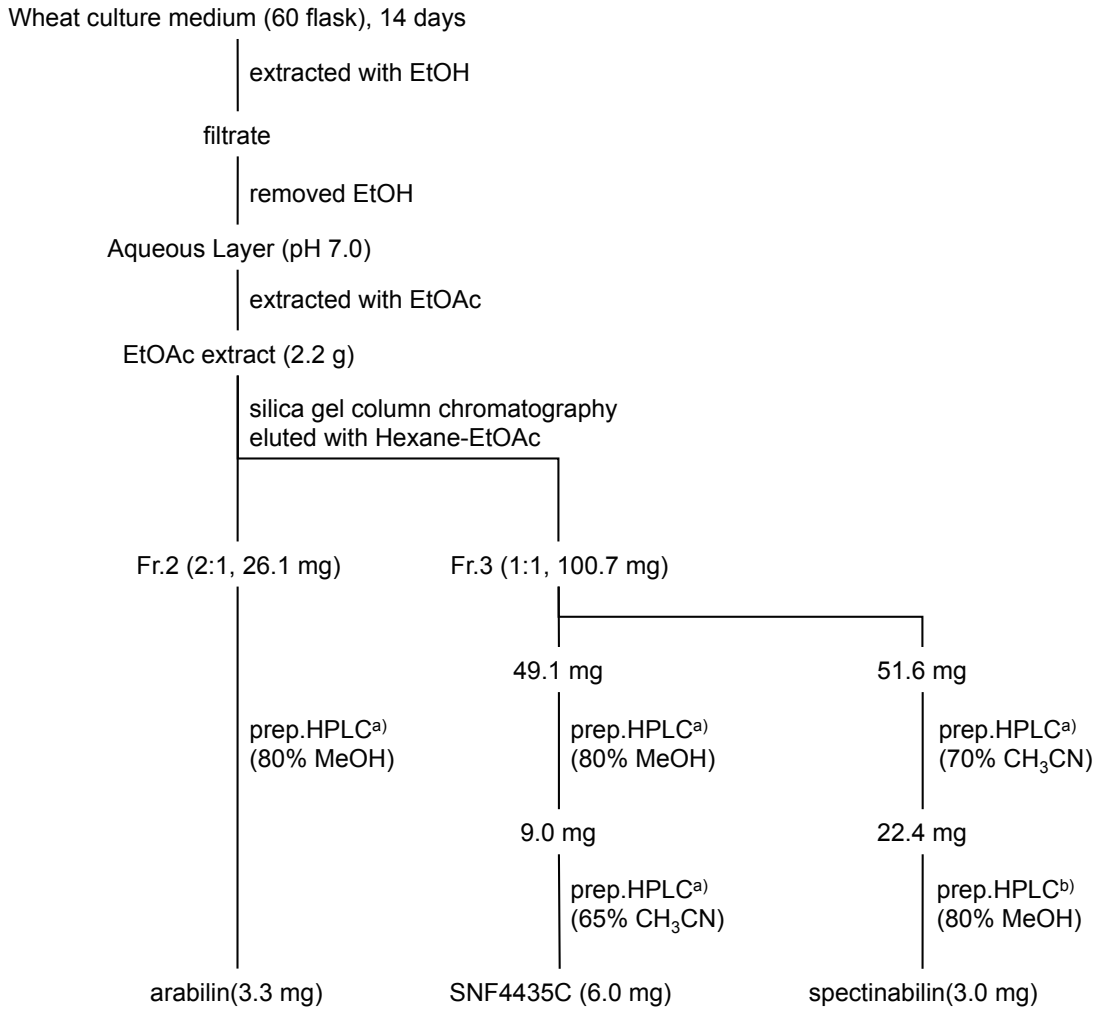

a) Column, Sun Fire, ODS(Waters, 10μm, 19 mmI.D.×250 mm); Mobile phase, aqMeOH or aqCH_3CN; flow rate, 10 mL/minute

b) Column, CAPCELL PAC, ODS(SHISEIDO, 5μm, 20 mmI.D.×250 mm) Mobile phase, aqMeOH; flow rate, 10 mL/minute

Figure 2-2. Isolation procedure of arabilin, SNF4435C and spectinabilin from *Streptomyces* sp. MK756-CF1.

2-2-4. Structure elucidation of arabilin

The physico-chemical properties of arabilin as well as spectinabilin and SNF4435C are summarized in Table 2-1 [43,45]. From HRESI-MS measurements in combination with ^{1}H and ^{13}C NMR data (Figure 2-4 and 2-5), the molecular formula of arabilin was determined to be $C_{28}H_{31}NO_6$ (Found: 478.2215 $[M+H]^+$, Calcd: 478.2224), the same as spectinabilin and SNF4435C. The IR spectrum revealed that arabilin possesses a ketone conjugated with a double bond (1666 cm^{-1}) and a nitro group (1516 and 1342 cm^{-1}), as does spectinabilin and SNF4435C (Figure 2-3 and Table 2-1).

On the other hand, the UV spectrum of arabilin (λ_{max}: 263 nm (ε 18,400), 315 nm (sh, ε 10,300)) was different from that of spectinabilin (λ_{max}: 252 nm (ε 17,600), 268 nm (ε 18,200), 367 nm (ε 15,500) (Figure 2-3 and Table 2-1).

Since the ^{1}H and ^{13}C NMR spectral data of arabilin were partially similar to those of spectinabilin [43,46], structural studies of arabilin were performed by comparing with spectinabilin. The structure of arabilin was mainly determined by NMR spectral analyses as follows. The author established direct connectivity between each proton and carbon by the HMQC spectrum (Figure 2-7); the ^{1}H and ^{13}C spectral data for arabilin are shown in Table 2-2. The ^{1}H-^{1}H COSY and HMBC spectra proved that arabilin possesses a *p*-nitrophenyl group (C-16 to C-19), as does spectinabilin (Figure 2-6, 2-8, Table 2-2, and Jacobsen *et al* [46]). Arabilin's HMBC spectra (from H-1a to C-1, from H-2a to C-1, C2 and C3, from H-4a to C-3, C-4 and C-5), degrees of unsaturation, IR absorption at 1666 cm^{-1} and the chemical shift at C-1 (δ 162.1) and C-5 (δ 154.2)

indicated that C-1 and C-5 were conjugated to the same oxygen atom, and formed 2-methoxy-3,5-dimethyl-γ-pyrone moiety (C-1 to C-5) [43,45]. This finding and the difference between the UV spectrum of arabilin and that of spectinabilin imply that the tetraene moiety combined with a substituted furan moiety in spectinabilin is not preserved in arabilin. In the ^{1}H NMR spectra, one singlet methylene signal (δ_H 2.91, H-13, 2H) was observed only in arabilin (Table 2-2 and Jacobsen *et al* [46]). In the HMBC spectrum of arabilin, ^{1}H-^{13}C long-range couplings from two methyl protons (δ_H 1.73, H-12a and δ_H 1.81, H-14a) to an sp^3 carbon (δ_C 44.2, C-13) were observed (Figure 2-10), whereas no ^{1}H-^{13}C long-range coupling from the methyl proton to sp^3 carbon was observed in that of spectinabilin. In addition, ^{1}H-^{13}C long-range couplings from a methine proton (δ_H 6.48, H-8a) to a methine carbon bearing oxygen (δ_C 77.2, C-6), a methylene carbon (δ_C 35.6, C-7) and a quaternary sp^2 carbon (δ_C 114.9, C-8) indicated that C-8 and C-8a are connected by a double bond in arabilin but not in spectinabilin. Thus, the partial structures of arabilin other than a substituted γ-pyrone ring and a *p*-nitrophenyl group (C-5 ~ C-16) were also determined on the basis of ^{1}H-^{1}H COSY and HMBC analyses (Figure 2-6, 2-8, and 2-10).

The geometries of C-8/C-8a, C-9/C-10, C-11/C-12 and C-14/C-15 were determined to be *E*, *Z*, *Z* and *E* by NOE observation between H-8a (δ_H 6.48) and H-9 (δ_H 5.91), H-9 and H-10a (δ_H 1.88), H-11 (δ_H 5.99) and H-12a (δ_H 1.73), and H-13 (δ_H 2.91) and H-15 (δ_H 6.32), respectively (Figure 2-9 and 2-10). From the above findings, the planar structure of arabilin was determined as shown in Figure 2-1. Thus, it was revealed that all arabilin and its structural isomers, spectinabilin and SNF4435C, had a *p*-nitrophenyl

group and a substituted γ-pyrone ring.

The stereochemistry of arabilin at C-6 had not been determined, but Lim, H. N. *et al* assumed this to be (R) by a analogy to that of its congeners in 2011 [47].

Table 2-1. Physico-chemical properties of arabilin, spectinabilin and SNF4435C.

	arabilin	spectinabilin	SNF4435C
Appearance	Pale yellow powder	Pale yellow powder	Pale yellow powder
Molecular formula	$C_{28}H_{31}NO_6$	$C_{28}H_{31}NO_6$	$C_{28}H_{31}NO_6$
Molecular weight	477	477	477
HRESI-MS (m/z, Pos)			
Calcd.	478.2224 (as $C_{28}H_{32}NO_6$)	-	-
Found.	478.2215	-	-
Optical rotation $[\alpha]_D$	-166.2° (*c* 0.13, $CHCl_3$, 25℃)	+60.6° [c)] (*c* 5.0, $CHCl_3$, 26℃)	-105.6° [d)] (*c* 0.1, $CHCl_3$, 26℃)
IR ν_{max} cm^{-1} (KBr)	2956, 2854, 1666, 1597, 1516, 1342	1520, 1340, 1670 [c)]	2950, 2850, 1695, 1600, 1520, 1350 [d)]
UV λ_{max} nm (ε)	263 (18400), 315 (sh, 10300) (MeOH)	218 (19100), 252 (17600), 268 (18200), 367 (15500) (EtOH) [c)]	271 (19300) (MeOH) [d)]
TLC (Rf)[a)]	0.68	0.51	0.55
HPLC (Rt, min)[b)]	25.2 (85%MeOH)	23.5 (85%MeOH)	16.7 (85%MeOH)
Solubility			
Soluble	$CHCl_3$, MeOH	$CHCl_3$, MeOH	$CHCl_3$, MeOH
Insoluble	*n*-hexane, H_2O	*n*-hexane, H_2O	*n*-hexane, H_2O

[a)] Silica gel TLC (Kieselgel 60F_{254}, Merck); mobile phase, *n*-hexane-EtOAc (1:2)

[b)]Column, SunFire ODS (Waters, 5 μm, 4.6×250 mm); mobile phase, aqMeOH; flow rate, 0.7 ml/minute

[c)]Kakinuma K. *et al.*, *Tetrahedron* **32**, 217-222 (1976)

[d)]Takahashi K. *et al.*, *J. Antibiot.*, **54**, 548-553 (2001)

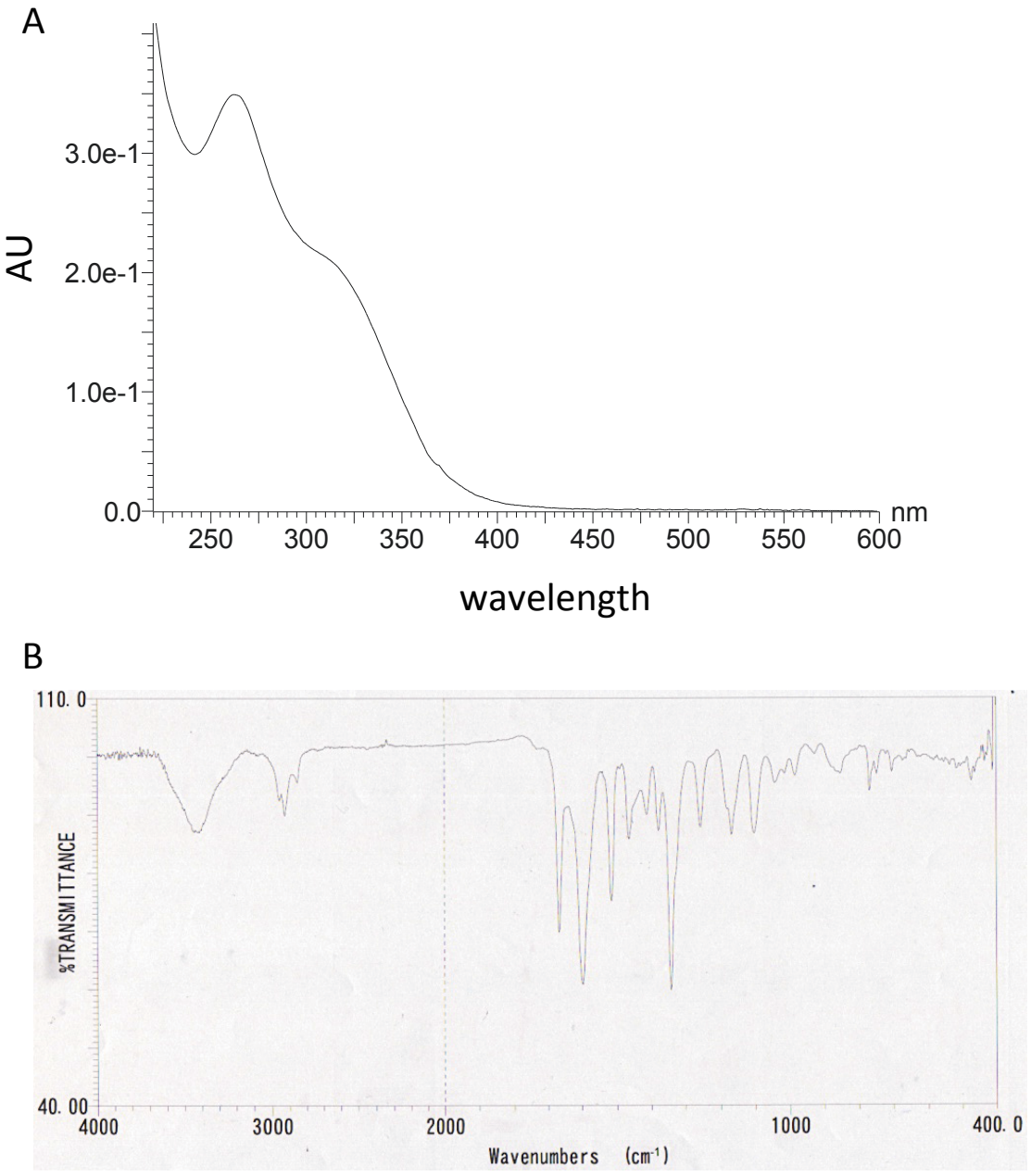

Figure 2-3. UV spectrum and IR spectrum of arabilin.

(a) UV spectrum of arabilin was measured at room temperature in MeOH.

(b) IR spectrum of arabilin was measured in a KBr disc.

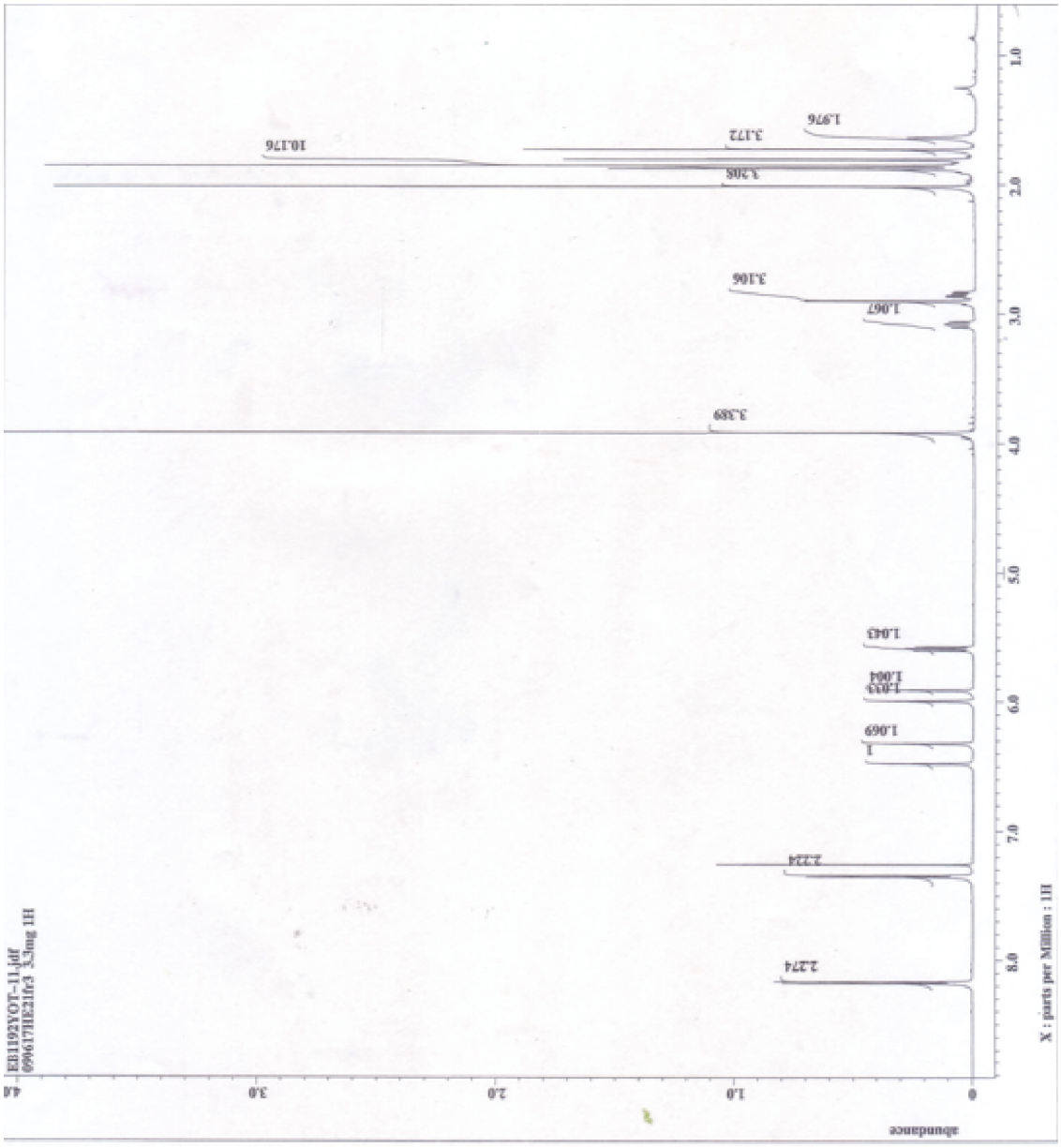

Figure 2-4. ^{1}H NMR spectrum of arabilin in $CDCl_3$ (600 MHz).

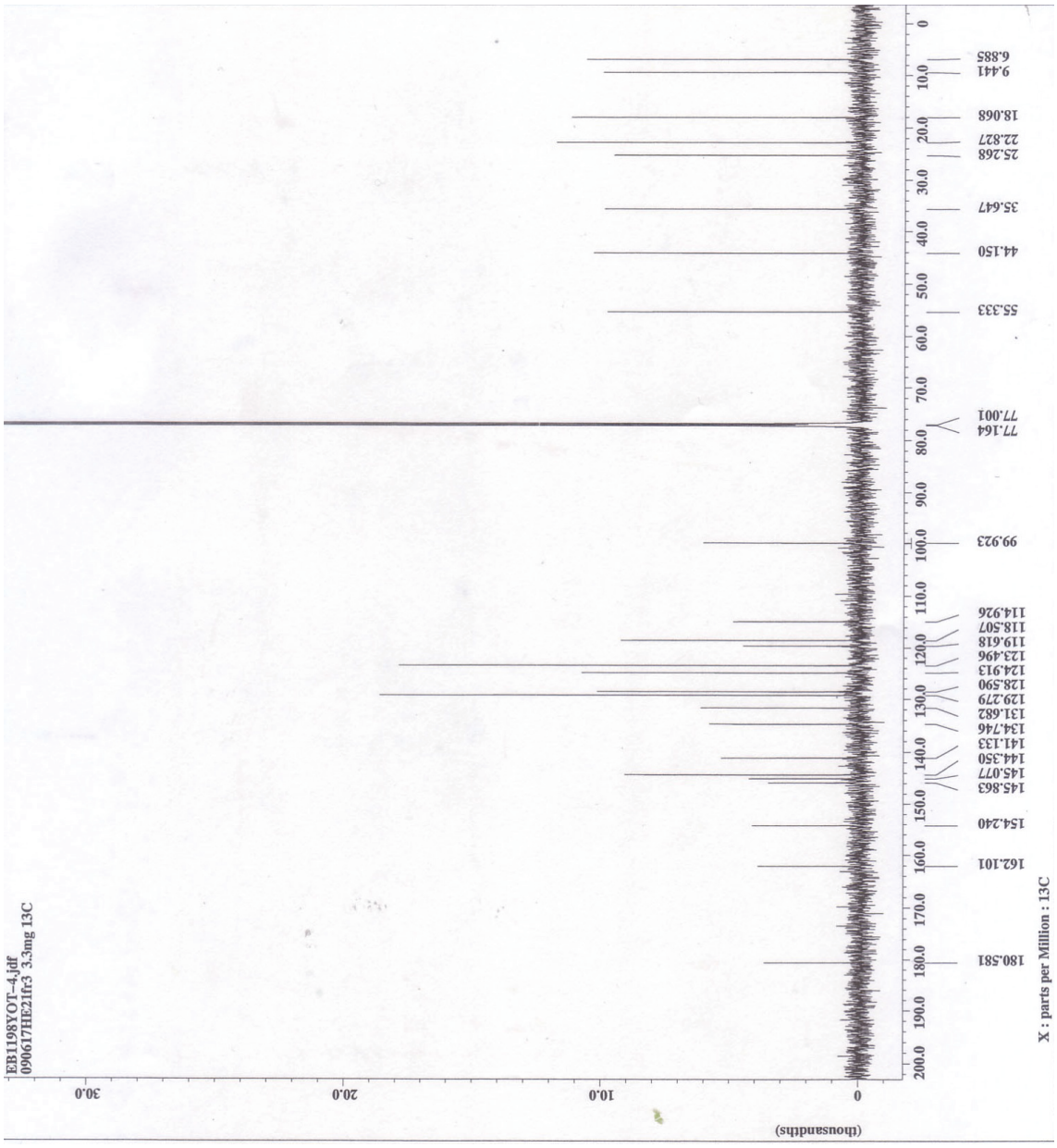

Figure 2-5. ^{13}C NMR spectrum of arabilin in $CDCl_3$ (150 MHz).

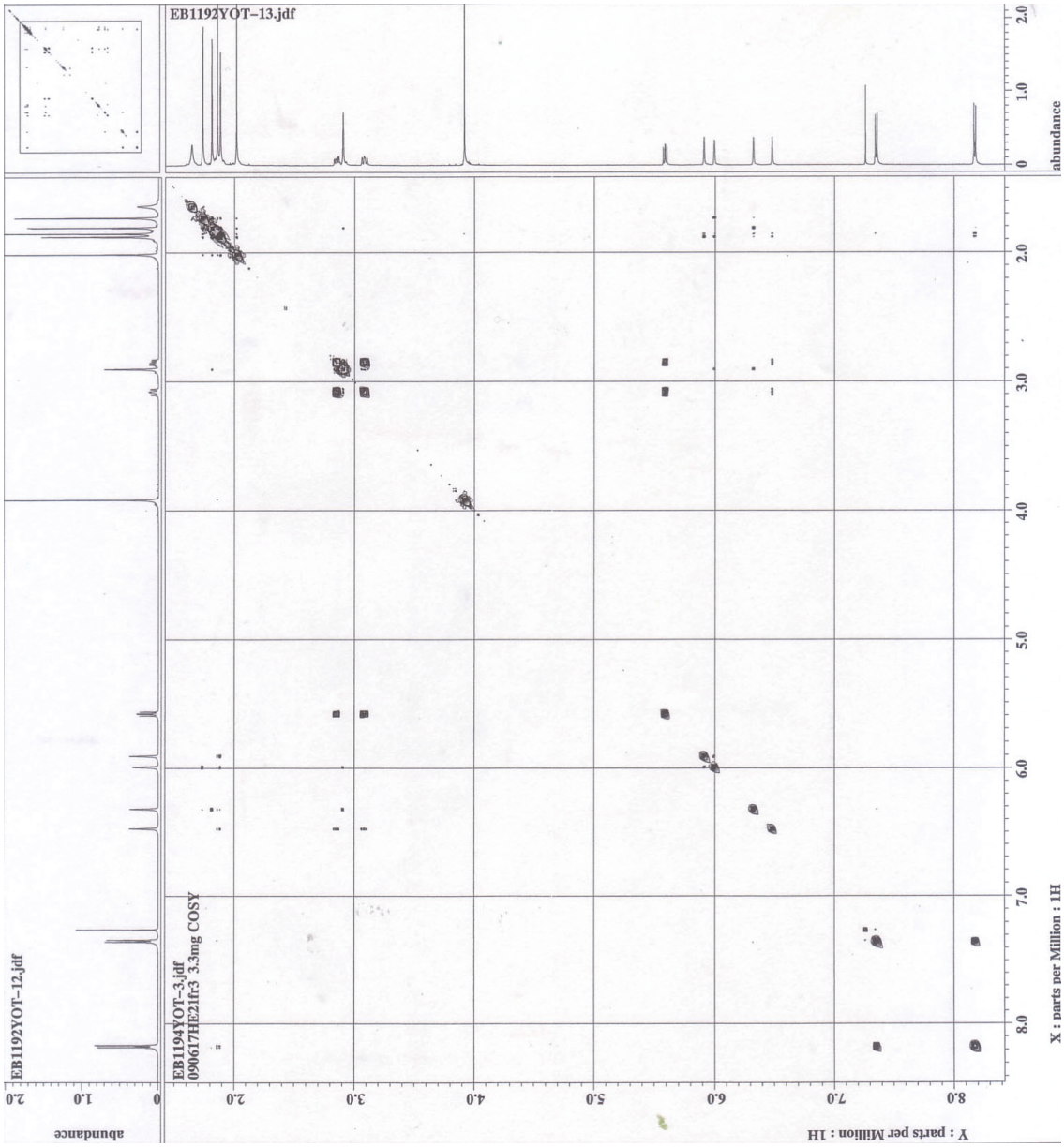

Figure 2-6. ^{1}H-^{1}H COSY spectrum of arabilin in $CDCl_3$.

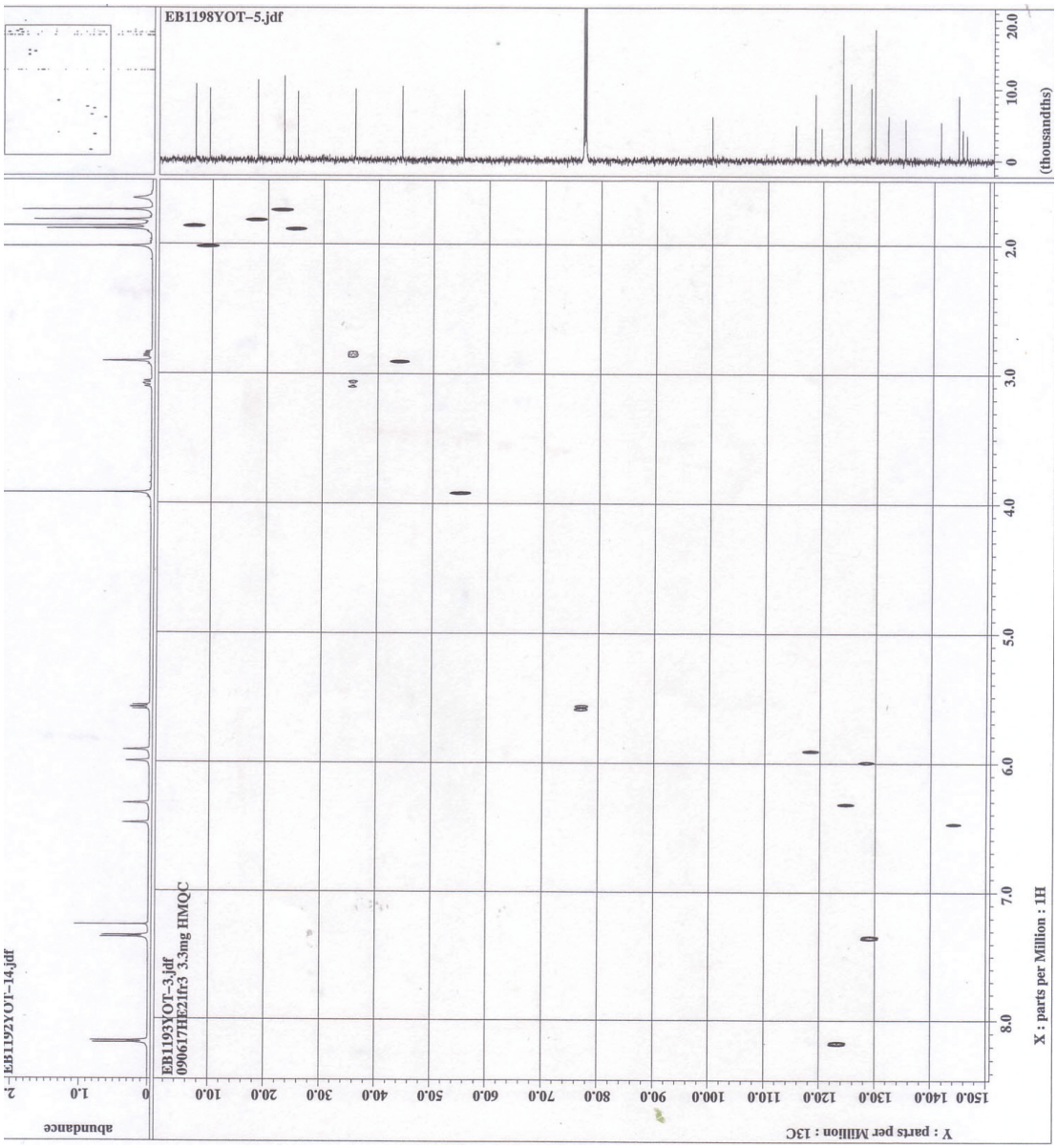

Figure 2-7. HMQC spectrum of arabilin in $CDCl_3$.

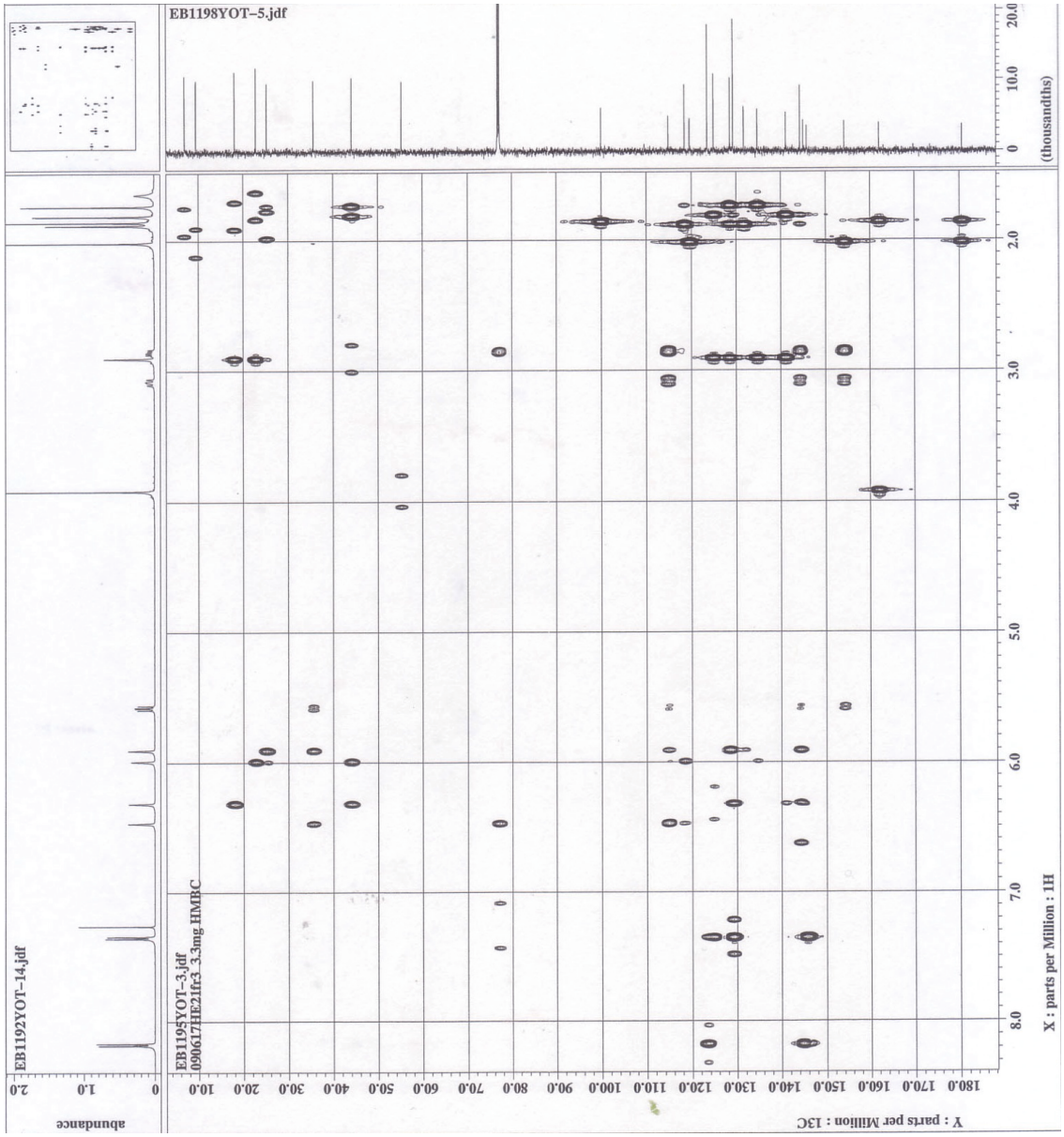

Figure 2-8. HMBC spectrum of arabilin in $CDCl_3$.

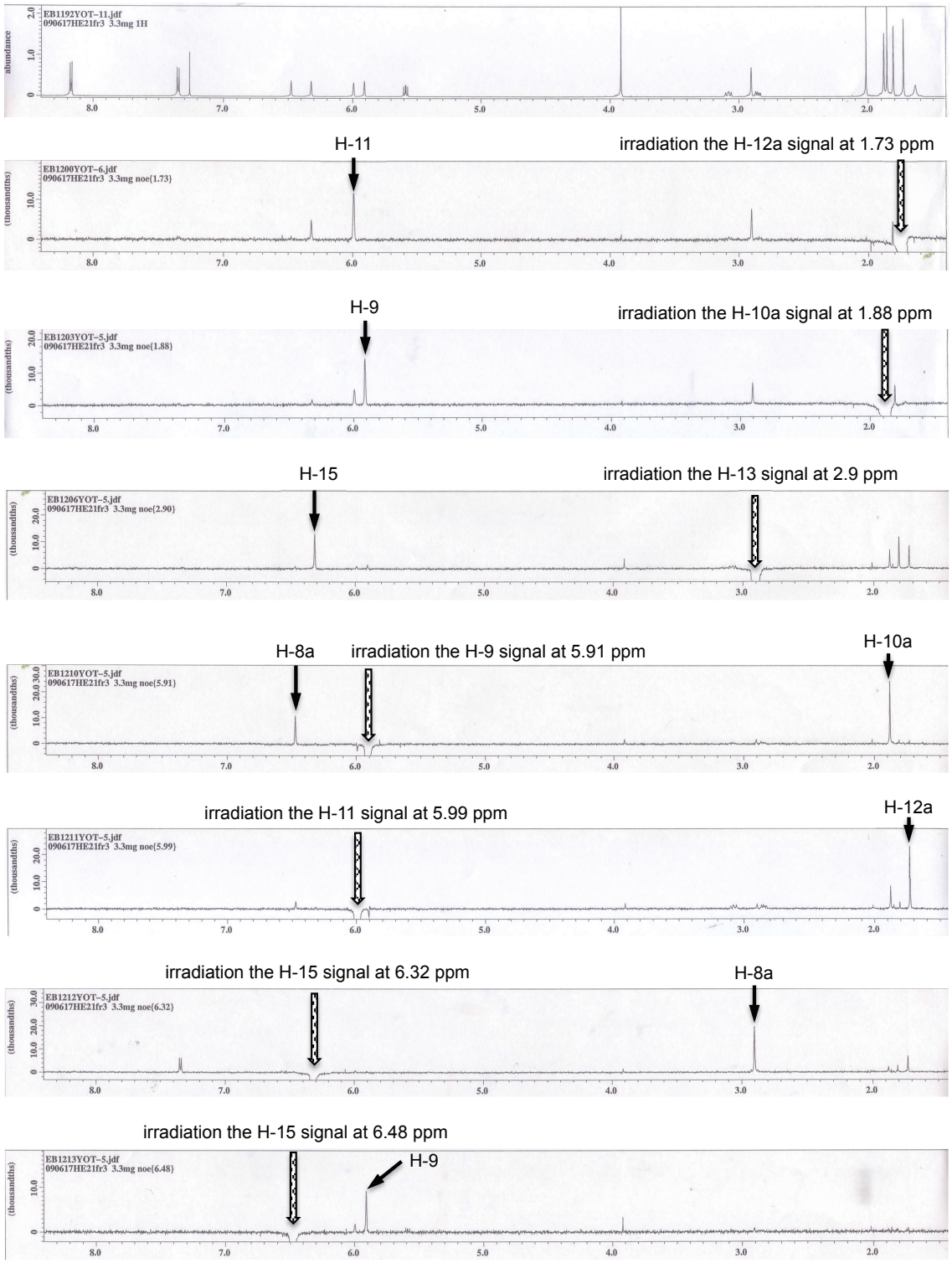

Figure 2-9. Difference NOE spectra of arabilin in $CDCl_3$.

Table 2-2. ^{13}C- and ^{1}H-NMR data for arabilin in $CDCl_3$.

No.	δc (ppm)	δ_H (ppm)
1	162.1	
1a	55.3	3.92 (3H, s)
2	99.9	
2a	6.9	1.86 (3H, s)
3	180.6	
4	119.6	
4a	9.4	2.02 (3H, s)
5	154.2	
6	77.2	5.59 (1H, dd, *J* = 7.7, 11.0 Hz)
7	35.6	2.85 (1H, dd, *J* = 7.7, 15.2 Hz) 3.08 (1H, dd, *J* = 11.0, 15.2 Hz)
8	114.9	
8a	144.4	6.48 (1H, s)
9	118.5	5.91 (1H, s)
10	131.7	
10a	25.3	1.88 (3H, bs)
11	128.6	5.99 (1H, s)
12	134.7	
12a	22.8	1.73 (3H, bd)
13	44.2	2.91 (2H, s)
14	141.1	
14a	18.1	1.81 (3H, bd)
15	124.9	6.32 (1H, s)
16	145.1	
17	129.3	7.35 (2H, d, *J* = 8.8 Hz)
18	123.5	8.17 (2H, d, *J* = 8.8 Hz)
19	145.9	

Chemical shifts in ppm from TMS as an internal standard

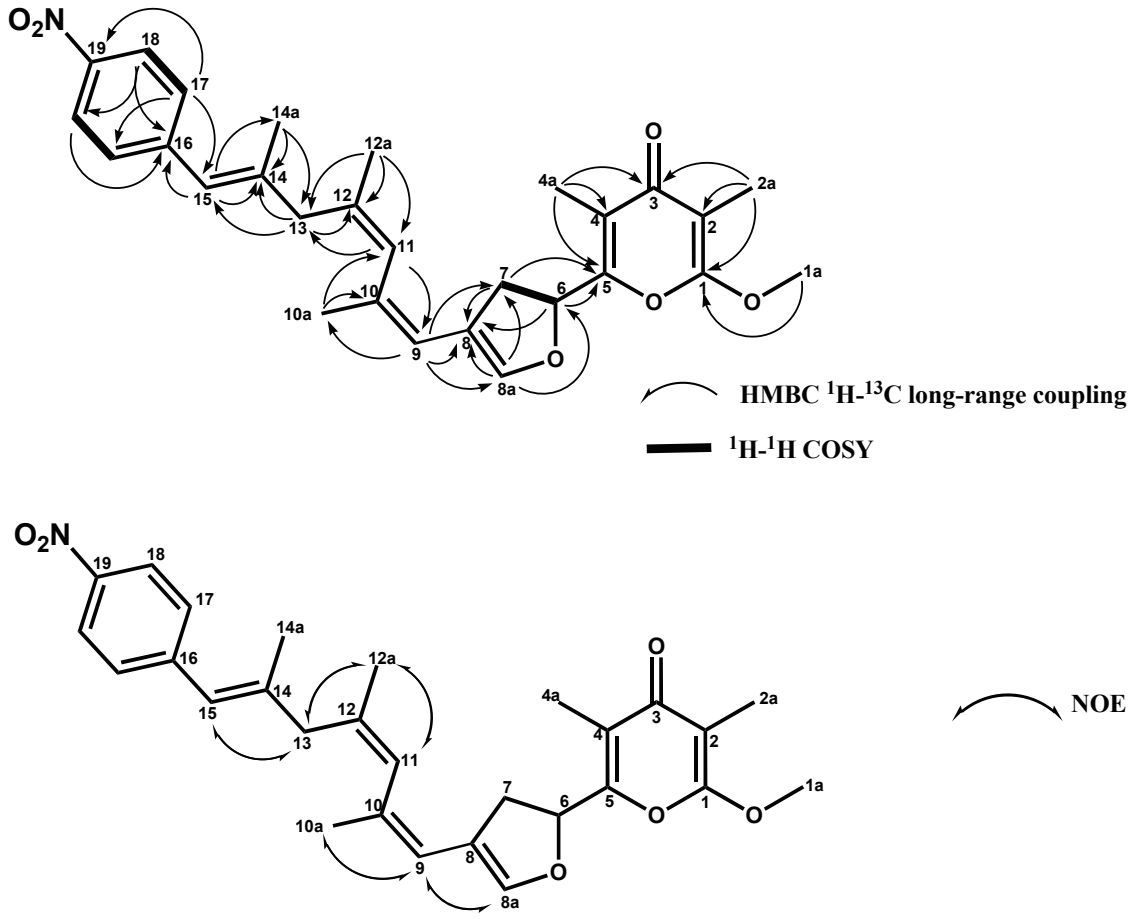

Figure 2-10. Structures of arabilin elucidated by ^{1}H-^{1}H COSY, NOE and HMBC experiments.

2-2-5. Effects of arabilin, spectinabilin and SNF4435C on binding of DHT to AR

Arabilin, spectinabilin and SNF4435C inhibited the binding of DHT to AR in a dose-dependent manner (Figure 2-11). The IC_{50} values of arabilin, spectinabilin and SNF4435C were 11 μM, 13 μM and 7 μM, respectively. Furthermore, these inhibitory activities were more potent than that of flutamide, which was clinically used for the treatment for prostatic diseases.

On the other hand, arabilin, spectinabilin and SNF4435C did not show inhibitory activity against binding of estradiol to estrogen receptor (ER) up to 100 μM (Figure 2-12). These data suggested that arabilin potent and specific blocked the binding of androgen to the ligand-binding domain of AR *in vitro*.

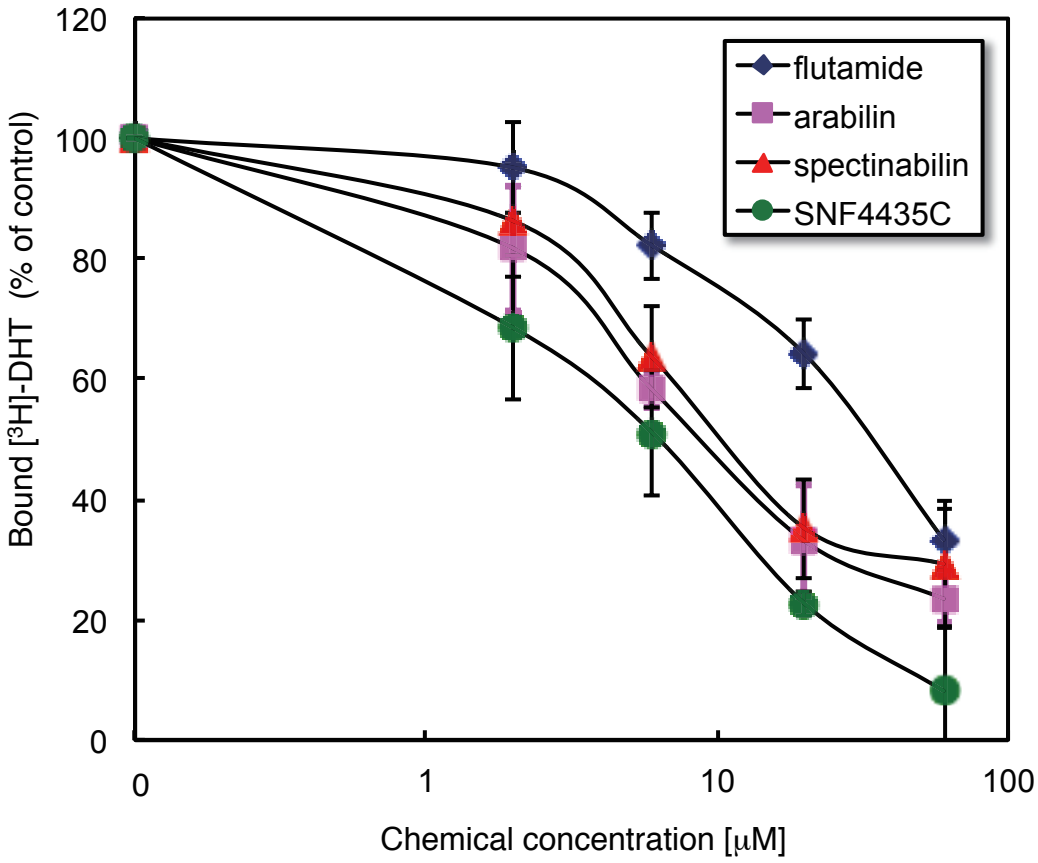

Figure 2-11. Effects of arabilin, spectinabilin, SNF4435C and flutamide on binding of DHT to AR.

Fifty μg/ml MBP-AR-LBD, 2 nM [^{3}H] DHT and the indicated concentrations of test compounds were incubated at 4°C for 3 hours. Then, the radioactivity of [^{3}H] DHT bound to MBP-AR-LBD was measured with a liquid scintillation counter.
Values are the means of four samples; bars, SD.

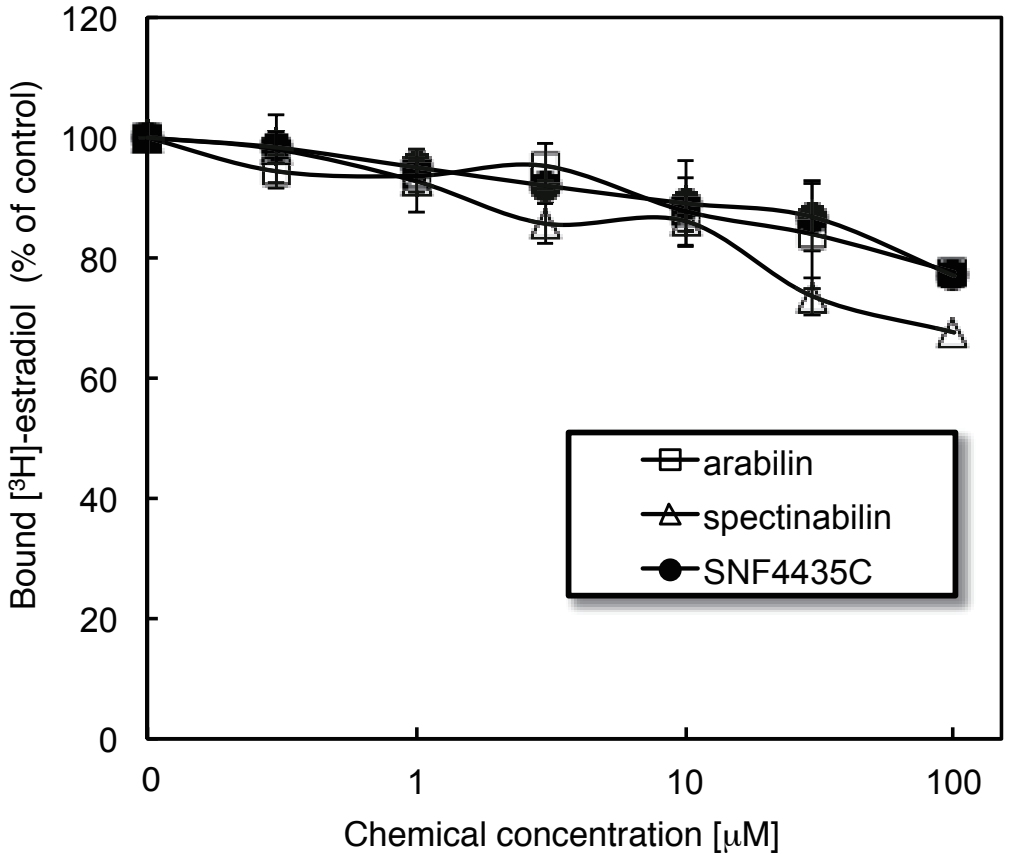

Figure 2-12. Effects of arabilin, spectinabilin, SNF4435C and flutamide on binding of estradiol to ER.

Five hundred ng/ml MBP-ER, 1 nM [^{3}H] estradiol and the indicated concentrations of test compounds were incubated at 4°C for 15 min. Then, the radioactivity of [^{3}H] estradiol bound to MBP-ER was measured with a liquid scintillation counter. Values are the means of four samples; bars, SD.

2-2-6. Effects of arabilin, spectinabilin and SNF4435C on DHT-induced PSA expression

To determine whether arabilin, spectinabilin and SNF4435C show AR antagonistic activity, the author examined the effects of these compounds on DHT-induced expression of Prostate-specific antigen (PSA) mRNA in LNCaP cells, DHT-responded prostate cancer cells. PSA is a 33-kDa serine protease, whose expression in the prostate is induced by androgen-mediated action of AR, therefore AR antagonist can suppress expression of PSA mRNA.

As shown in Figure 2-13, arabilin, spectinabilin and SNF4435C inhibited the DHT-induced expression of endogenous PSA mRNA in LNCaP cells with IC_{50} values of 210 nM, 1.75 nM and 274 nM, respectively. Although the author does not know why spectinabilin showed 100-fold potent inhibition activity of androgen-dependent PSA mRNA expression when compared with arabilin and SNF4435C, it is possibly due to the membrane-permeable ability of these compounds, or due to the difference of antagonistic mechanism by these compounds. Although there are difference in the potency of antagonism by these three compounds, these not work as AR agonist, but do as AR antagonist.

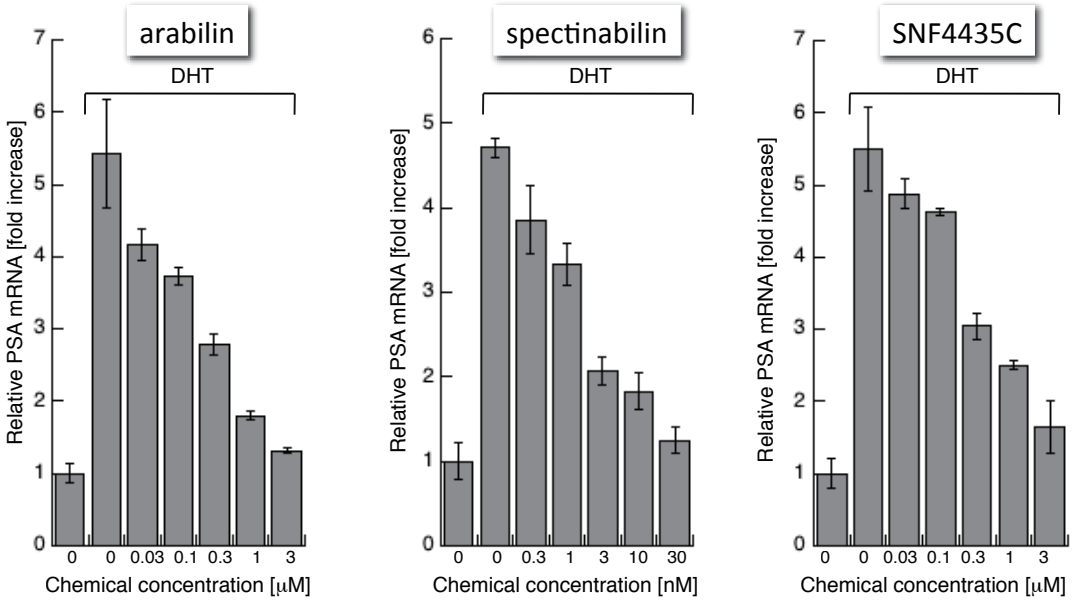

Figure 2-13. Effects of arabilin, spectinabilin and SNF4435C on DHT-induced PSA mRNA expression.

LNCaP cells were treated with 0.1 nM of DHT and the indicated concentrations of test compounds. After 12 hours, PSA mRNA were measured by real-time quantitative RT-PCR. Values are the means of triplicate samples; bars, SD.

2-2-7. Effects of arabilin, spectinabilin and SNF4435C on DHT-induced prostate cancer cell proliferation

To investigate whether arabilin, spectinabilin and SNF4435C show anti-prostate cancer activity due to AR antagonist activity, the author examined the effects of these compounds on DHT-dependent cell proliferation in LNCaP cells.

Arabilin, spectinabilin and SNF4435C effectively dose-dependent inhibited proliferation in LNCaP cells with IC_{50} values of 90 nM, 0.9 nM and 220 nM, respectively (Figure2-14). These IC_{50} values are almost similar in inhibitory activity of DHT-induced PSA expression with IC_{50} values.

On the other hand, arabilin, spectinabilin and SNF4435C did not showed that proliferation inhibitory activity even 1000 nM in PC3 cells, androgen-independent prostate cancer cells (Figure 2-15).

Therefore, arabilin, spectinabilin and SNF4435C may exert cancer cell proliferation inhibitory activity by working as AR antagonists in LNCaP cells. Thus, the author obtained a new type of AR antagonists with non-steroidal/non-anilide-type structures.

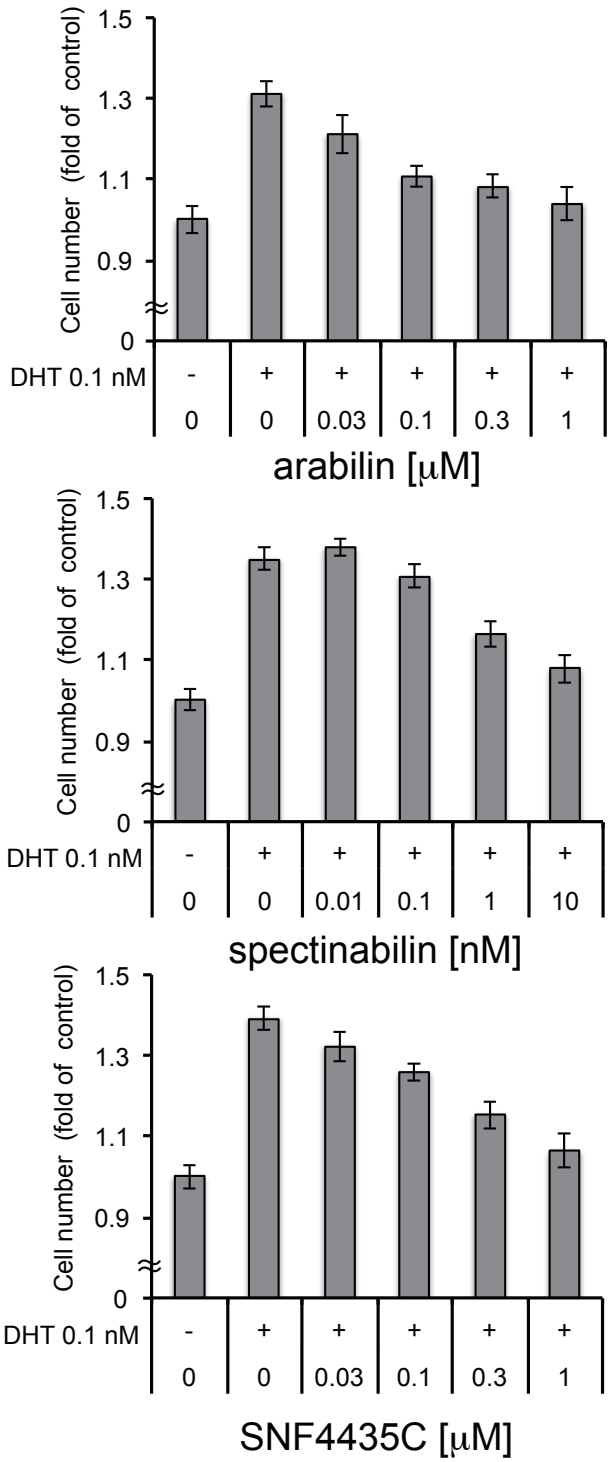

Figure 2-14. Effects of arabilin, spectinabilin and SNF4435C on DHT-dependent proliferation in LNCaP cells.

LNCaP cells were treated with 0.1 nM of DHT and the indicated concentrations of test compounds. After 72 hours, cell proliferations were measured by crystal violet staining assay. Values are the means of triplicate samples; bars, SD.

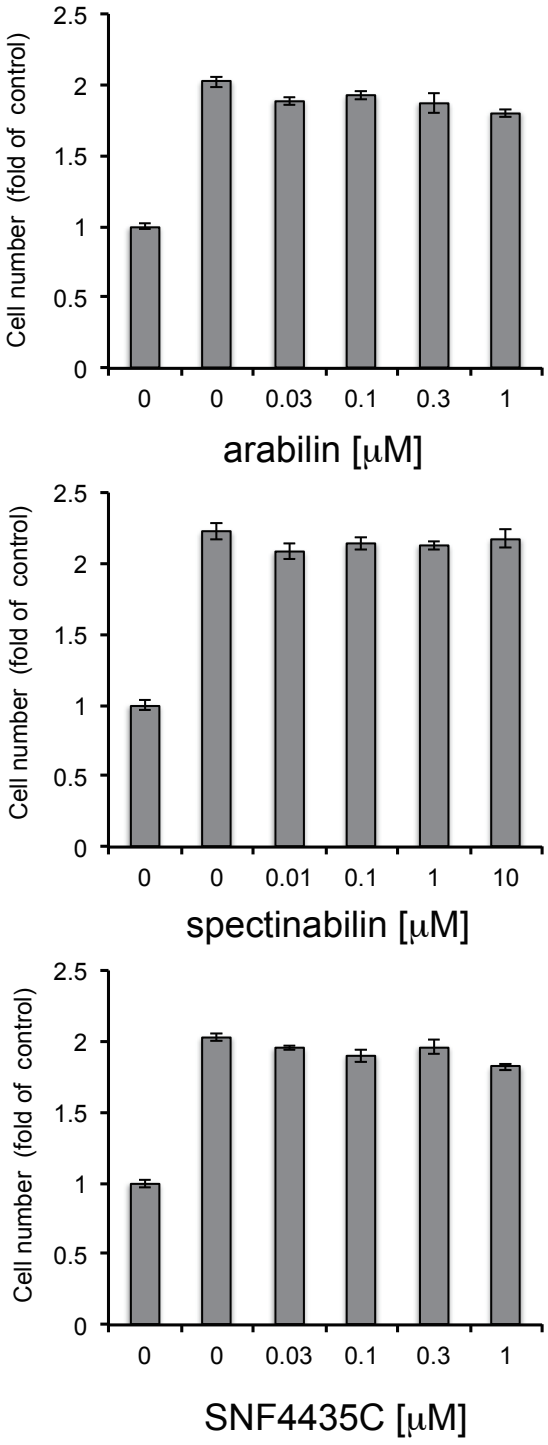

Figure 2-15. Effects of arabilin, spectinabilin and SNF4435C on DHT-independent proliferation in PC3 cells.

PC3 cells were treated with the indicated concentrations of test compounds. After 72 hours, cell proliferations were measured by crystal violet staining assay. Values are the means of triplicate samples; bars, SD.

2-3. Experimental procedures

General experimental procedures

Mass spectra were measured with a JEOL JMS-T100LC mass spectrometer. Optical rotations were made with a JASCO P-1030 polarimeter using a micro-cell (light path 100 mm). UV spectra and IR spectra were recorded on a Hitachi U-1800 spectrophotometer and a Horiba FT-210 spectrometer in KBr disc, respectively. ^{1}H and ^{13}C NMR spectra were recorded on a JEOL JNM-ECA600 spectrometer operating at 600 MHz and 150 MHz, respectively. An LC-PDA-MS system (Waters Corp., USA) with a photo diode array detector (2996) and mass analyzer (micromass ZQ) was used for analysis and preparation.

Taxonomic studies

The producing strain, MK756-CF1, was isolated from a soil sample collected in Kochi prefecture, Japan. The morphological characteristics of strain MK756-CF1 were determined on yeast-starch agar. The 16S ribosomal RNA (rRNA) gene was amplified by PCR using genomic DNA of the strain and sequenced. The most related sequences were searched using the BLAST algorithm in the DNA Data Bank of Japan (DDBJ).

Fermentation

A slant culture of arabilin producing organism was inoculated in a 500-ml baffled Erlenmeyer flask containing 110 ml of a seed medium consisting of galactose 2%,

dextrin 2%, Bacto-soytone (Difco) 1.0%, corn steep liquor (Oji Cornstarch Co. Ltd.) 0.5%, $(NH_4)_2SO_4$ 0.2% and $CaCO_3$ 0.2% in deionized water (pH7.4 before sterilization). The culture was incubated on a rotary shaker (180 rpm) at 27°C for 3 days. The seed culture (7 ml) of the strain was transferred into a 500-ml Erlenmeyer flask containing autoclaved press wheat (15 g) with deionized water (25 ml). The fermentation was carried out by a solid-state cultivation at 30°C for 14 days.

[^{3}H] DHT-AR *in vitro* binding assay

This assay was performed according to the method described previously [48]. In brief, the gene sequence corresponding to the ligand-binding domain (AR-LBD, 609–919 a.a.) in the C-terminus of AR was expressed in *E. coli* strain DH5α as a maltose-binding protein-fused protein (MBP-AR-LBD), followed by purification using amylose resin (BIO-RAD). Thus, the obtained recombinant MBP-AR-LBD (50 μg/ml), [^{3}H] dihydrotestosterone (DHT, 2 nM) and test samples were incubated at 4°C for 3 hours. Then, [^{3}H] DHT-bound MBP-AR-LBD was precipitated with hydroxyapatite and radioactivity was measured with a liquid scintillation counter.

[^{3}H] estradiol-ER *in vitro* binding assay

The gene sequence corresponding to the ligand-binding domain (ER-LBD, 301–551 a.a.) of ER was expressed in *E. coli* strain DH5α as a maltose-binding protein-fused protein (MBP-ER-LBD), followed by purification using amylose resin (BIO-RAD). Thus, the obtained recombinant MBP-ER-LBD (0.5 μg/ml), [^{3}H] estradiol (1 nM) and

test samples were incubated at 4°C for 15 min. Then, [^{3}H] estradiol-bound MBP-ER-LBD was precipitated with hydroxyapatite and radioactivity was measured with a liquid scintillation counter.

Detection of PSA mRNA by real-time RT-PCR

LNCaP cells were incubated in RPMI 1640 medium supplemented with 2% charcoal-stripped serum for 24 hours. The cells were then treated with DHT (0.1 nM) and test compounds. After 12 hours, RNA from the cells was isolated, and the expression of PSA genes was determined by real-time quantitative reverse transcription-PCR (RT-PCR), and normalized to GAPDH mRNA. The primer sequences used were as follows: for PSA, 5'-AGG TCG GAG TCA ACG GAT TT-3' (forward) and 5'-TAG TTG AGG TCA ATG AAG GG-3' (reverse); for GAPDH, 5'-GGT CCT CAC AGC TGC CCA TC-3' (forward) and 5'-CAG CCT GAG GCG TAG CAG GT-3' (reverse).

Evaluation of DHT-dependent cell proliferation by crystal violet staining assay

LNCaP cells were plated at a density of 1 x 10^4 cells per 48-well dish, and incubated in RPMI 1640 medium supplemented with 2% charcoal-stripped serum for 24 hours. The cells were then treated with DHT (0.1 nM) and test compounds. After 72 hours, cell were fixed with 3% paraformaldehyde, washed with PBS, and then stained with 0.1% crystal violet solution (Wako Pure Chemical Industries, Ltd., Japan). Stained-cells were wash with water, and then solubilized with 1 M citric acid (Kanto Chemical Co., Japan)

buffer. The solution was transfer 96-well plate and monitored spectrophotometrically by measuring absorbance at 570 nm.

Evaluation of DHT-independent cell proliferation by crystal violet staining assay

PC3 cells were plated at a density of 0.5 x 10^4 cells per 48-well dish, and incubated in RPMI 1640 medium supplemented with 2% charcoal-stripped serum for 24 hours. The cells were then treated with test compounds. The method of crystal violet staining assay is as above.

Chapter 3

Identification of licopyranocoumarin and glycyrurol from herbal medicines as neuroprotective compounds for Parkinson's disease treatment

3-1. Introduction

Mitochondrial dysfunction, including impediment of the mitochondrial electron transport chain mainly relying on complex I activity, has been implicated in Parkinson's disease (PD). For instance, postmortem brains, skeletal muscle and platelets of PD patients have been found in disorder of mitochondrial complex I [49,50,51,52,53] and cybrid cells containing mitochondrial DNA (mtDNA) derived from PD platelets have indicated complex I defects [54,55]. Furthermore, mitochondria complex I inhibitors such as rotenone (Figure 1-5), MPTP (Figure 1-5), and its toxic metabolite MPP^+ (Figure 1-5) have been shown to induce disorder of movement associated with selective loss of dopaminergic neurons on various rodents, therefore they have been widely used as acquired PD-like models [56,57,58,59,60,61].

Some candidate compounds of treatment for PD have been found using by these models. Selegiline (Figure 3-1), a medication widely used at present, has been revealed the capacity to protect dopamine neurons by inhibiting MAO-B oxidation for conversion of MPTP into MPP^+ and blocking the formation of free radicals derived from the oxidative metabolism of dopamine [62,63]. MPP^+ models also have found that unexploited therapeutic potential for some atypical antipsychotics (olanzapine, aripiprazole, and ziprasidone) and the anticonvulsant zonisamide in PD, and new mechanisms of neuroprotective activity of FLZ (which activates HSP27/HSP70) and paeoniflorin (which modulates autophagy) have led to treatments for PD (Figure 3-1) [64,65,66,67].

Herbal medicines are used to treat PD in ancient medical systems in Asian countries such as India, China, Japan, and Korea based on anecdotal and experience-based theories [68]. The traditional herbal medicines *yi-gan san* and *modified yeoldahanso-tang* have neuroprotective effects and can rescue dopaminergic neurons from MPP^+/MPTP-induced toxicity using both *in vitro* and *in vivo* methods [69,70]. Several compounds derived from herbal medicines also exert anti-Parkinsonian activities. For instance, ginsenoside Rb1 isolated from *Panax ginseng C. A. Meyer,* 3-*O*-demethylswertipunicoside isolated from *S. punicea* and salidroside isolated from *Rhodiola rosea L.* have been reported to attenuate MPP^+-induced neurotoxicity in PC12 cells *in vitro* (Figure 3-2) [71,72,73]. However, clinical evidence for the efficacy and safety of these herbal medicines for PD is insufficient [74].

Therefore, in this study, we screened a library containing 128 traditional herbal medicines, which have been used clinically for at least 10 years in Japan (especially called *kanpo* in Japan), focusing on their neuroprotective activity using PD-like cellular models. As a result, the author found the anti-Parkinsonian herbal medicines *choi-joki-to* and *daio-kanzo-to*. Moreover, the author identified licopyranocoumarin (LPC) and glycyrurol (GCR) derived from the genus *Glycyrrhiza* as the potent neuroprotective agents against MPP^+-induced toxicity.

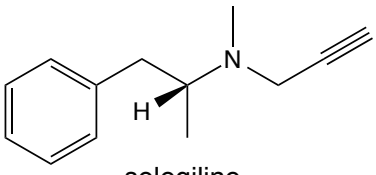

selegiline

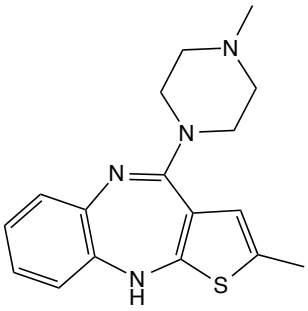

olanzapine

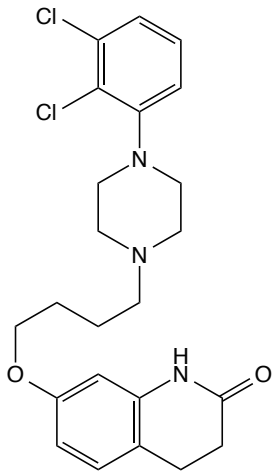

aripiprazole

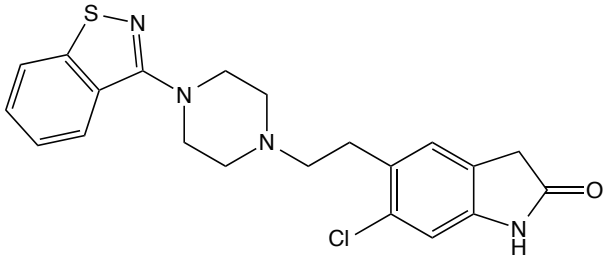

ziprasidone

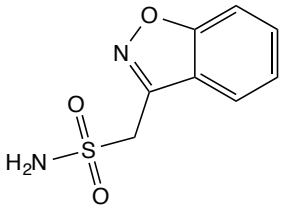

zonisamide

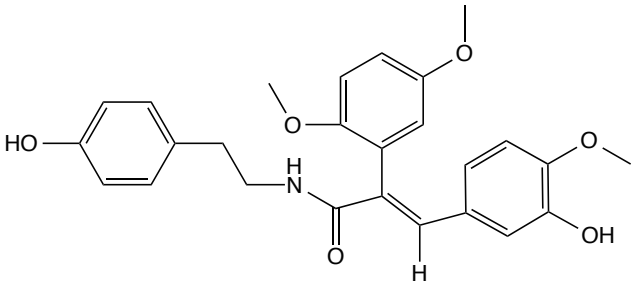

FLZ

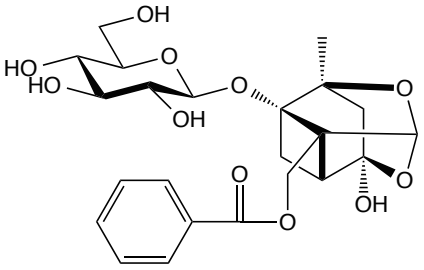

paeoniflorin

Figure 3-1. Structures of candidate compounds for treatment of PD.

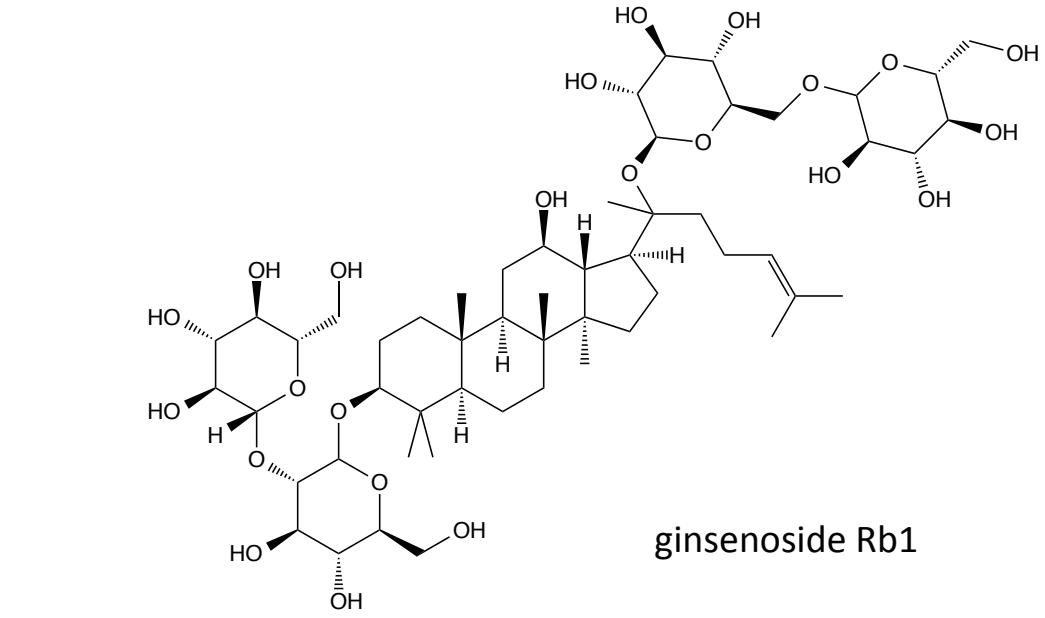

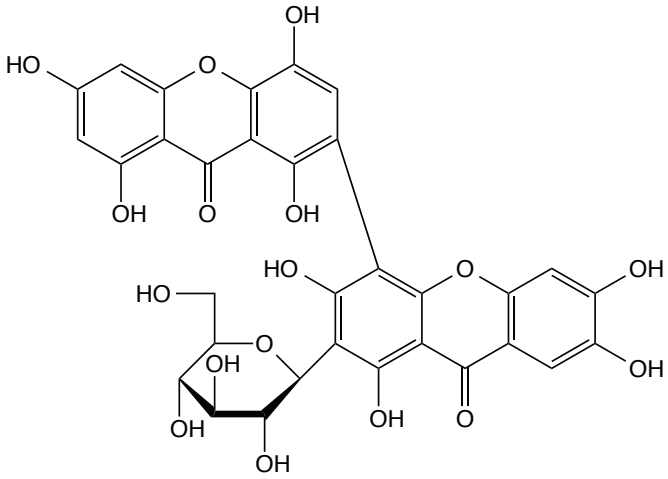

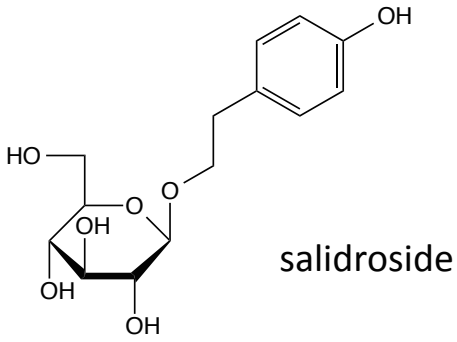

Figure 3-2. Structures of candidate compounds for treatment of PD derived from herbal medicine.

3-2. Result

3-2-1. Identification of *choi-joki-to* and *daio-kanzo-to* as potent neuroprotective herbal medicines using PD-like model screening

Rotenone, a direct inhibitor of mitochondria complex I, is usually used to mimic Parkinsonism *in vitro* and *in vivo* [75]. Treatment of NGF-differentiated PC12D cells with 0.3 μM of rotenone for 48 hours lead to salient cell death as evaluated by the trypan blue dye exclusion assay. Using this PD-like cellular model, the author screened a library containing 128 traditional herbal medicines, which have been used clinically in Japan, paying attention on preventive effects against rotenone-induced cell death of NGF-differentiated PC12D cells.

As a result, several ethyl acetate (EtOAc) extracts of herbal medicines showed prevention against rotenone-induced cell death generally, but two traditional herbal medicines, *choi-joki-to* and *daio-kanzo-to* exerted significant neuroprotective effects against rotenone-induced neurotoxicity (Figure 3-3A). Furthermore, the EtOAc extracts of *choi-joki-to* or *daio-kanzo-to* also gave dose-dependent protection from neuronal cell death induced by MPP^+, another well-known neurotoxicity for cellular model of PD (Figure 3-3B).

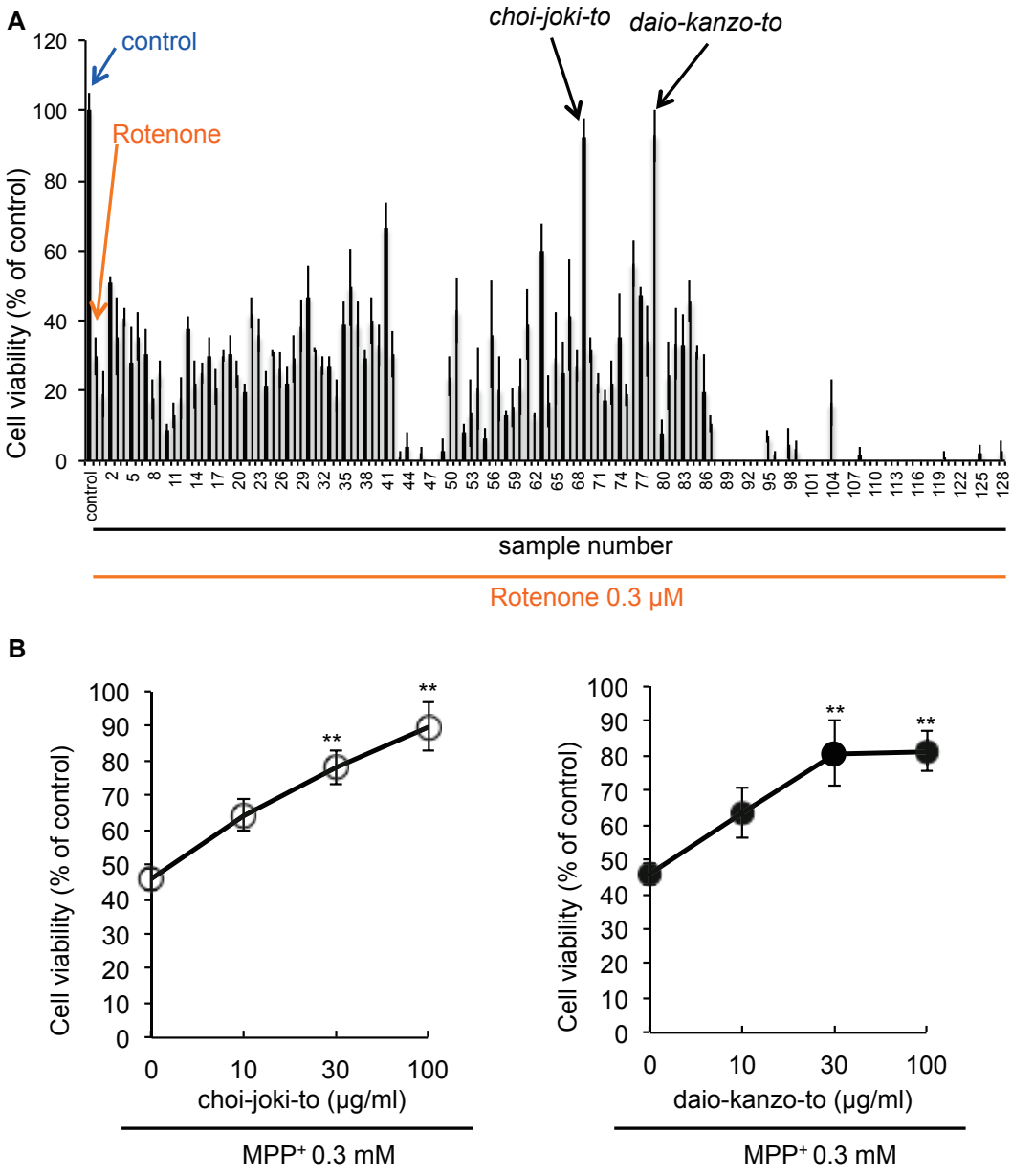

Figure 3-3. Two herbal medicines, *Daio-kanzo-to* and *Choi-joki-to*, identified as neuroprotective agents in the course of screening.

(**A**) NGF-differentiated PC12D cells were treated with 0.3 μM rotenone and herbal medicine extract for 48 hours. Cell viability was evaluated by trypan blue dye exclusion assay. (**B**) NGF-differentiated PC12D cells were treated with various concentrations of *choi-joki-to* or *daio-kanzo-to* in the presence of 0.3 mM MPP^+ for 48 hours. Cell viability was evaluated by trypan blue dye exclusion assay. Values are the means of triplicate samples; bars, s.d. $^{**}p<0.01$ compared with MPP^+ group cells.

3-2-2. LPC and GCR isolated from *Glycyrrhiza* as potent neuroprotective compounds

Next, the author attempted to identify the major compounds responsible for neuroprotective effects contained in *choi-joki-to* and *daio-kanzo-to*. First, the author noted that both *choi-joki-to* and *daio-kanzo-to* commonly contain rhubarb and *Glycyrrhiza* species, at the ratio of 2:1 (Table 3-1): therefore, the author analyzed whether this 2:1 ratio of rhubarb to *Glycyrrhiza* is important for neuroprotective effects against MPP^+-induced toxicity. As shown in Figure 3-4, rhubarb and *Glycyrrhiza* contained in *choi-joki-to* and *daio-kanzo-to* at 2:1 is not a particular ratio necessary for neuroprotective effects, but rather increased *Glycyrrhiza* content potentiated the neuroprotective effects against MPP^+-induced cell death.

Thus, the author tried to isolate the active principle responsible for neuroprotective effects from EtOAc extract of *Glycyrrhiza* by monitoring the neuroprotective activity against MPP^+-induced cell death in PC12D cells using a trypan blue dye exclusion assay. As a result, the author isolated two compounds from *Glycyrrhiza* powder as potent neuroprotective agents, and identified these two compounds as LPC and GCR by NMR analysis, respectively (Figure 3-5~3-9, 3-10A, B).

Both LPC and GCR markedly prevented MPP^+-induced cell death in a dose-dependent manner with IC_{50} values of 0.9 μM and 1.2 μM, respectively (Figure 3-10C). Furthermore, both LPC and GCR did not show cytoprotective effects against other toxins, such as taxol and cisplatin (CDDP) even at 3 μM concentration, which

significantly suppressed MPP^+-induced cell death in PC12D cells. Therefore, cytoprotective effects of LPC and GCR may specific for mitochondrial toxins (Figure 3-11).

To further confirm the neuroprotective effects of LPC and GCR against MPP^+-induced cell death, PC12D cells were labeled with propidium iodide (PI) and histogram analysis-related nuclear DNA contents were verified by flow cytometry. By the treatment of PC12D cells with 0.3 mM of MPP^+, NGF-differentiated PC12D cells with DNA content below G1 phase levels (defined as hypodiploid sub-G1 peak) were distinguishable in the population as compared with control levels (49.63 ± 6.41% versus 7.23 ± 1.04% of cells in sub-G1, respectively) (Figure 3-12A, B). LPC or GCR alone did not indicate any effects on the overall population of cells. However, they decreased the percentage of MPP^+-induced cell death by 11.2–29.0% and 11.4–28.0% (values are the mean of average of three data), respectively (Figure 3-12A, B). These result indicated that LPC and GCR certainly exert neuroprotective activity against MPP^+-induced cell death.

Table 3-1. Crude drugs constituents of *"choi-joki-to"* and *"daio-kanzo-to".*

Choui-jyouki-to		Daio-kanzo-to	
scientific names	contents(g)	scientific names	contents(g)
rhubarb	2	rhubarb	4
glycyrrhiza	1	glycyrrhiza	2
salt cake	0.5		

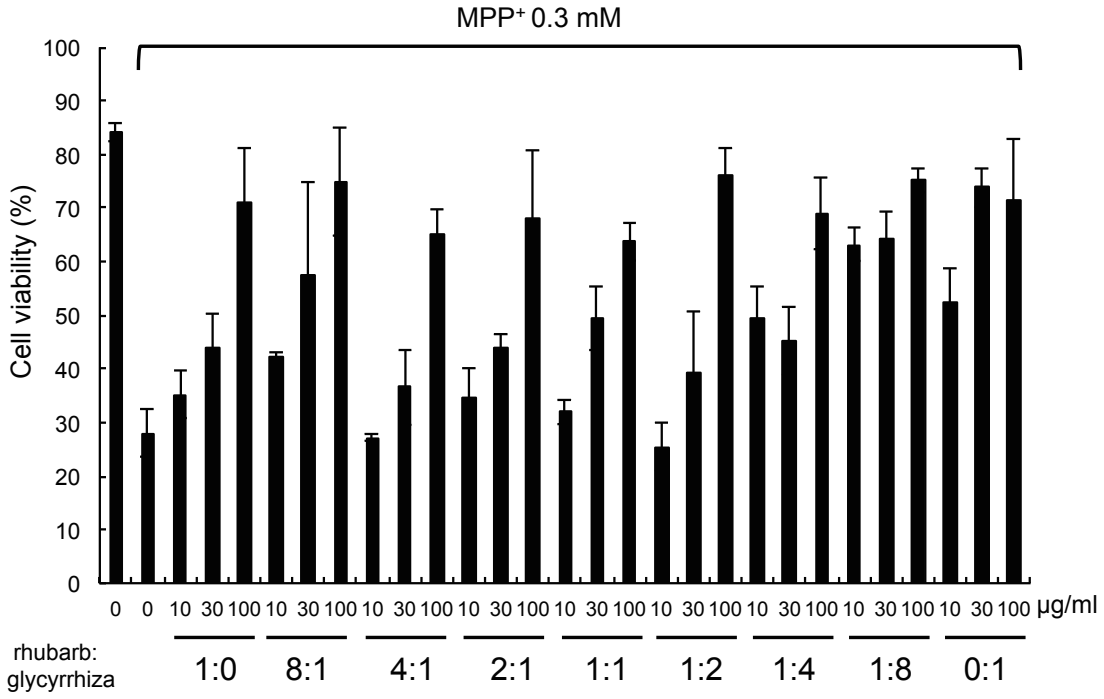

Figure 3-4. *Glycyrrhiza* prevented MPP^+-induced cell death more potently than rhubarb.

NGF-differentiated PC12D cells were treated with various concentrations of rhubarb and *Glycyrrhiza* (rhubarb:*Glycyrrhiza* ratio = 1:0, 8:1, 4:1, 2:1, 1:1, 1:2, 1:4, 1:8, 0:1) in the presence of 0.3 mM MPP^+ for 48 hours. Cell viability was evaluated by trypan blue exclusion assay. Values are the means of three independent experiments; bars, s.d.
$^{**}p<0.01$ compared with MPP^+ group cells.

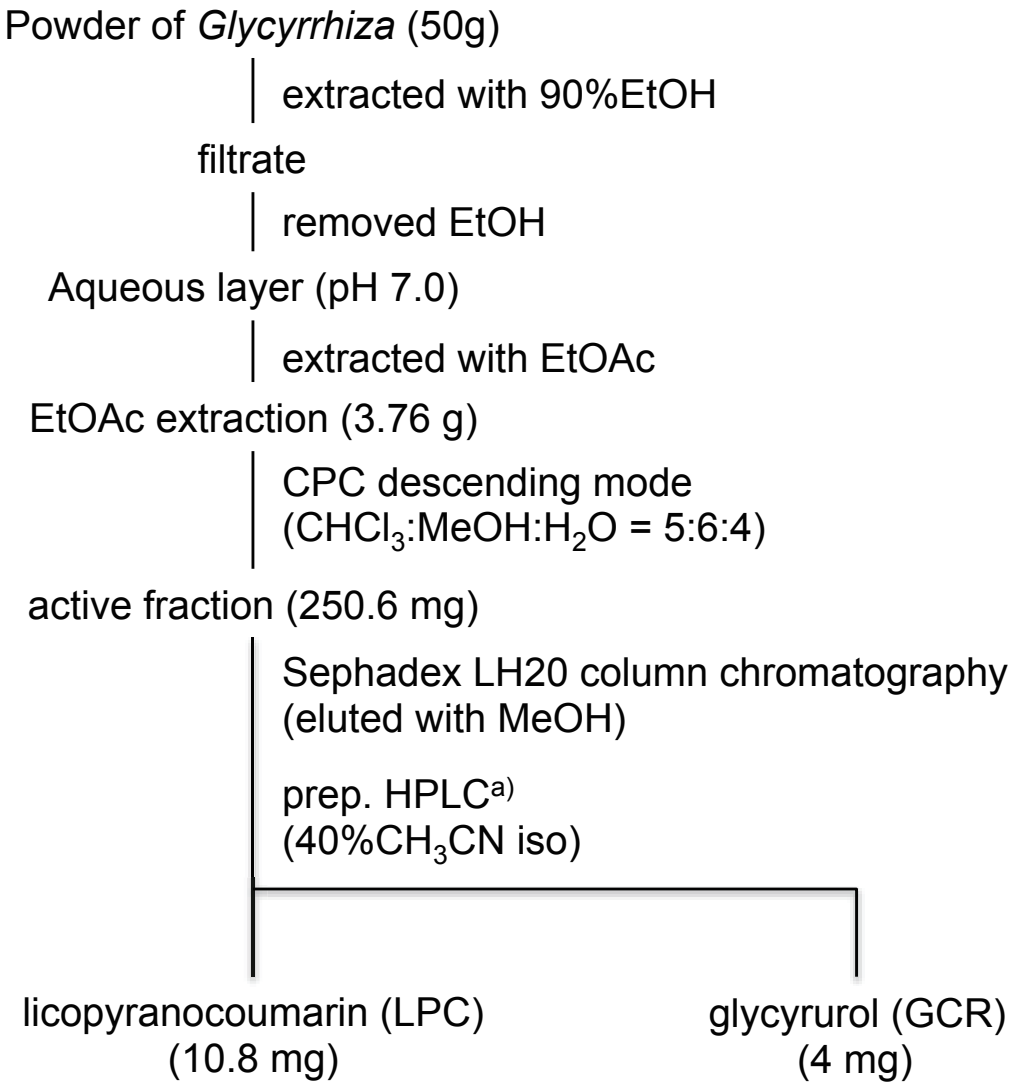

a) YMC-Pack ODS-AQ, YMC Co. Ltd., Japan, 10ml/minutes

Figure 3-5. Isolation procedure of LPC and GCR from *Glycyrrhiza.*

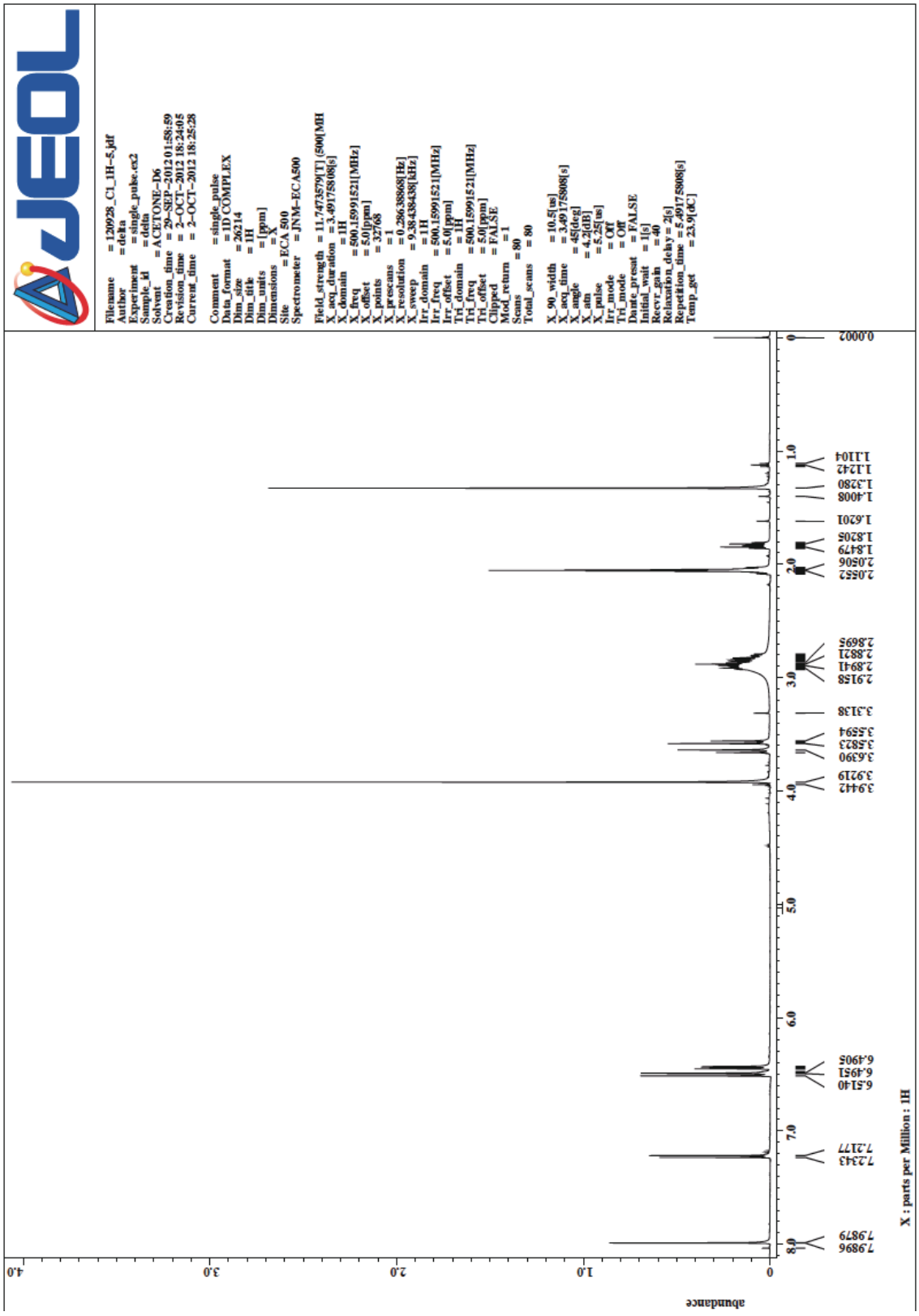

Figure 3-6. ^{1}H NMR spectrum of LPC in acetone-d$_6$ (500 MHz).

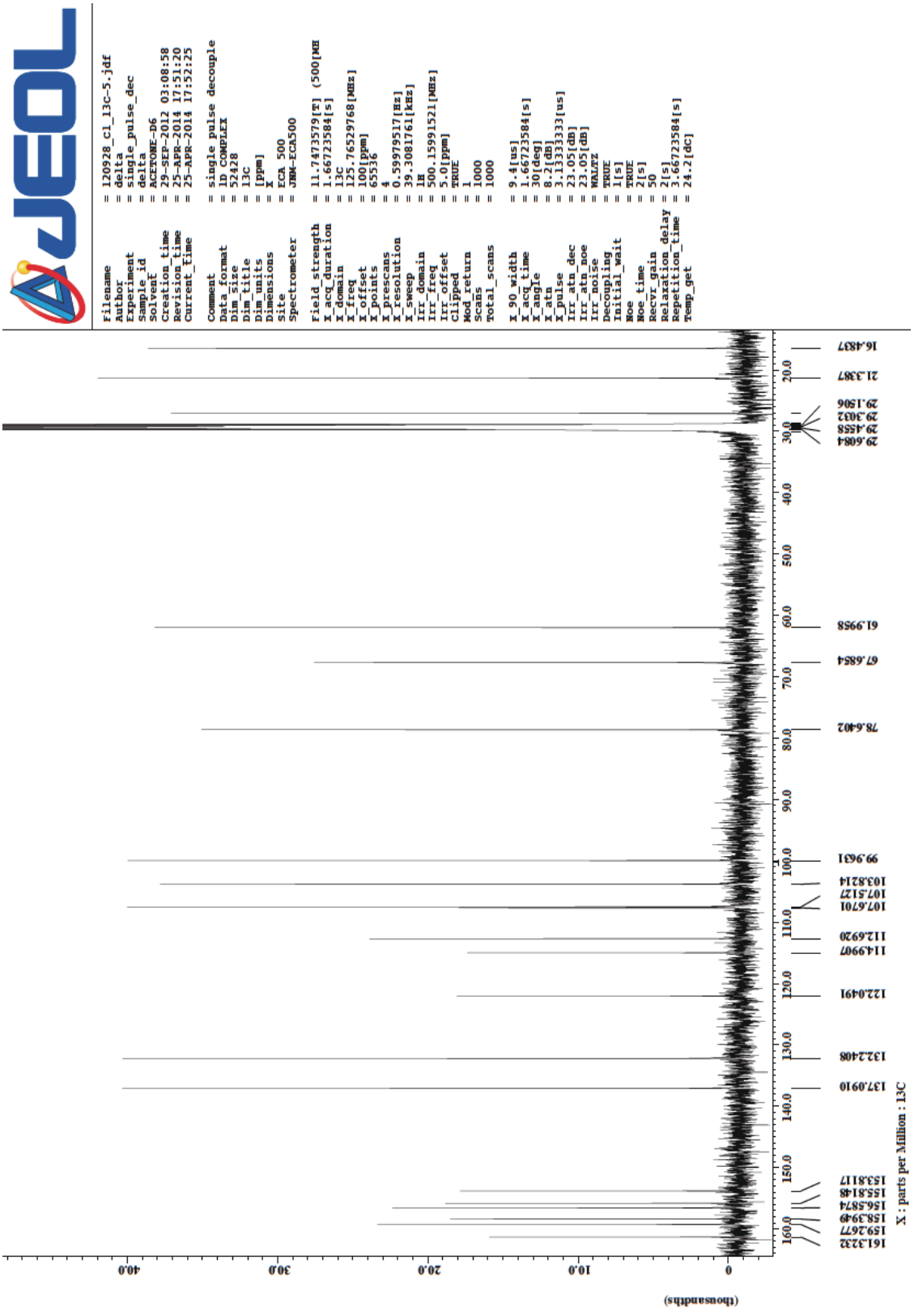

Figure 3-7. ^{13}C NMR spectrum of LPC in acetone-d$_6$ (500 MHz).

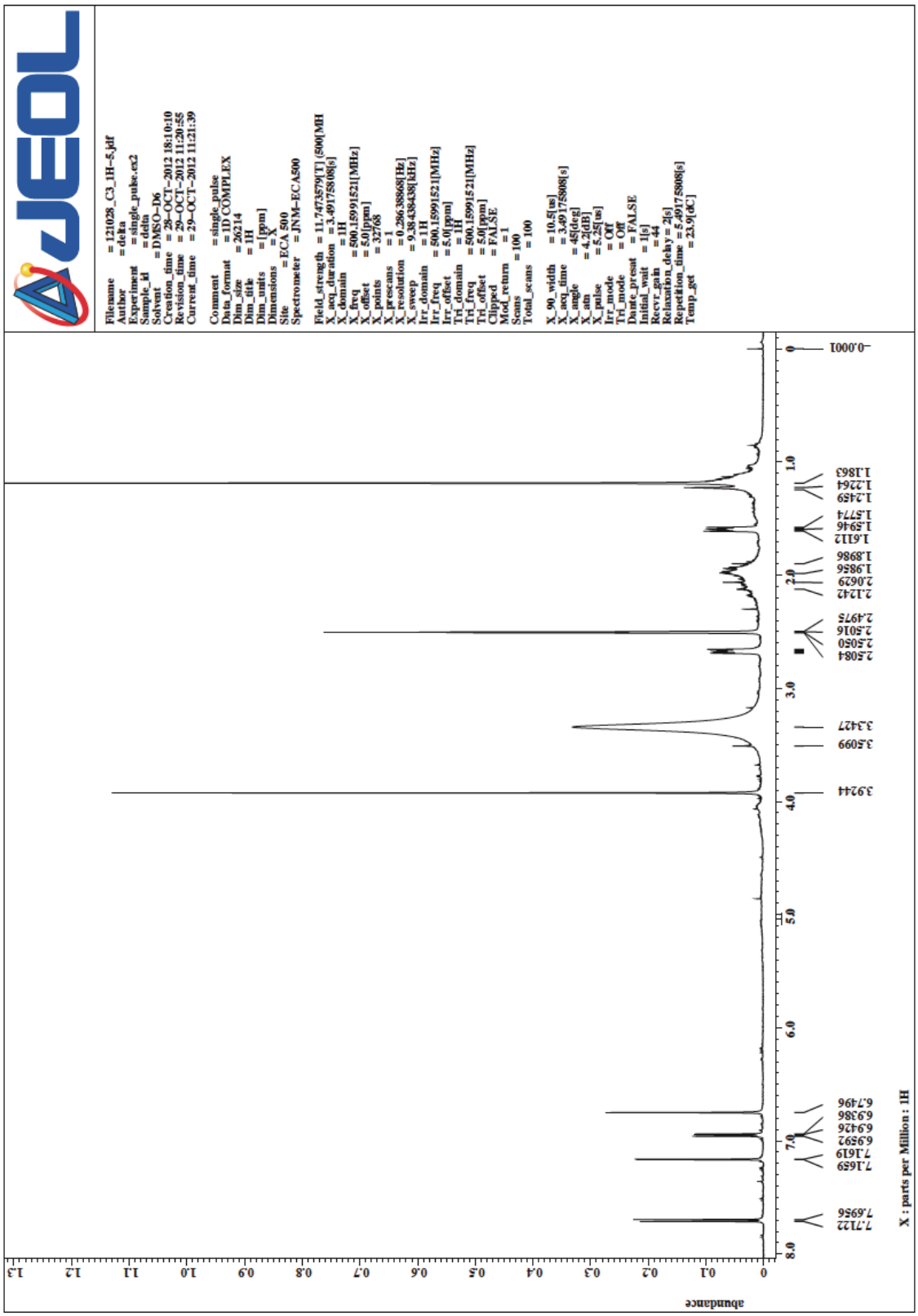

Figure 3-8. ^{1}H NMR spectrum of GCR in DMSO-d_6 (500 MHz).

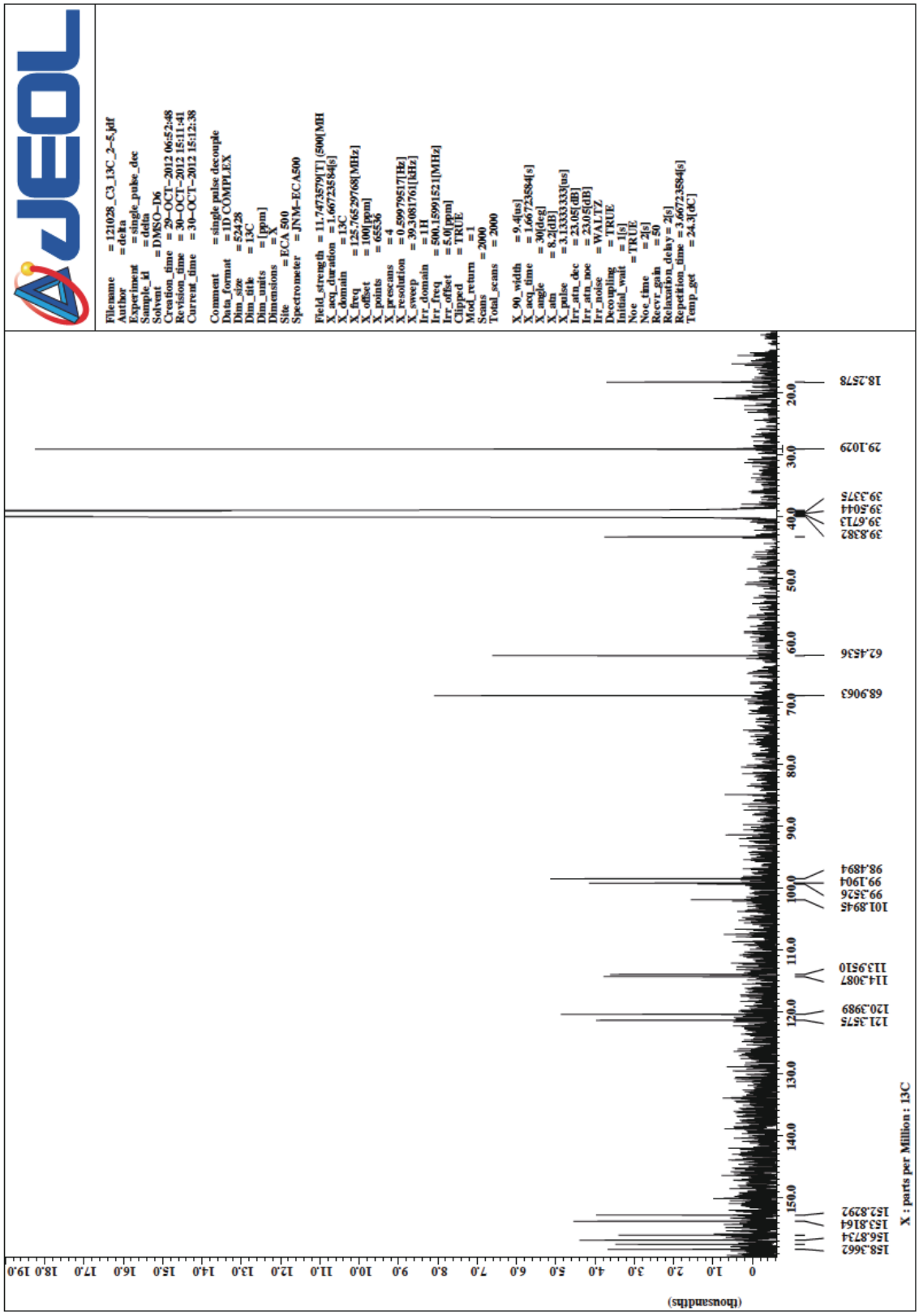

Figure 3-9. ^{13}C NMR spectrum of GCR in DMSO-d_6 (500 MHz).

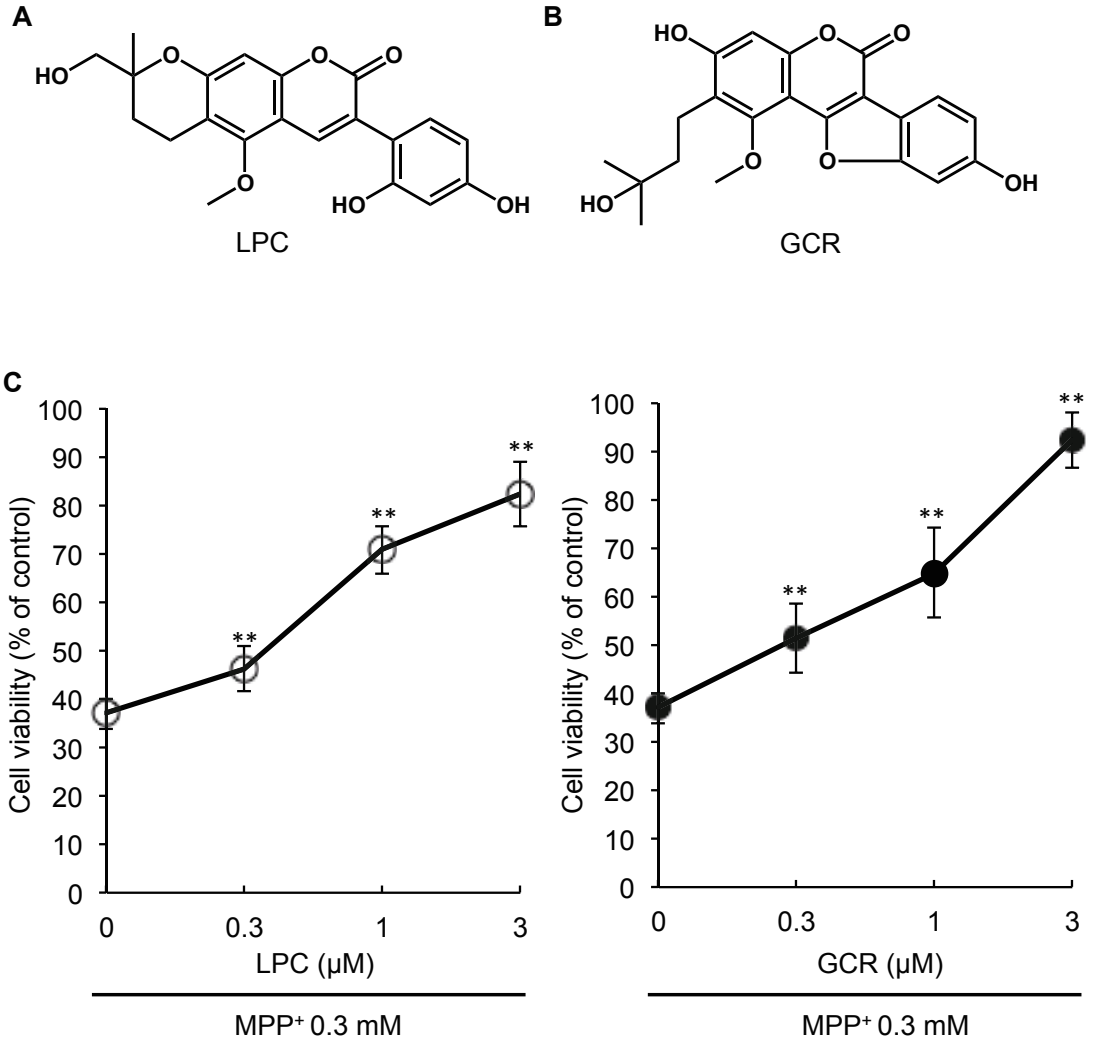

Figure 3-10. LPC and GCR prevented MPP^+-induced cell death.

Structures of (**A**) LPC and (**B**) GCR. (**C**) NGF-differentiated PC12D cells were treated with various concentrations of LPC or GCR in the presence of 0.3 mM MPP^+ for 48 hours. Cell viability was evaluated by trypan blue dye exclusion assay. Values are the means of three independent experiments; bars, s.d. $^{**}p<0.01$ compared with MPP^+ group cells.

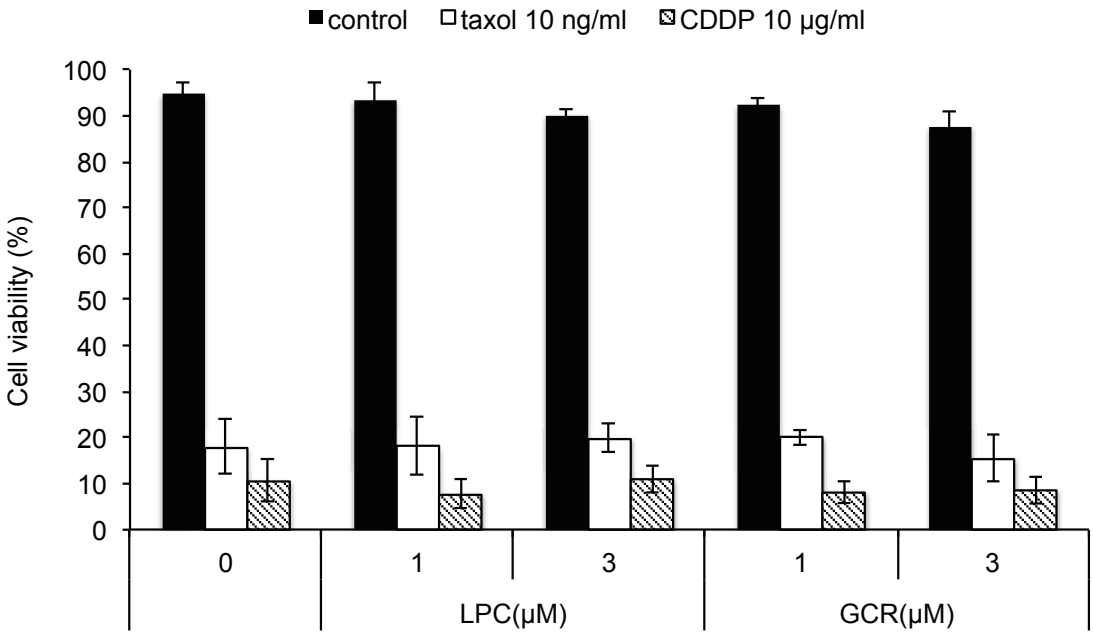

Figure 3-11. LPC and GCR did not show cytoprotective effect against other toxins in PC12D cells.

PC12D cells were treated with various concentration of LPC or GCR in the presence of 10 ng/ml taxol or 10 μg/ml cisplatin (CDDP) for 48 hours.

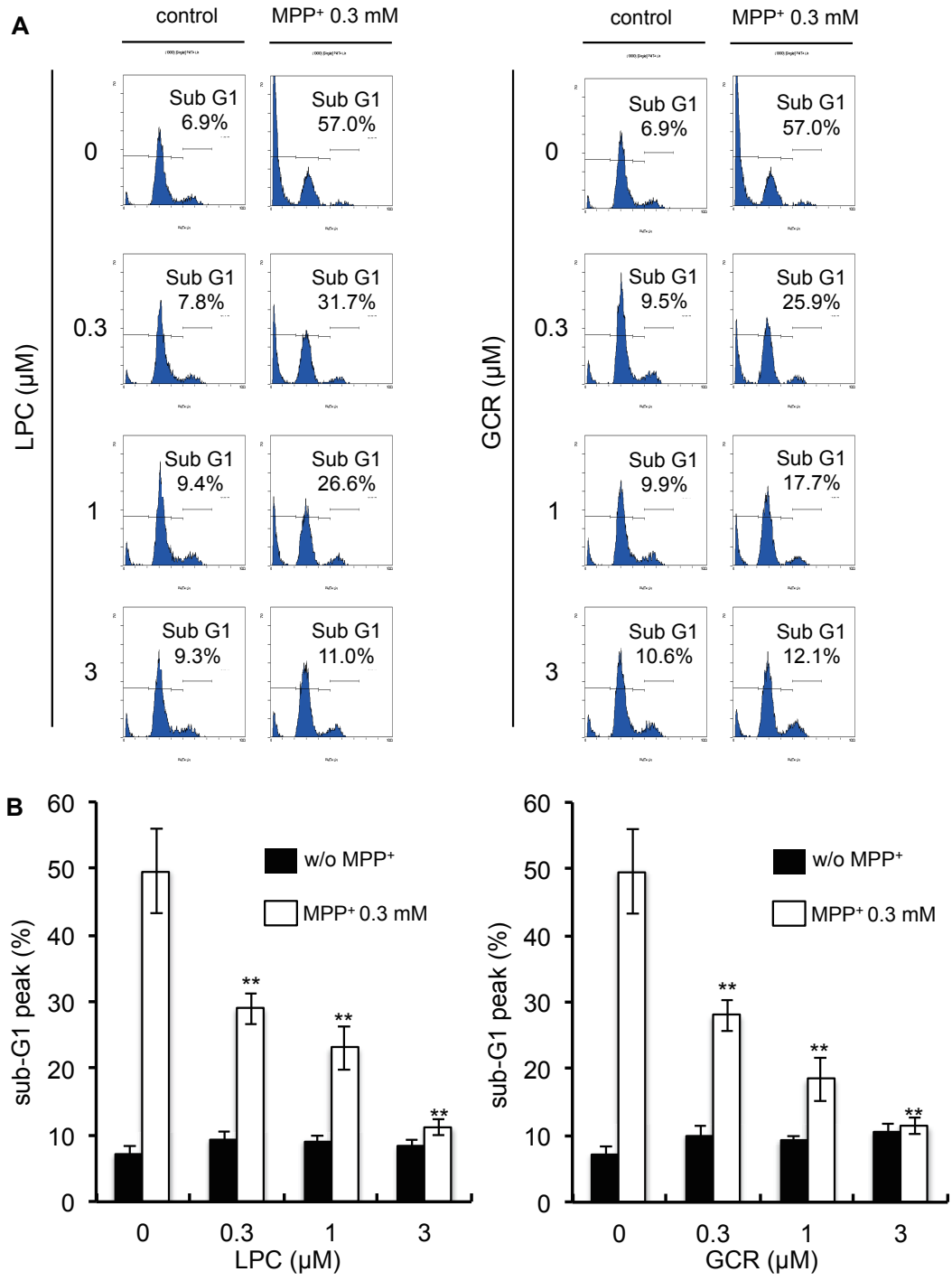

Figure 3-12. LPC and GCR attenuated MPP$^+$-induced apoptosis.

(**A**) NGF-differentiated PC12D cells were treated with various concentrations of LPC or GCR in the presence of 0.3 mM MPP$^+$ for 48 hours. Collected cells were stained with PI and analyzed by flow cytometry. (**B**) The sub-G1 ratio was analyzed. Values are the means of three independent experiments; bars, s.d. $^{**}p<0.01$ compared with MPP$^+$ group cells.

3-2-3. LPC and GCR attenuate the MPP^+-induced decrease in mitochondrial membrane potential

MPP^+ is a well-known inhibitor of mitochondria complex I and induces mitochondrial dysfunction. Because LPC or GCR suppressed MPP^+-induced cell death, the author next investigated the effect of LPC and GCR on MPP^+-mediated loss of mitochondrial membrane potential ($\Delta\Psi_{mit}$) using JC-1 dyes. As shown in Figure 3-13, by the treatment of differentiated PC12D cells with 0.3 mM of MPP^+ for 48 hours, $\Delta\Psi_{mit}$ was decreased to 45–50% with reduction of JC-1 aggregate fluorescence. However, significant increase in $\Delta\Psi_{mit}$ was observed following cotreatment with LPC and GCR. These results suggested that LPC and GCR each inhibit MPP^+-induced decrease of $\Delta\Psi_{mit}$.

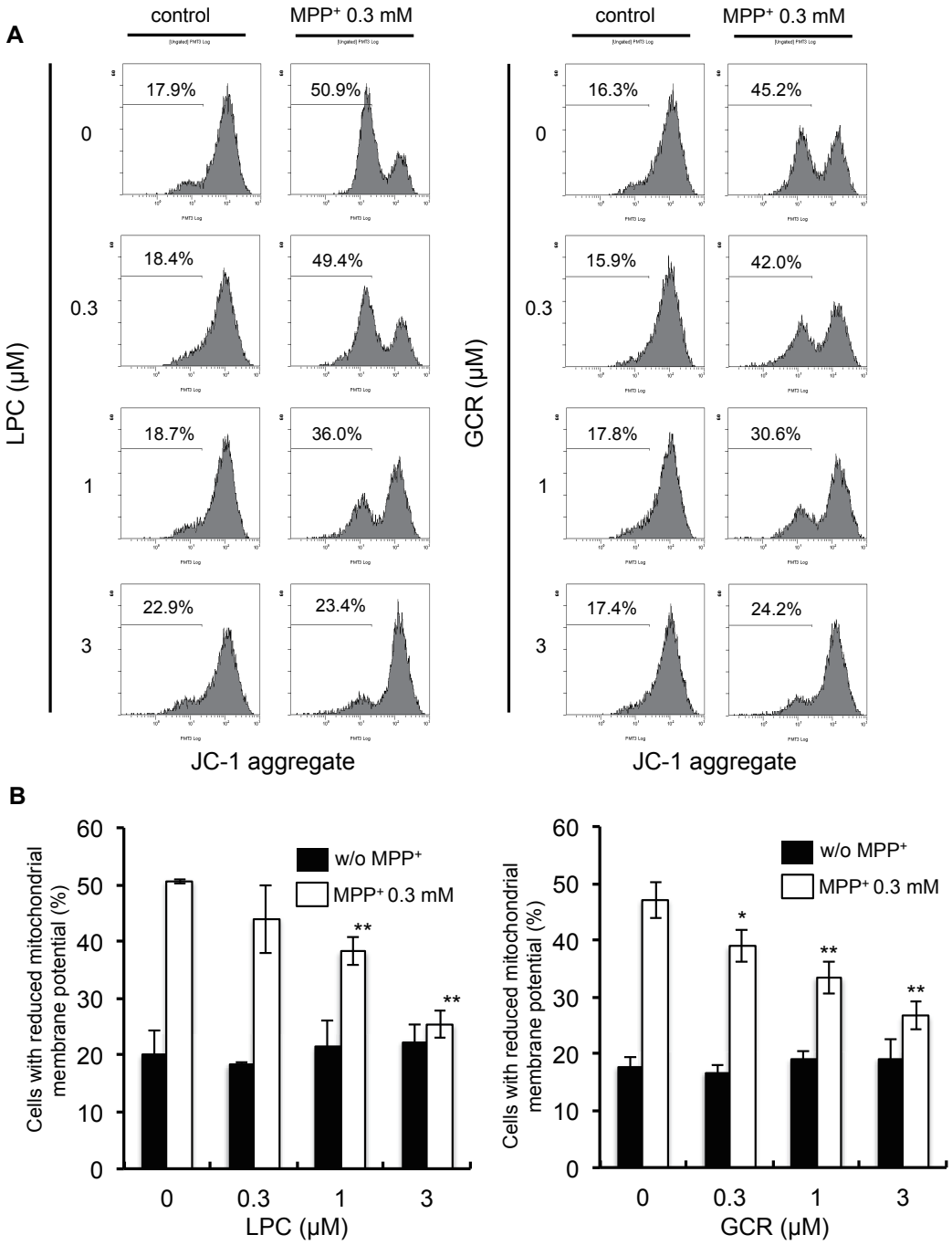

Figure 3-13. LPC and GCR protected cells against MPP^+-induced disappearance of mitochondrial membrane potential.

(**A**) NGF-differentiated PC12D cells were treated with various concentrations of LPC or GCR in the presence of 0.3 mM MPP^+ for 48 hours. Collected cells were stained with JC-1 and analyzed by flow cytometry. (**B**) The ratio of cells exhibiting disappearance of mitochondrial membrane potential was analyzed. Values are the means of three independent experiments; bars, s.d. $^{*}p<0.05$, $^{**}p<0.01$ compared with MPP^+ group cells.

3-2-4. LPC and GCR counteract MPP^+-induced ROS production

MPP^+ has been extensively reported to evoke generation of reactive oxygen species (ROS). Therefore the author examined the effect of LPC and GCR on MPP^+-mediated ROS generation. As shown in Figure 3-14, cytofluorometric histograms of NGF-differentiated PC12D cells after 12 hours of treatment with 0.3 mM MPP^+ upon staining with CMH_2DCFDA. ROS levels were significantly increased from 100 ± 7.8% (control level) to 247 ± 14.9% ($p<0.001$). However, the generation of intracellular ROS was reduced to 164 ± 15.7% ($p<0.01$) and 153 ± 13.0% ($p<0.01$) by the addition of 3 μM LPC and 3 μM GCR, respectively. These data suggested that LPC and GCR inhibit MPP^+-induced intracellular ROS generation.

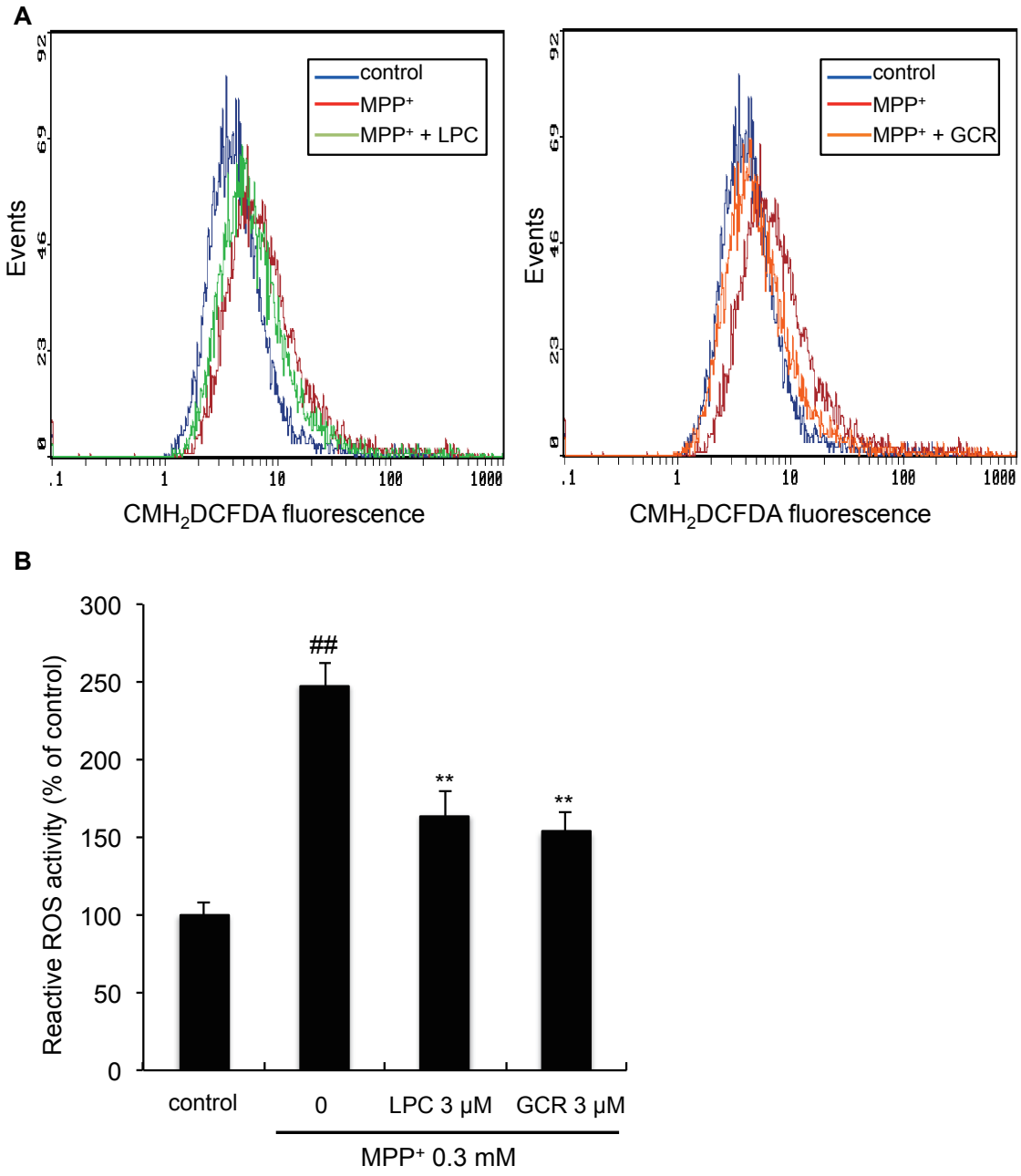

Figure 3-14. LPC and GCR decreased MPP^+-induced intracellular ROS generation.

(**A**) NGF-differentiated PC12D cells were pre-incubated for 1 hour with 3 μM LPC or 3 μM GCR, then treated with 0.3 mM MPP^+ for 12 hours. Then, the samples were loaded with 2.5 μM CM-H_2DCFDA and the fluorescence intensities were measured by flow cytometry. (**B**) The ratio of cells exhibiting ROS production was analyzed. Values are the means of four independent experiments; bars, s.d. $^{\#\#}p<0.01$ compared with control cells. $^{**}p<0.01$ compared with MPP^+ group cells.

3-2-5. Antioxidant activities of LPC and GCR *in vitro*

Because treatment of PC12D cells with LPC and GCR each effectively reduced MPP^+-induced intracellular ROS generation, the free radical scavenging activities of these two compounds were examined. When the antioxidant activity was evaluated by β-carotene bleaching assay, kaempferol (positive control) indicated potent scavenging activity (60.9 ± 2.5%), but LPC and GCR inhibited less than 10% of the carotene bleaching even at the final concentration of 30 μM (Figure 3-15A). The DPPH free radical scavenging potentials of LPC and GCR at 30 μM each showed little to no scavenging activity compared with kaempferol (80.9 ± 1.7%) (Figure 3-15B). These results indicated that LPC and GCR did not possess antioxidant activity *in vitro*.

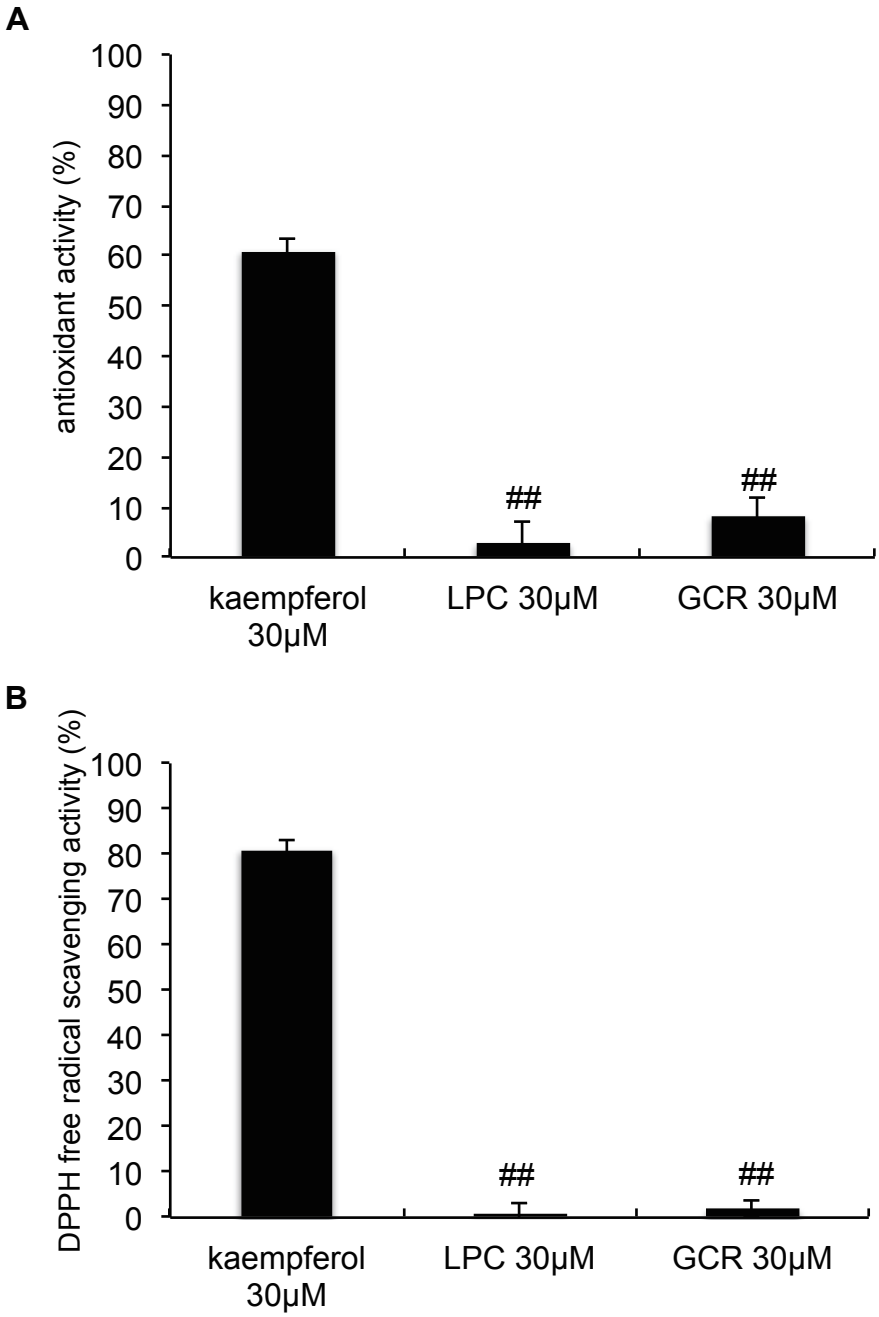

Figure 3-15. LPC and GCR lacked potency for scavenging free radicals.

Antioxidant activities of LPC and GCR were measured by (**A**) a β-carotene bleaching assay system and (**B**) a DPPH radical scavenging assay. Kaempferol served as the positive control. Values are the means of three independent experiments; bars, s.d.
$^{##}p<0.01$ compared with antioxidant activity of kaempferol.

3-2-6. LPC and GCR attenuate JNK activity induced by MPP^+

It is well-established that JNK plays a pivotal role in the mediation of MPP^+-induced neurotoxicity [76,77,78,79]. Particularly, MPP^+-induced ROS generation is closely related to JNK activation [80]. Thus, the author investigated whether the ability of LPC or GCR to reduce MPP^+-induced cell death involves the alteration of JNK signaling in MPP^+-induced neurotoxicity. As shown in Figure 3-16, phosphorylated JNK levels were increased after exposure to MPP^+ for 36 hours, and treatment with LPC or GCR significantly reduced the expression levels of the phosphorylated protein.

In addition, a JNK inhibitor, SP600125, led to attenuation of the MPP^+-induced neuronal cell death and decreased $\Delta\Psi_{mit}$ just like LPC and GCR as shown in Figure 3-10, 3-12 and 3-13 (Figure 3-17B, C). These results suggested that MPP^+-induced disappearance of $\Delta\Psi_{mit}$, which leads to neuronal cell death, were mediated by JNK, and neuroprotective activity of LPC and GCR against MPP^+-induced neuronal cell death might be due to downregulation of ROS generation, resulting in the inhibition of JNK activation.

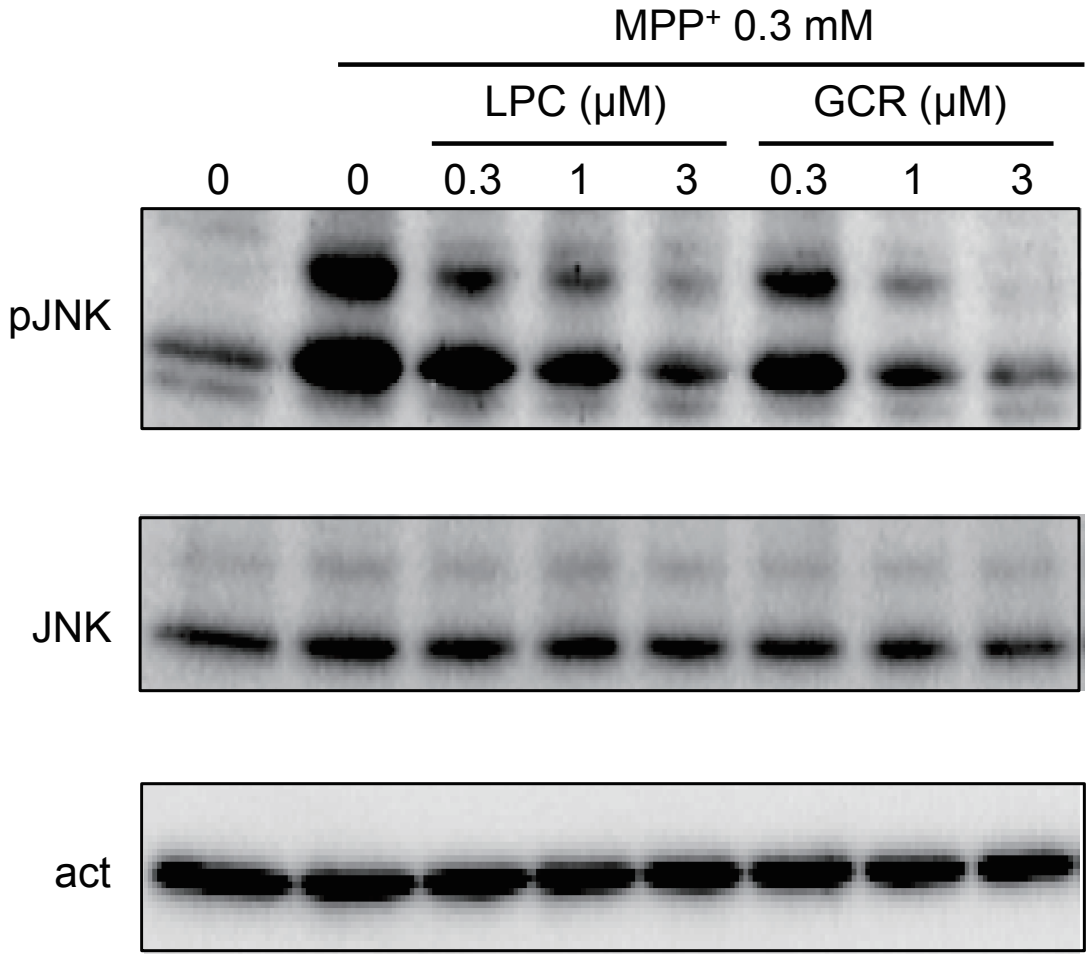

Figure 3-16. LPC and GCR attenuated MPP^+-induced JNK activation.
NGF-differentiated PC12D cells were treated with various concentrations of LPC or GCR and 0.3 mM MPP^+ for 36 hours, and JNK and phosphorylated JNK level were detected by Western blot.

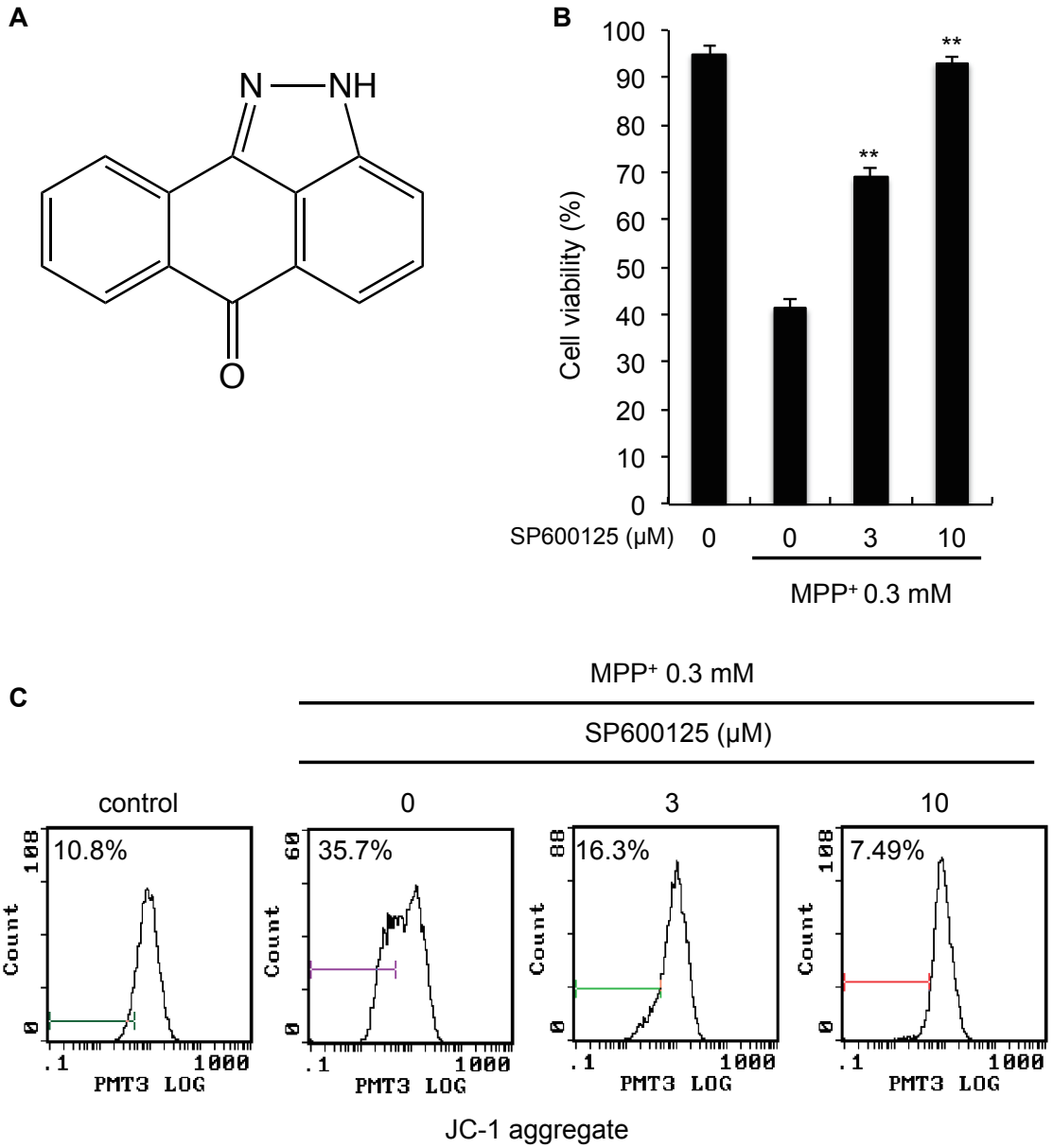

Figure 3-17. SP600125 attenuated MPP^+-induced cell death and disappearance of mitochondrial membrane potential.

(**A**) structure of SP600125. (**B**), (**C**) NGF-differentiated PC12D cells were treated with SP600125 and 0.3 mM MPP^+ for 48 hours. Thereafter, cell viability was measured by trypan blue dye exclusion assay (B) and mitochondrial membrane potentials were assessed by JC-1 assay (C). Values of (B) are the means of three independent experiments; $^{**}p<0.01$ compared with MPP^+ group cells.

3-3. Discussion

Both *choi-joki-to* and *daio-kanzo-to* are traditional herbal medicines available in Japan (called *kanpo* in Japan in particular) that are mainly used for laxative products. In the laboratory, *choi-joki-to* exhibited oxygen radical scavenging capacity [81] and inhibited the progression of atheroma in a KHC rabbit model [82], On the other hand, *daio-kanzo-to* has provided inhibition of amylase activity in mouse plasma and gastrointestinal tube [83], inhibition of cholera toxin [84], and inhibitory effects on drug oxidations [85].

In this study, the author have demonstrated that *choi-joki-to* and *daio-kanzo-to* had neuroprotective effects against MPP^+- and rotenone-induced toxicity in NGF-differentiated neuronal PC12D cells. Because these herbal medicines are provided enough to evidence of safety, it could be the state of being real that these herbal medicines are approved for use in PD in the near future.

Furthermore, the author confirmed that *Glycyrrhiza,* commonly contained in these two herbal medicines, indicated potent neuroprotective activity against MPP^+-induced toxicity. *Glycyrrhiza* is known to be included in a number of traditional herbal medicines, and its major components are triterpenoid saponins, and glycyrrhizin and its metabolite. These compounds show several physiologically activities including anti-inflammatory, anti-viral, hepatoprotective, anti-cancer, and immunomodulatory effects [86]. Therefore, at first the author expected that glycyrrhizin might be an active

principle contained in *Glycyrrhiza* that suppressed MPP^+- and rotenone-induced toxicity, but glycyrrhizin did not show such activities. Alternatively, the author isolated two coumarin derivatives, LPC and GCR, as the most potent neuroprotective compounds in *Glycyrrhiza.* LPC isolated from *Glycyrrhiza* sp. has been reported to show several bioactivities, including anti-HIV effects, inhibitory activity of CYP3A4 and the aryl hydrocarbon receptor antagonist [87,88,89]. On the other hand, GCR, which was very recently isolated from *Glycyrrhiza uralensis,* shows antithrombotic effects [90]. However, the neuroprotective effects of these two compounds have not yet been reported so far. This study has indeed revealed, for the first time, the potent neuroprotective activity of LPC and GCR in a PD-like cellular model system.

Oxidative stress is responsible for a general dysfunction of mitochondrial homeostasis that is a leading hypothesis as a potential mechanism for dopaminergic neuronal degeneration in PD [91]. Postmortem analyses of the substantia nigra from PD patients confirm several oxidative stress-related alterations [92,93,94], and several toxins (rotenone, paraquat and MPP^+) used to produce PD-like models directly and/or indirectly inhibit mitochondrial function, induce the production of ROS, and promote oxidative damage. Therefore, antioxidant agents are considered to be promising approach to prevent the disease progression. For example, α-tocopherol, coenzyme Q_{10}, and catechols have been reported to show neuroprotective effects by attenuating rotenone-induced oxidative stress on PD-like models *in vitro* and *in vivo* [26,27,28].

Likewise, the author found that LPC and GCR attenuated the MPP^+-induced elevation of intracellular ROS generation (Figure 3-14A, B), indicating that inhibition of

MPP^+-mediated ROS generation is closely related to the neuroprotective effects of LPC and GCR.

Several evidences have suggested that ROS generation induces the activation of JNK signaling, and JNK represents one of the major signaling pathways implicated in PD pathogenesis. JNK activity is increased in MPTP animal models [95,96,97,98], MPP^+-treated cellular models [80,96] and rotenone neurotoxicity [99,100]. Moreover, ROS-mediated activation of JNK almost certainly leads to cell death. Indeed, the author also verified that a JNK inhibitor, SP600125, suppressed MPP^+-induced cell death (Figure 3-17 B). Furthermore, MPP^+-induced activation of JNK and cell death were found to be inhibited by LPC and GCR under conditions where these compounds inhibited the MPP^+-mediated ROS generation (Figure 3-16). Although the potential mechanisms by which JNK participates in MPP^+-induced cell death remains to be fully elucidated, activation of JNK has been reported to mediate cell death by taking part in the induction of mitochondrial permeability transition (mPT) and decrease of $\Delta\Psi_{mit}$ in subsets of cell types [101,102]. Because in our assay system SP600125 inhibited both cell death and the disappearance of $\Delta\Psi_{\mathrm{mit}}$ induced by MPP^+ (Figure 3-17B, C), the author considers the inhibition of the decrease in MPP^+-induced $\Delta\Psi_{\mathrm{mit}}$ caused by LPC and GCR (Figure 3-13) to be due to the inhibition of ROS-mediated JNK activation.

Several neuroprotective compounds have significant antioxidant and free radical-scavenging activities. There have been several reports on the antioxidant activities of coumarin derivative [103,104,105], and LPC and GCR each inhibited MPP^+-induced ROS generation and are member of the coumarin compound family.

Nevertheless, neither LPC nor GCR showed ROS scavenging activity *in vitro*. Increased amount of ROS can be generated by an imbalance of activation of the oxidase system and antioxidant enzymes. Membrane-bound nicotinamide adenine dinucleotide phosphate (NADPH) oxidase is known to be a neurotoxin-related oxidase enzyme system [106,107], and enzymatic antioxidants include superoxide dismutase (SOD), glutathione peroxidase (GPx), thioredoxin reductase (TPx) and catalase [108]. Therefore, it is likely that LPC and GCR might regulate the balance of these systems by inhibiting oxidase activity enzymatically or neurotoxin-induced activation of oxidase system. Furthermore, the author can't exclude the possibility that LPC and GCR could induce the expression or activation of antioxidant enzymes.

In summary, the author identified *choi-joki-to* and *daio-kanzo-to* as neuroprotective herbal medicines, and both LPC and GCR were identified as neuroprotective substances from *Glycyrrhiza* contained in *choi-joki-to* and *daio-kanzo-to*. LPC or GCR exert their neuroprotective effects by inhibiting MPP^+-induced ROS production and thus limiting JNK activation, and causing a subsequent decrease in $\Delta\Psi_{mit}$. Our proposed mechanism is illustrated in Figure 3-18. Further studies are required to elucidate the molecular mechanisms for the suppression of ROS generation by LPC and GCR in PC12D cells. Our findings enliven the prospect of using LPC, GCR, *choi-joki-to*, and *daio-kanzo-to* as effective and safe natural therapeutic agents in PD; *in vivo* trials in MPTP animal models are needed.

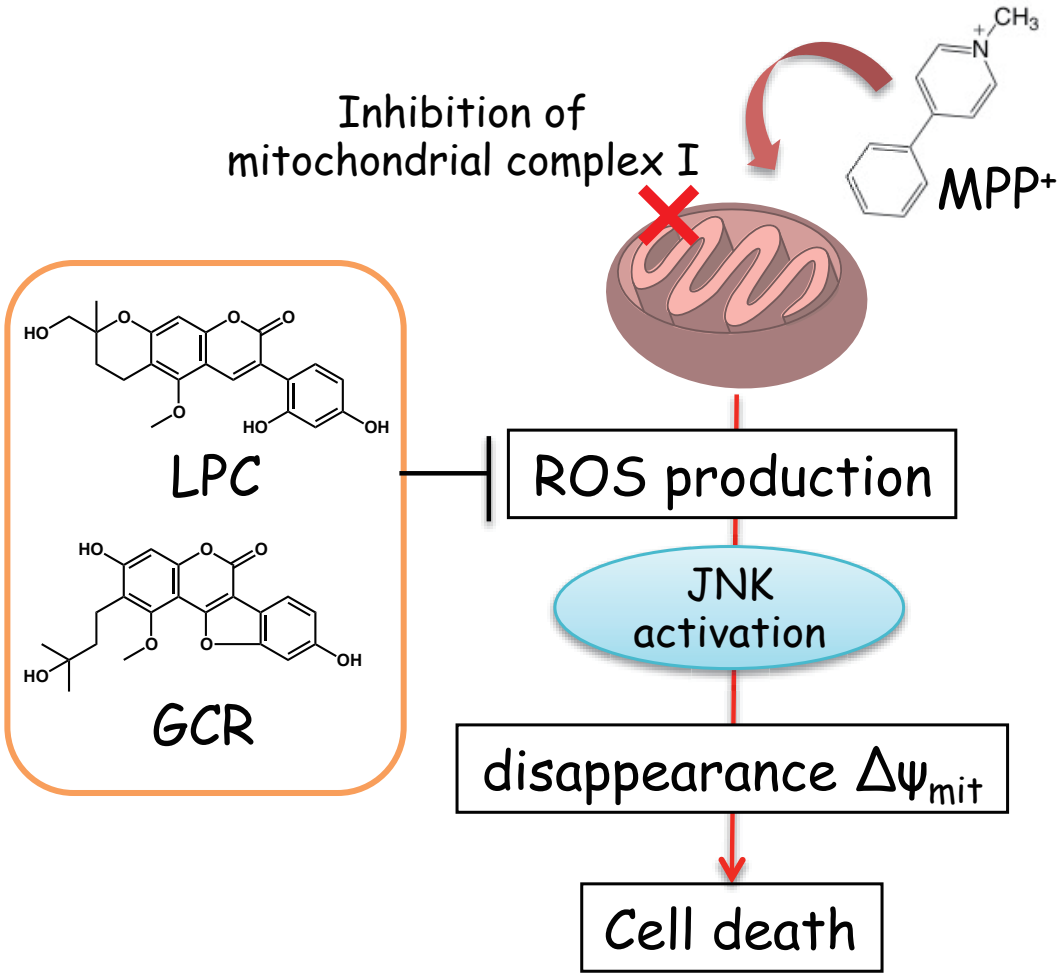

Figure 3-18. Suggested model for neuroprotection of LPC and GCR against MPP^+-induced toxicity in PC12D cells.

Both LPC and GCR exert neuroprotective effects against MPP^+-induced toxicity via suppression of ROS generation and of JNK activation.

3-4. Experimental procedures

Reagents

MPP^+, Rotenone, linoleic acid, 2,2-Diphenyl-1-pocrylhydrazyl (DPPH), SP600125, and mouse monoclonal anti-β-actin antibodies were purchased from Sigma Chemical Co. (St. Louis, MO). Taxol, cisplatin, pyridinium iodide (PI) and 5,5′,6,6′-tetrachloro-1,1′,3,3′-tetraehylbenzimidazolylcarbocyanineiodide (JC-1) were purchased from Wako Pure Chemical Industries, Ltd. (Osaka, Japan). Nerve growth factors, CM-H_2DCFDA, and β-carotene standard were purchased from Alomone Labs (Jerusalem, Israel), Life Technologies (Carlsbad, CA), and Kanto Chemical Co. (Tokyo, Japan), respectively. Rabbit polyclonal anti-JNK antibody and rabbit monoclonal anti-phospho-JNK antibody were purchased from Santa Cruz Biotechnology (Santa Cruz, CA) and Cell Signaling (Beverly, MA), respectively. Horseradish peroxidase-conjugated anti-mouse and anti-rabbit IgG used as a secondary antibodies were from GE Healthcare (Little Chalfont, UK).

Cell cultures

PC12D cells were cultured in Dulbecco's modified Eagle medium supplemented with 5% (v/v) inactivated fetal bovine serum, 10% (v/v) inactivated horse serum, 100 U/mL penicillin G, 0.6 mg/mL L-glutamine, and 0.1 mg/mL kanamycin at 37ºC with 5% CO_2. PC12D cells were differentiated by 100 ng/mL NGF treatment for 48 hours.

Cell viability assays

For the trypan blue dye exclusion assay, differentiated or undifferentiated PC12D cells were cultured in 48-well dishes. Drug-treated or untreated cells were stained with trypan blue (Sigma Chemical Co.), and the ratio of viable cells was determined using a hemocytometer. Cell viability (%) means the ratio of the number of trypan blue-impermeable cells to total cell count. IC_{50} values were calculated by linear regression analysis from the inhibition of MPP^+-induced cell death at different concentrations of the drug.

Cell cycle analysis

To examine apoptosis, differentiated PC12D cells were harvested after drug treatment. The cells were washed with PBS and fixed with 70% ethanol at 4ºC for more than 1 hour. The cells were then stained with propidium iodide (PI) solution according to a previously reported protocol [109]. The labeled nuclei were subjected to flow cytometry (FCM, Beckman-Coulter, Miami, FL).

Measurements of mitochondrial membrane potential

Changes in mitochondrial membrane potentials were assessed JC-1 was used according to the manufacturer's protocol. Briefly, treated cells were collected by pipetting and removing medium. Next, the cells were incubated in medium containing 2.5 μg/ml JC-1 for 20 min at 37ºC. Cells were then washed with PBS. JC-1 fluorescence was measured by a flow cytometer.

Measurement of intracellular ROS

Intracellular ROS production was measured using CM-H_2DCFDA. The cells were plated at a density of 12 x 10^4 cells per 12-well dish. The cells were treated with MPP^+ and test compounds for 12 hours, and then trypsinized and collected. After the cells were washed with PBS, incubated with 2.5 μM CM-H_2DCFDA in HBSS at 37°C for 30 min, and then washed again with PBS three times. The relative levels of fluorescence were quantified by using a flow cytometer.

β-carotene bleaching assay

This assay was carried out according to the β-carotene bleaching method [110]. A mixture of β-carotene and linoleic acid was prepared by adding a mixture of 0.3 mg of β-carotene in 3 mL chloroform, 40 mg linoleic acid, and 400 mg Tween 20. Chloroform was removed and 100 mL of distilled water was added to form an emulsion with continuous shaking. Aliquots (0.1 mL) of the β-carotene/linoleic acid emulsion were mixed with 1 μL of sample solution and incubated in a water bath at 50ºC. The oxidation of the emulsion was monitored spectrophotometrically by measuring absorbance at 470 nm. Control samples contained 1 μL of methanol. Antioxidant activity is expressed as percent inhibition relative to control after 60 min incubation using the following equation:

$AA(\%) = 100(DR_c - DR_s)/DR_c$,

where AA = antioxidant activity; DR_c = degradation rate of the control =[ln(*a/b*)/60]; DR_s = degradation rate in presence of the sample = [ln(*a/b*)/60]; *a* = absorbance at time

0; *b* = absorbance at 60 min.

DPPH radical scavenging assay

The DPPH radical scavenging effect of test compounds was determined according to the previously described method [110]. The reaction mixtures contained 100 μl ethanol, 125 μM DPPH, and test compounds. After 2 min of incubation at room temperature, the absorbance was recorded at 517 nm.

Extraction and isolation of LPC and GCR from Licorice

Compounds were extracted from dried and pulverized licorice (50 g) with 90% EtOH, then filtrated and concentrated *in vacuo*. This suspension was adjusted to pH 7.0, followed by extraction with EtOAc (5 L) twice; the organic layer was concentrated to yield residue (3.76 g). The EtOAc extract was fractionated by centrifugal partition chromatography (CPC) with $CHCl_3$-MeOH:H_2O (5:6:4). The obtained crude active extract was applied on Sephadex LH20 column chromatography (Sephadex LH-20, 70 μM; GE Healthcare, NJ, USA), and eluted with MeOH. The active fraction (250.6 mg) was further purified by preparative octadecyl silyl (ODS) HPLC (YMC-Pack ODS-AQ, YMC Co. Ltd., Japan) with 40% aqueous CH_3CN to give pure licopyranocoumarin (10.8 mg) and glycyrurol (4 mg), respectively.

Western blotting

Cells were lysed in RIPA buffer (25 mM HEPES (pH 7.2), 1.5% Triton X-100 (Wako),

1% sodium deoxycholate (Wako), 0.1% SDS, 0.5 M NaCl (Wako), 5 mM EDTA, 50 mM NaF (Sigma), 0.1 mM sodium vanadate (Sigma), and 1 mM phenylmethylsulfonyl fluoride (PMSF) with sonication. The lysates were centrifuged at 13,000 rpm for 15 min to yield the soluble cell lysates. For immunoblotting, cell lysates were subjected to SDS-polyacrylamide gel electrophoresis. Proteins were transferred onto a polyvinylidene fluoride membrane (Millipore) by electroblotting and then incubated with appropriate antibodies. Immune complexes were detected with an Immobilon Western kit (Millipore), and luminescence was detected with a LAS-1000 mini (Fujifilm Co., Tokyo, Japan).

Statistical analysis

All statistical analyses in bar plots were performed with a two-tailed paired Student's *t*-test.

Chapter 4

Conclusion

Both prostate cancer and PD are progressive age-dependent diseases, therefore it is urgently necessary for our country to treat for these two diseases because of the rapid progression of aging in Japan. However, the present therapies of these two diseases have the separate problems, respectively.

Although androgen antagonists are established prostate cancer treatments, prostate cancer almost always has drug-resistant caused by insufficient structure variation of clinical drug. On the other hand, the pathogenesis mechanisms of PD remain to be clarified, and current therapy is limited to a symptomatic treatment.

In this study, the author screened for new drug-seeds for prostate cancer and PD from second metabolites of microbes and traditional herbal medicine, respectively. The results, significance and speculation about this study are summarized below.

[chapter 2] In the course of screening for a new type of androgen receptor (AR) antagonist, the author isolated a novel compound, arabilin, with two structural isomers, spectinabilin and SNF4435C, produced by *Streptomyces* sp. MK756-CF1. Structure elucidation on the basis of the spectroscopic properties showed that arabilin is a novel polypropionate-derived metabolite with a *p*-nitrophenyl group and a substituted γ-pyrone ring.

Arabilin competitively blocked the binding of androgen to the ligand-binding domain of AR *in vitro*. In addition, arabilin inhibited androgen-induced PSA mRNA expression and proliferation in prostate cancer LNCaP cells.

However, whether arabilin can overcome hormone-refractory prostate cancer is still

unknown. Therefore, further study such as binding assay or reporter gene assay using mutant ARs (e.g., T877A, W741C, W741L) are going now.

[chapter 3] In the course of screening for the anti-Parkinsonian drugs from a library of traditional herbal medicines, the author found that the extracts of *choi-joki-to* and *daio-kanzo-to* protected cells from MPP^+-induced cell death.

Because *choi-joki-to* and *daio-kanzo-to* commonly contain the genus *Glycyrrhiza*, the author isolated licopyranocoumarin (LPC) and glycyrurol (GCR) as potent neuroprotective principals from *Glycyrrhiza*.

LPC and GCR markedly blocked MPP^+-induced neuronal PC12D cell death and disappearance of mitochondrial membrane potential, which were mediated by JNK. LPC and GCR inhibited MPP^+-induced JNK activation through the suppression of reactive oxygen species (ROS) generation, thereby inhibiting MPP^+-induced neuronal PC12D cell death.

These results indicated that LPC and GCR derived from *choi-joki-to* and *daio-kanzo-to* would be promising drug leads for PD treatment and biological tool to understand the underlying mechanism of PD in the future. Interestingly, both LPC and GCR did not possess ROS scavenging activity *in vitro.* Therefore, the investigation of other mechanism for inhibition of cellular ROS generation by LPC and GCR, such as NADPH oxidase inhibitory activity and up-regulation of glutathione, are going now.

References

1. Drews J (2000) Drug discovery: a historical perspective. *Science* 287: 1960-1964.
2. Beutler JA (2009) Natural Products as a Foundation for Drug Discovery. *Current Protocols in Pharmacology / Editorial Board, SJ Enna* 46: 9 11 11-19 11 21.
3. Fleming A (2001) On the antibacterial action of cultures of a penicillium, with special reference to their use in the isolation of *B. influenzae*. 1929. *Bulletin of the World Health Organization* 79: 780-790.
4. Chain E, Florey HW, Gardner AD, Heatley NG, Jennings MA, Orr-Ewing J, Sanders AG (1940) Penicillin as a chemotherapeutic agent. *Lancet* 236: 226-228.
5. Wani MC, Wall ME (1969) Plant antitumor agents. II. The structure of two new alkaloids from *Camptotheca acuminata. J Org Chem* 34: 1364-1367.
6. Thali M (1995) Cyclosporins: immunosuppressive drugs with anti-HIV-1 activity. *Mol Med Today* 1: 287-291.
7. Horsburgh T, Wood P, Brent L (1980) Suppression of in vitro lymphocyte reactivity by cyclosporin A: existence of a population of drug-resistant cytotoxic lymphocytes. *Nature* 286: 609-611.
8. Towle MJ, Salvato KA, Budrow J, Wels BF, Kuznetsov G, Aalfs KK, Welsh S, Zheng W, Seletsky BM, Palme MH, Habgood GJ, Singer LA, Dipietro LV, Wang Y, Chen JJ, Quincy DA, Davis A, Yoshimatsu K, Kishi Y, Yu MJ, Littlefield BA (2001) In vitro and in vivo anticancer activities of synthetic macrocyclic ketone analogues of halichondrin B. *Cancer Res* 61: 1013-1021.
9. Hirata Y, Uemura D (1986) Halichondrins - Antitumor Polyether Macrolides from a Marine Sponge. *Pure and Applied Chemistry* 58: 701-710.
10. Smith JA, Wilson L, Azarenko O, Zhu X, Lewis BM, Littlefield BA, Jordan MA (2010) Eribulin binds at microtubule ends to a single site on tubulin to suppress dynamic instability. *Biochemistry* 49: 1331-1337.

11. Newman DJ, Cragg GM (2012) Natural products as sources of new drugs over the 30 years from 1981 to 2010. *J Nat Prod* 75: 311-335.

12. Meimetis LG, Williams DE, Mawji NR, Banuelos CA, Lal AA, Park JJ, Tien AH, Fernandez JG, de Voogd NJ, Sadar MD, Andersen RJ (2012) Niphatenones, glycerol ethers from the sponge *Niphates digitalis* block androgen receptor transcriptional activity in prostate cancer cells: structure elucidation, synthesis, and biological activity. *J Med Chem* 55: 503-514.

13. Miyamoto H, Messing EM, Chang C (2004) Androgen deprivation therapy for prostate cancer: current status and future prospects. *Prostate* 61: 332-353.

14. Tenbaum S, Baniahmad A (1997) Nuclear receptors: structure, function and involvement in disease. *Int J Biochem Cell Biol* 29: 1325-1341.

15. Shore N, Mason M, de Reijke TM (2012) New developments in castrate-resistant prostate cancer. *BJU Int* 109 Suppl 6: 22-32.

16. Attard G, Reid AH, Yap TA, Raynaud F, Dowsett M, Settatree S, Barrett M, Parker C, Martins V, Folkerd E, Clark J, Cooper CS, Kaye SB, Dearnaley D, Lee G, de Bono JS (2008) Phase I clinical trial of a selective inhibitor of CYP17, abiraterone acetate, confirms that castration-resistant prostate cancer commonly remains hormone driven. *J Clin Oncol* 26: 4563-4571.

17. Yin L, Hu Q, Hartmann RW (2013) Recent progress in pharmaceutical therapies for castration-resistant prostate cancer. *International Journal of Molecular Sciences* 14: 13958-13978.

18. Tran C, Ouk S, Clegg NJ, Chen Y, Watson PA, Arora V, Wongvipat J, Smith-Jones PM, Yoo D, Kwon A, Wasielewska T, Welsbie D, Chen CD, Higano CS, Beer TM, Hung DT, Scher HI, Jung ME, Sawyers CL (2009) Development of a second-generation antiandrogen for treatment of advanced prostate cancer. *Science* 324: 787-790.

19. Scher HI, Beer TM, Higano CS, Anand A, Taplin ME, Efstathiou E, Rathkopf D, Shelkey J, Yu EY, Alumkal J, Hung D, Hirmand M, Seely L, Morris MJ, Danila

DC, Humm J, Larson S, Fleisher M, Sawyers CL (2010) Antitumour activity of MDV3100 in castration-resistant prostate cancer: a phase 1-2 study. *Lancet* 375: 1437-1446.

20. Chen CD, Welsbie DS, Tran C, Baek SH, Chen R, Vessella R, Rosenfeld MG, Sawyers CL (2004) Molecular determinants of resistance to antiandrogen therapy. *Nature Medicine* 10: 33-39.

21. Taplin ME, Bubley GJ, Shuster TD, Frantz ME, Spooner AE, Ogata GK, Keer HN, Balk SP (1995) Mutation of the androgen-receptor gene in metastatic androgen-independent prostate cancer. *The New England Journal of Medicine* 332: 1393-1398.

22. Korpal M, Korn JM, Gao X, Rakiec DP, Ruddy DA, Doshi S, Yuan J, Kovats SG, Kim S, Cooke VG, Monahan JE, Stegmeier F, Roberts TM, Sellers WR, Zhou W, Zhu P (2013) An F876L mutation in androgen receptor confers genetic and phenotypic resistance to MDV3100 (enzalutamide). *Cancer Discovery* 3: 1030-1043.

23. Lees AJ, Hardy J, Revesz T (2009) Parkinson's disease. *Lancet* 373: 2055-2066.

24. Lewitt PA (2008) Levodopa for the treatment of Parkinson's disease. *The New England Journal of Medicine* 359: 2468-2476.

25. Dawson TM, Dawson VL (2002) Neuroprotective and neurorestorative strategies for Parkinson's disease. *Nat Neurosci* 5 Suppl: 1058-1061.

26. Song JX, Sze SC, Ng TB, Lee CK, Leung GP, Shaw PC, Tong Y, Zhang YB (2012) Anti-Parkinsonian drug discovery from herbal medicines: what have we got from neurotoxic models? *J Ethnopharmacol* 139: 698-711.

27. Testa CM, Sherer TB, Greenamyre JT (2005) Rotenone induces oxidative stress and dopaminergic neuron damage in organotypic substantia nigra cultures. *Brain Res Mol Brain Res* 134: 109-118.

28. Yang L, Calingasan NY, Wille EJ, Cormier K, Smith K, Ferrante RJ, Beal MF (2009) Combination therapy with coenzyme Q10 and creatine produces additive

neuroprotective effects in models of Parkinson's and Huntington's diseases. *J Neurochem* 109: 1427-1439.

29. Blesa J, Phani S, Jackson-Lewis V, Przedborski S (2012) Classic and new animal models of Parkinson's disease. *Journal of Biomedicine & Biotechnology* 2012: 845618.

30. Dauer W, Przedborski S (2003) Parkinson's disease: mechanisms and models. *Neuron* 39: 889-909.

31. Dawson TM, Ko HS, Dawson VL (2010) Genetic animal models of Parkinson's disease. *Neuron* 66: 646-661.

32. Dexter DT, Jenner P (2013) Parkinson disease: from pathology to molecular disease mechanisms. *Free Radical Biology & Medicine* 62: 132-144.

33. Gao W, Dalton JT (2007) Expanding the therapeutic use of androgens via selective androgen receptor modulators (SARMs). *Drug Discov Today* 12: 241-248.

34. Gao W, Bohl CE, Dalton JT (2005) Chemistry and structural biology of androgen receptor. *Chem Rev* 105: 3352-3370.

35. Scher HI, Steineck G, Kelly WK (1995) Hormone-refractory (D3) prostate cancer: refining the concept. *Urology* 46: 142-148.

36. Taplin ME, Rajeshkumar B, Halabi S, Werner CP, Woda BA, Picus J, Stadler W, Hayes DF, Kantoff PW, Vogelzang NJ, Small EJ (2003) Androgen receptor mutations in androgen-independent prostate cancer: Cancer and Leukemia Group B Study 9663. *J Clin Oncol* 21: 2673-2678.

37. Gaddipati JP, McLeod DG, Heidenberg HB, Sesterhenn IA, Finger MJ, Moul JW, Srivastava S (1994) Frequent detection of codon 877 mutation in the androgen receptor gene in advanced prostate cancers. *Cancer Res* 54: 2861-2864.

38. Hara T, Miyazaki J, Araki H, Yamaoka M, Kanzaki N, Kusaka M, Miyamoto M (2003) Novel mutations of androgen receptor: a possible mechanism of bicalutamide withdrawal syndrome. *Cancer Res* 63: 149-153.

39. Tan J, Sharief Y, Hamil KG, Gregory CW, Zang DY, Sar M, Gumerlock PH,

deVere White RW, Pretlow TG, Harris SE, Wilson EM, Mohler JL, French FS (1997) Dehydroepiandrosterone activates mutant androgen receptors expressed in the androgen-dependent human prostate cancer xenograft CWR22 and LNCaP cells. *Molecular Endocrinology* 11: 450-459.

40. van Bokhoven A, Varella-Garcia M, Korch C, Johannes WU, Smith EE, Miller HL, Nordeen SK, Miller GJ, Lucia MS (2003) Molecular characterization of human prostate carcinoma cell lines. *Prostate* 57: 205-225.

41. Steketee K, Timmerman L, Ziel-van der Made AC, Doesburg P, Brinkmann AO, Trapman J (2002) Broadened ligand responsiveness of androgen receptor mutants obtained by random amino acid substitution of H874 and mutation hot spot T877 in prostate cancer. *Int J Cancer* 100: 309-317.

42. Yoshida T, Kinoshita H, Segawa T, Nakamura E, Inoue T, Shimizu Y, Kamoto T, Ogawa O (2005) Antiandrogen bicalutamide promotes tumor growth in a novel androgen-dependent prostate cancer xenograft model derived from a bicalutamide-treated patient. *Cancer Res* 65: 9611-9616.

43. Kakinuma K, Hanson CA, Rinehart KLJ (1976) Spectinabilin, a new nitro-containing metabolite isolated from *Streptomyces spectabilis*. *Tetrahedron* 32: 217-222.

44. Kurosawa K, Takahashi K, Tsuda E (2001) SNF4435C and D, novel immunosuppressants produced by a strain of *Streptomyces spectabilis*. I. Taxonomy, fermentation, isolation and biological activities. *J Antibiot (Tokyo)* 54: 541-547.

45. Takahashi K, Tsuda E, Kurosawa K (2001) SNF4435C and D, novel immunosuppressants produced by a strain of *Streptomyces spectabilis*. II. Structure elucidation. *J Antibiot (Tokyo)* 54: 548-553.

46. Jacobsen MF, Moses JE, Adlington RM, Baldwin JE (2005) The total synthesis of spectinabilin and its biomimetic conversion to SNF4435C and SNF4435D. *Org Lett* 7: 2473-2476.

47. Lim HN, Parker KA (2011) Total synthesis of the potent androgen receptor antagonist (-)-arabilin: a strategic, biomimetic [1,7]-hydrogen shift. *J Am Chem Soc* 133: 20149-20151.

48. Nagamine N, Shirakawa T, Minato Y, Torii K, Kobayashi H, Imoto M, Sakakibara Y (2009) Integrating statistical predictions and experimental verifications for enhancing protein-chemical interaction predictions in virtual screening. *PLoS Comput Biol* 5: e1000397.

49. Bindoff LA, Birch-Machin M, Cartlidge NE, Parker WD, Jr., Turnbull DM (1989) Mitochondrial function in Parkinson's disease. *Lancet* 2: 49.

50. Parker WD, Jr., Parks JK, Swerdlow RH (2008) Complex I deficiency in Parkinson's disease frontal cortex. *Brain Res* 1189: 215-218.

51. Parker WD, Jr., Swerdlow RH (1998) Mitochondrial dysfunction in idiopathic Parkinson disease. *Am J Hum Genet* 62: 758-762.

52. Schapira AH, Cooper JM, Dexter D, Clark JB, Jenner P, Marsden CD (1990) Mitochondrial complex I deficiency in Parkinson's disease. *J Neurochem* 54: 823-827.

53. Smigrodzki R, Parks J, Parker WD (2004) High frequency of mitochondrial complex I mutations in Parkinson's disease and aging. *Neurobiol Aging* 25: 1273-1281.

54. Esteves AR, Domingues AF, Ferreira IL, Januario C, Swerdlow RH, Oliveira CR, Cardoso SM (2008) Mitochondrial function in Parkinson's disease cybrids containing an nt2 neuron-like nuclear background. *Mitochondrion* 8: 219-228.

55. Trimmer PA, Borland MK, Keeney PM, Bennett JP, Jr., Parker WD, Jr. (2004) Parkinson's disease transgenic mitochondrial cybrids generate Lewy inclusion bodies. *J Neurochem* 88: 800-812.

56. Heikkila RE, Hess A, Duvoisin RC (1984) Dopaminergic neurotoxicity of 1-methyl-4-phenyl-1,2,5,6-tetrahydropyridine in mice. *Science* 224: 1451-1453.

57. Eberhardt O, Schulz JB (2003) Apoptotic mechanisms and antiapoptotic therapy in

the MPTP model of Parkinson's disease. *Toxicol Lett* 139: 135-151.

58. Burns RS, Chiueh CC, Markey SP, Ebert MH, Jacobowitz DM, Kopin IJ (1983) A primate model of parkinsonism: selective destruction of dopaminergic neurons in the pars compacta of the substantia nigra by N-methyl-4-phenyl-1,2,3,6-tetrahydropyridine. *Proc Natl Acad Sci U S A* 80: 4546-4550.

59. Davis GC, Williams AC, Markey SP, Ebert MH, Caine ED, Reichert CM, Kopin IJ (1979) Chronic Parkinsonism secondary to intravenous injection of meperidine analogues. *Psychiatry Res* 1: 249-254.

60. Betarbet R, Sherer TB, MacKenzie G, Garcia-Osuna M, Panov AV, Greenamyre JT (2000) Chronic systemic pesticide exposure reproduces features of Parkinson's disease. *Nat Neurosci* 3: 1301-1306.

61. Martinez TN, Greenamyre JT (2012) Toxin models of mitochondrial dysfunction in Parkinson's disease. *Antioxid Redox Signal* 16: 920-934.

62. Heikkila RE, Manzino L, Cabbat FS, Duvoisin RC (1984) Protection against the dopaminergic neurotoxicity of 1-methyl-4-phenyl-1,2,5,6-tetrahydropyridine by monoamine oxidase inhibitors. *Nature* 311: 467-469.

63. Cohen G, Pasik P, Cohen B, Leist A, Mytilineou C, Yahr MD (1984) Pargyline and deprenyl prevent the neurotoxicity of 1-methyl-4-phenyl-1,2,3,6-tetrahydropyridine (MPTP) in monkeys. *Eur J Pharmacol* 106: 209-210.

64. Cao BY, Yang YP, Luo WF, Mao CJ, Han R, Sun X, Cheng J, Liu CF (2010) Paeoniflorin, a potent natural compound, protects PC12 cells from MPP+ and acidic damage via autophagic pathway. *J Ethnopharmacol* 131: 122-129.

65. Kong XC, Zhang D, Qian C, Liu GT, Bao XQ (2011) FLZ, a novel HSP27 and HSP70 inducer, protects SH-SY5Y cells from apoptosis caused by MPP(+). *Brain Res* 1383: 99-107.

66. Park SW, Lee CH, Lee JG, Kim LW, Shin BS, Lee BJ, Kim YH (2011) Protective

effects of atypical antipsychotic drugs against MPP(+)-induced oxidative stress in PC12 cells. *Neurosci Res* 69: 283-290.

67. Yurekli VA, Gurler S, Naziroglu M, Uguz AC, Koyuncuoglu HR (2013) Zonisamide attenuates MPP+-induced oxidative toxicity through modulation of Ca2+ signaling and caspase-3 activity in neuronal PC12 cells. *Cell Mol Neurobiol* 33: 205-212.

68. Manyam BV, Sanchez-Ramos JR (1999) Traditional and complementary therapies in Parkinson's disease. *Adv Neurol* 80: 565-574.

69. Bae N, Ahn T, Chung S, Oh MS, Ko H, Oh H, Park G, Yang HO (2011) The neuroprotective effect of modified Yeoldahanso-tang via autophagy enhancement in models of Parkinson's disease. *J Ethnopharmacol* 134: 313-322.

70. Doo AR, Kim SN, Park JY, Cho KH, Hong J, Eun-Kyung K, Moon SK, Jung WS, Lee H, Jung JH, Park HJ (2010) Neuroprotective effects of an herbal medicine, Yi-Gan San on MPP+/MPTP-induced cytotoxicity *in vitro* and *in vivo*. *J Ethnopharmacol* 131: 433-442.

71. Hashimoto R, Yu J, Koizumi H, Ouchi Y, Okabe T (2012) Ginsenoside Rb1 Prevents MPP(+)-Induced Apoptosis in PC12 Cells by Stimulating Estrogen Receptors with Consequent Activation of ERK1/2, Akt and Inhibition of SAPK/JNK, p38 MAPK. *Evid Based Complement Alternat Med* 2012: 693717.

72. Li X, Ye X, Sun X, Liang Q, Tao L, Kang X, Chen J (2011) Salidroside protects against MPP(+)-induced apoptosis in PC12 cells by inhibiting the NO pathway. *Brain Res* 1382: 9-18.

73. Zhou J, Sun Y, Zhao X, Deng Z, Pu X (2013) 3-O-demethylswertipunicoside inhibits MPP(+)-induced oxidative stress and apoptosis in PC12 cells. *Brain Res* 1508: 53-62.

74. Chung V, Liu L, Bian Z, Zhao Z, Leuk Fong W, Kum WF, Gao J, Li M (2006) Efficacy and safety of herbal medicines for idiopathic Parkinson's disease: a systematic review. *Mov Disord* 21: 1709-1715.

75. Beal MF (2001) Experimental models of Parkinson's disease. *Nat Rev Neurosci* 2: 325-334.

76. Yao S, Li Y, Kong L (2006) Preparative isolation and purification of chemical constituents from the root of Polygonum multiflorum by high-speed counter-current chromatography. *J Chromatogr A* 1115: 64-71.

77. Mielke K, Herdegen T (2000) JNK and p38 stresskinases--degenerative effectors of signal-transduction-cascades in the nervous system. *Prog Neurobiol* 61: 45-60.

78. Tatton WG, Chalmers-Redman R, Brown D, Tatton N (2003) Apoptosis in Parkinson's disease: signals for neuronal degradation. *Ann Neurol* 53 Suppl 3: S61-70; discussion S70-62.

79. Voss T, Ravina B (2008) Neuroprotection in Parkinson's disease: myth or reality? *Curr Neurol Neurosci Rep* 8: 304-309.

80. Kim SY, Kim MY, Mo JS, Park JW, Park HS (2007) SAG protects human neuroblastoma SH-SY5Y cells against 1-methyl-4-phenylpyridinium ion (MPP+)-induced cytotoxicity via the downregulation of ROS generation and JNK signaling. *Neurosci Lett* 413: 132-136.

81. Nishimura K, Osawa T, Watanabe K (2011) Evaluation of oxygen radical absorbance capacity in kampo medicine. *Evid Based Complement Alternat Med* 2011: 812163.

82. Iizuka A, Iijima OT, Kondo K, Matsumoto A, Itakura H, Yoshie F, Komatsu Y, Takeda H, Matsumiya T (2000) Antioxidative effects of Choi-oki-to and its ability to inhibit the progression of atheroma in KHC rabbits. *J Atheroscler Thromb* 6: 49-54.

83. Kobayashi K, Funayama N, Suzuki R, Yoshizaki F (2002) Survey of the influence of Chinese medicinal prescriptions on amylase activity in mouse plasma and gastrointestinal tube. *Biol Pharm Bull* 25: 1108-1111.

84. Oi H, Matsuura D, Miyake M, Ueno M, Takai I, Yamamoto T, Kubo M, Moss J, Noda M (2002) Identification in traditional herbal medications and confirmation

by synthesis of factors that inhibit cholera toxin-induced fluid accumulation. *Proc Natl Acad Sci U S A* 99: 3042-3046.

85. Hasegawa A, Kawaguchi Y, Nakasa H, Nakamura H, Ohmori S, Ishii I, Kitada M (2002) Effects of Kampo extracts on drug metabolism in rat liver microsomes: Rhei Rhizoma extract and Glycyrrhizae Radix extract inhibit drug oxidation. *Jpn J Pharmacol* 89: 164-170.

86. Asl MN, Hosseinzadeh H (2008) Review of pharmacological effects of Glycyrrhiza sp. and its bioactive compounds. *Phytother Res* 22: 709-724.

87. Hatano T, Yasuhara T, Fukuda T, Noro T, Okuda T (1989) Phenolic constituents of licorice. II. Structures of licopyranocoumarin, licoarylcoumarin and glisoflavone, and inhibitory effects of licorice phenolics on xanthine oxidase. *Chem Pharm Bull (Tokyo)* 37: 3005-3009.

88. Tsukamoto S, Aburatani M, Yoshida T, Yamashita Y, El-Beih AA, Ohta T (2005) CYP3A4 inhibitors isolated from Licorice. *Biol Pharm Bull* 28: 2000-2002.

89. Kasai A, Hiramatsu N, Hayakawa K, Yao J, Kitamura M (2008) Blockade of the dioxin pathway by herbal medicine Formula Bupleuri Minor: identification of active entities for suppression of AhR activation. *Biol Pharm Bull* 31: 838-846.

90. Tao WW, Duan JA, Yang NY, Tang YP, Liu MZ, Qian YF (2012) Antithrombotic phenolic compounds from *Glycyrrhiza uralensis*. *Fitoterapia* 83: 422-425.

91. Seaton TA, Cooper JM, Schapira AH (1997) Free radical scavengers protect dopaminergic cell lines from apoptosis induced by complex I inhibitors. *Brain Res* 777: 110-118.

92. Alam ZI, Jenner A, Daniel SE, Lees AJ, Cairns N, Marsden CD, Jenner P, Halliwell B (1997) Oxidative DNA damage in the parkinsonian brain: an apparent selective increase in 8-hydroxyguanine levels in substantia nigra. *J Neurochem* 69: 1196-1203.

93. Dexter DT, Carter CJ, Wells FR, Javoy-Agid F, Agid Y, Lees A, Jenner P, Marsden CD (1989) Basal lipid peroxidation in substantia nigra is increased in

Parkinson's disease. *J Neurochem* 52: 381-389.

94. Floor E, Wetzel MG (1998) Increased protein oxidation in human substantia nigra pars compacta in comparison with basal ganglia and prefrontal cortex measured with an improved dinitrophenylhydrazine assay. *J Neurochem* 70: 268-275.

95. Saporito MS, Brown EM, Miller MS, Carswell S (1999) CEP-1347/KT-7515, an inhibitor of c-jun N-terminal kinase activation, attenuates the 1-methyl-4-phenyl tetrahydropyridine-mediated loss of nigrostriatal dopaminergic neurons In vivo. *J Pharmacol Exp Ther* 288: 421-427.

96. Xia XG, Harding T, Weller M, Bieneman A, Uney JB, Schulz JB (2001) Gene transfer of the JNK interacting protein-1 protects dopaminergic neurons in the MPTP model of Parkinson's disease. *Proc Natl Acad Sci U S A* 98: 10433-10438.

97. Hunot S, Vila M, Teismann P, Davis RJ, Hirsch EC, Przedborski S, Rakic P, Flavell RA (2004) JNK-mediated induction of cyclooxygenase 2 is required for neurodegeneration in a mouse model of Parkinson's disease. *Proc Natl Acad Sci U S A* 101: 665-670.

98. Park SW, Kim SH, Park KH, Kim SD, Kim JY, Baek SY, Chung BS, Kang CD (2004) Preventive effect of antioxidants in MPTP-induced mouse model of Parkinson's disease. *Neurosci Lett* 363: 243-246.

99. Newhouse K, Hsuan SL, Chang SH, Cai B, Wang Y, Xia Z (2004) Rotenone-induced apoptosis is mediated by p38 and JNK MAP kinases in human dopaminergic SH-SY5Y cells. *Toxicol Sci* 79: 137-146.

100. Klintworth H, Newhouse K, Li T, Choi WS, Faigle R, Xia Z (2007) Activation of c-Jun N-terminal protein kinase is a common mechanism underlying paraquat- and rotenone-induced dopaminergic cell apoptosis. *Toxicol Sci* 97: 149-162.

101. Hanawa N, Shinohara M, Saberi B, Gaarde WA, Han D, Kaplowitz N (2008) Role of JNK translocation to mitochondria leading to inhibition of mitochondria bioenergetics in acetaminophen-induced liver injury. *J Biol Chem* 283:

13565-13577.

102. Lin X, Wang YJ, Li Q, Hou YY, Hong MH, Cao YL, Chi ZQ, Liu JG (2009) Chronic high-dose morphine treatment promotes SH-SY5Y cell apoptosis via c-Jun N-terminal kinase-mediated activation of mitochondria-dependent pathway. *Febs J* 276: 2022-2036.

103. Ng TB, Liu F, Wang ZT (2000) Antioxidative activity of natural products from plants. *Life Sci* 66: 709-723.

104. Fernandez-Puntero B, Barroso I, Iglesias I, Benedi J, Villar A (2001) Antioxidant activity of Fraxetin: *in vivo* and *ex vivo* parameters in normal situation versus induced stress. *Biol Pharm Bull* 24: 777-784.

105. Vladimirov Iu A, Parfenov EA, Epanchintseva OM, Smirnov LD (1991) [The antiradical activity of coumarin reductones]. *Biull Eksp Biol Med* 112: 472-475.

106. Infanger DW, Sharma RV, Davisson RL (2006) NADPH oxidases of the brain: distribution, regulation, and function. *Antioxid Redox Signal* 8: 1583-1596.

107. Sawada M, Imamura K, Nagatsu T (2006) Role of cytokines in inflammatory process in Parkinson's disease. *Journal of Neural Transmission Supplementum*: 373-381.

108. Jin H, Kanthasamy A, Ghosh A, Anantharam V, Kalyanaraman B, Kanthasamy AG (2013) Mitochondria-targeted antioxidants for treatment of Parkinson's disease: Preclinical and clinical outcomes. *Biochimica et Biophysica Acta*.

109. Kawatani M, Uchi M, Simizu S, Osada H, Imoto M (2003) Transmembrane domain of Bcl-2 is required for inhibition of ceramide synthesis, but not cytochrome c release in the pathway of inostamycin-induced apoptosis. *Exp Cell Res* 286: 57-66.

110. Kumazawa S, Taniguchi M, Suzuki Y, Shimura M, Kwon MS, Nakayama T (2002) Antioxidant activity of polyphenols in carob pods. *J Agric Food Chem* 50: 373-377.

謝辞

本研究は慶應義塾大学理工学部教授　井本正哉博士のご指導のもとに行いました。終始親身にご指導ご高配賜りましたことを謹んで感謝の意を表します。
また本研究を遂行するにあたり、多くのご指導、ご助言頂きました慶應義塾大学理工学部専任講師　田代悦博士に深く感謝の意を表します。
本論文の執筆にあたり、ご指導、ご助言頂きました慶應義塾大学理工学部教授　佐藤智典博士、慶應義塾大学理工学部准教授　宮本憲二博士、慶應義塾大学理工学部准教授　末永聖武博士に厚く感謝致します。
Arabilin の構造解析並びに arabilin 生産菌の同定及び培養に際し、ご指導を承りました微生物化学研究センター　高橋良和博士、五十嵐雅之博士、木下直子氏に厚く感謝致します。
共同研究者として漢方薬からの PD 治療薬探索研究を多方面からサポートして頂きました順天堂大学医学部教授　服部信孝博士に厚く御礼申し上げます。
漢方薬からの PD 治療薬探索研究において、多大なるご指導、ご鞭撻賜りました順天堂大学医学部　斉木臣二博士に厚く御礼申し上げます。
In vivo PD マウスモデルにより漢方薬の薬効を評価して頂いた順天堂大学医学部　山田大介氏に厚く御礼申し上げます。
漢方薬をご提供頂いたツムラ株式会社には感謝の意を表します。
化合物の構造解析を行うに際し、ご指導、ご鞭撻賜りました日本女子大学家政学部教授　新藤一敏博士に心より感謝致します。
天然物からの化合物の探索研究をご指導頂きました河村達郎博士、北川光洋博士に厚く感謝致します。
PD 研究を行うに際し、丁寧にご指導頂いた笹澤有紀子博士に厚く感謝致します。
Arabilin に関する研究に際し、ご協力頂いた慶應義塾大学ケミカルバイオロジー研究室卒業生である、小林大貴博士、濱中奈月氏、白川峰征博士、鳥居健太郎氏には厚く御礼申し上げます。
本研究を行うにあたり多くのご指導ご激励頂きました慶應義塾大学理工学部ケミカルバイオロジー研究室卒業生の諸先輩方、切瑳琢磨しあった同期、協力して頂いた後輩達に心より感謝致します。